

Functional Genomics of Cell Wall Biogenesis in Fungi

by

Edimarlyn González

A dissertation submitted to the Graduate Faculty in Biology in partial fulfillment of the requirements for the degree of Doctor of Philosophy, The City University of New York

2009

This manuscript has been read and accepted for the Graduate Faculty in Biology in satisfaction of the dissertation requirement for the degree of Doctor of Philosophy.

Date

**Chair of Examining Committee
Dr. Peter N. Lipke, Brooklyn College**

Date

**Executive Officer
Dr. Laurel A. Eckhardt**

Dr. Derrick T. Brazill, Hunter College

Dr. Weigang Qiu, Hunter College

Dr. Timothy W. Short, Queens College

Dr. Anne M. Dranginis, St. John's University

Supervising Committee

The City University of New York

Abstract

Functional Genomics of Cell Wall Biogenesis in Fungi

Edimarlyn González

Advisor: Professor Peter N. Lipke

In pathogenic fungi, glycosylphosphatidyl inositol cell wall proteins (GPI-CWPs) mediate adhesion of the fungus to a host during infection –a step that is necessary for the fungus to be able to initiate and establish infection. Genes involved in the biosynthetic pathway that incorporate GPI-CWPs to the wall thus represent excellent targets for antifungal drug design. A mechanistically-based genomic screen was developed and applied to search for genes involved in fungal cell wall biogenesis. Specifically, the screen identifies genes required for the cross-linking of glycoproteins (GPI-CWPs) to cell wall polysaccharides via GPI anchors. GPI-CWPs are the most abundant class of proteins at the wall and play both structural and biosynthetic functions.

The rationale for the screening assay was that cells unable to properly cross-link GPI-CWPs to the wall would either retain a GPI-CWP reporter protein within the cell (hypo-excretors) or excrete the reporter protein into the growth medium (hyper-excretors), relative to wild type cells. This idea was validated in cell wall mutants known to hyper-excrete GPI-CWPs. To screen for the hypo- and hyper-excretion phenotypes, a GPI-CWP-marker protein was made by fusing the green fluorescent protein (GFP) to the carboxyl end of the GPI-CWP α -agglutinin. The marker protein was expressed in 178 gene deletants missing genes previously implicated in cell wall biogenesis and in corresponding wild type parental strains. Strains expressing the

reporter protein were examined for deficiencies in anchoring the marker protein to the wall. The screen used conditions that facilitated sample processing at large-scale and enhanced marker protein yields while minimizing noise in marker protein expression. These conditions required expression of the reporter protein from the constitutive *S. cerevisiae* *GPD1* promoter at lower temperature than the standard 30 °C in the presence of 1 M sorbitol, and growth of the cell cultures to similar cell concentrations in medium buffered to pH 6.5. Sample analysis at large scale was possible by growing the cells as 3 ml cultures in glass test tubes from which OD measurements were taken directly. Microliter volumes of cell-free supernatants were evaluated for GFP levels using a 96-well plate reader fluorimeter. Interesting mutants were subjected to secondary screens using anti-GFP antibodies and by collecting complete fluorescence spectra. The strains were also analyzed for cell surface fluorescence and levels of cytosolic and total protein in the culture medium.

Deletions in *MCD4*, *GPI13*, *TDH3* and *GDA1* caused hyper-excretion of the reporter protein. *MCD4* and *GPI13* are essential genes that play a role in GPI-anchor biosynthesis, *GDA1* is involved in GPI-CWP O-glycosylation and *TDH3* is a glycolytic enzyme that resides at the cell wall and has been implicated in mediating adhesion of fungal cells to host surfaces. The genomic screen was performed without the use of pepstatin A, which was found to inhibit GFP degradation by extracellular protease activity and thus to enhance the sensitivity of the screening assay without affecting cell growth and viability. Identified mutants thus hyper-excrete large enough amounts of the GPI-CWP reporter protein to allow detection of the hyper-excretion phenotype even in the presence of GFP proteolysis. Deletion of the transglycosidases Dcwp1 and Dfg5p,

suspected of playing a direct role in cross-linking GPI-CWPs to the cell wall, hyper-excreted the reporter protein when grown in the presence of pepstatin A. Gene deletants subjected to secondary screens exhibited 1.5-2.0 fold less fluorescence at the wall than wild type cells except for *MCD4/mcd4* and *GPI13/gpi13* cells which hyper-express the marker protein at the wall 2-4-fold relative to wild type cells. This increase may be in compensation for the high failure rate of adding the GPI-anchor to GPI-CWPs precursors. All strains examined showed less than wild type levels of the cytosolic marker, 3-phosphoglycerate kinase (PGK) and wild type levels of total protein in cell-free supernatants.

Acknowledgments

I would like to express my deepest gratitude to Dr. Peter N. Lipke for being a generous and supportive mentor and friend.

Hunter College Biology Department Faculty and Students

Brooklyn College Biology Department Faculty and Students

Dissertation Committee

Dr. Derrick T. Brazill, Hunter College

Dr. Anne M. Dranginis, St. John's University

Dr. Timothy W. Short, Queens College

Dr. Weigang Qiu, Hunter College

Special Thanks to:

Dr. Rafael Ovalle. Brooklyn College, New York, NY

Dr. Ronald E. Gordon. Mount Sinai School of Medicine, New York, NY.

Dr. Thomass Hughes. Yale School of Medicine. New Haven, CT.

Dr. Charles G. Hicks. Nassau Community College, Garden City, NY.

Dedication

To my mother and the love of my life Charlie for your never-ending unconditional love, help, and support. It is difficult to imagine myself completing this work without you in my life. I love you both very much.

Table of Contents

Title	i
Dissertation Page	ii
Abstract	iii
Acknowledgments	vi
Dedication	vii
Table of Contents	vii
Figures	xii
Tables	xvi
Chapter 1	1
Introduction	1
1.1. On fungal infections and the need for new strategies to treat them	1
1.2. Cell wall synthesis and assembly as targets for drug design	6
1.2a. Cell wall composition and organization	7
1.2b. Cell wall polysaccharide synthesis and processing	10
1.2b1. Chitin	10
1.2b2. Mannan	10
1.2b3. β -1,6 glucan	12
1.2b4. β -1,3 glucan	13
1.2b5. GPI anchors	13
1.2c. Additional cell wall components	16
1.2d. Fungal cell wall function	17

1.3. Cell wall GPI-mannoproteins (GPI-CWPs)	18
1.3a. Synthesis and structure	18
1.3b. Functional roles as structural, biosynthetic, and virulent components of the cell wall	22
1.4. The <i>S. cerevisiae</i> gene deletion library as a tool for studying GPI-CWP anchorage to the fungal cell wall	23
Chapter 2	25
High expression yield and control of expression noise of a GFP-labeled GPI-CWP in <i>S. cerevisiae</i>	25
2.1. Introduction	25
2.2. Materials and Methods	30
2.2a. Strains, Media, and Reagents	30
2.2b. Construction of reporter plasmid, pGFP-Sag1p, and yeast transformation	30
2.2c. Fluorescence Microscopy	31
2.2d. Cell wall extraction	32
2.2e. Immunoelectron microscopy	32
2.2f. Dot blotting	33
2.2g. Methylene blue exclusion assay for estimating effect of pepstatin on cell viability	34
2.3 Results	35
2.3a. Construction and expression of the cell wall GPI-reporter protein GFP-Sag1p	35
2.3b. Fluorescence and immunoelectron microscopy show expression and localization of GFP-Sag1 to the cell wall	38

2.3c. 1 M sorbitol and 1 μ M pepstatin A increase yields of excreted GFP-Sag1p	42
2.3d. Growth at lower temperature increases yields of excreted GFP-Sag1p	48
2.3e. Expression variability of excreted GFP-Sag1p is minimal among clonal cultures grown to similar cell concentrations	49
2.4 Discussion and Conclusions	51
2.4a. Pepstatin A increases GFP-Sag1p yields	51
2.4b. 1 M sorbitol improves soluble GFP-Sag1p expression yields by promoting protein folding and enhancing transcription from the <i>GPD1</i> promoter	53
2.4c. Temperature dependence of GFP-Sag1p excretion	55
Chapter 3	56
Large-scale screening for new yeast mutants affected in anchorage of GPI-CWPs to the cell wall	56
3.1 Introduction	56
3.2 Materials and Methods	59
3.2a. Strains and Media	59
3.2b. High-throughput transformation and growth of gene deletion strains	60
3.2c. High-throughput quantification of GFP-Sag1p levels in mutant and wild-type supernatants by fluorescence spectroscopy and dot blot immunoanalysis	61
3.2d. Western Blotting	63
3.2e. Total protein assay	64
3.2f. Deletion strain confirmation by diagnostic PCR	65

3.3 Results	66
3.4 Discussion	99
3.4a. General Approach	99
3.4b Genes identified as required for GPI-CWP anchorage to the cell wall	102
3.4b1. <i>MCD4</i> and <i>GPI13</i>	102
3.4b2. <i>TDH3</i>	105
3.4b3. <i>GDA1</i>	107
3.4c. Advantages of the screening approach	109
3.4d. Other applications for the screening assay	110
Chapter 4	111
The homologous genes <i>DCW1</i> and <i>DFG5</i> are required for anchoring of GPI-CWPs to the fungal cell wall	111
4.1 Introduction	111
4.2 Materials and Methods	112
4.2a. Strains, media, plasmids, yeast transformation and growth conditions	112
4.2b. GFP quantification by dot-blot immunoanalysis and fluorescence microscopy	113
4.2c. Determination of effect of pepstatin A and PMSF on growth rate and cell viability	113
4.2d. Determination of cytosolic protein in culture supernatants	114
4.3. Results and Discussion	114
4.3a. <i>dcw1</i> and <i>dfg5</i> Null mutants hyper-excrete a GPI-CWP reporter protein when grown in the presence of the aspartyl protease inhibitor pepstatin A	114

4.3b. Pestatin A does not affect growth rate or lead to increases in cell death	120
Chapter 5	127
Concluding Remarks	127
5.1. A need for novel antifungals	127
5.2. GPI-CWP anchorage to the fungal cell wall: an ideal target for antifungal drug design	127
5.3. Development of a robust reporting assay of deficiencies in GPI-CWP anchorage to the cell wall	128
5.4. High-throughput application of the reporting assay to screen for genes required for GPI-CWP anchorage to the cell wall	129
5.5. Genes identified as required for GPI-CWP anchorage to the cell wall	131
5.6. Pepstatin A enhances sensitivity of the screening assay	131
References	133

Figures

Figure 1.1. Schematic of the <i>Saccharomyces cerevisiae</i> cell wall	9
Figure 1.2. A model for anchorage of GPI-CWPs to the cell wall in fungi	15
Figure 2.1. Schematic of pGFP-Sag1p reporter construct	36
Figure 2.2. Visualization of GFP-Sag1p at the cell wall by fluorescence microscopy	39
Figure 2.3. Visualization of GFP-Sag1p at the cell wall by immunoelectron microscopy and cell wall fractionation	41
Figure 2.4A. Growth in the presence of 1 M sorbitol increases GFP-Sag1p expression yields	44
Figure 2.4B. GFP-Sag1p is hyper-excreted from the cell wall mutant <i>KRE5/kre5</i>	45
Figure 2.4C. Growth at lower temperature increases GFP-Sag1p yields	45
Figure 2.4D. Determination of linear range for GFP-Sag1p excretion by immunoblotting	46
Figure 2.5. Growth in the presence of pepstatin A increases GFP-Sag1p yields	47
Figure 2.6. Clonal cultures grown to similar cell densities excrete comparable amounts of GFP-Sag1p	48
Figure 2.7A. Pepstatin A does not affect growth rate in wild type cells	50
Figure 2.7B. Pepstatin A does not affect cell viability in wild type cells	51
Figure 3.1A. Determination of GFP-Sag1p excretion from cell wall mutants 1-96 by fluorimetry	68
Figure 3.1B. Determination of GFP-Sag1p excretion from cell wall mutants 97-179 by fluorimetry	73
Figure 3.2. Secondary screening of cell wall mutants identified as hyper-excretors of GFP-Sag1p by fluorimetry	79

Figure 3.3A. Secondary screening of cell wall mutants identified as hyper-excretors of GFP-Sag1p by immunoblotting with anti-GFP antibodies	80
Figure 3.3B. Integrated GFP intensity from GFP-Sag1p hyper-excretors	81
Figure 3.3C. Determination of excretion of cytosolic 3-phosphoGlycerate kinase (PGK) from GFP-Sag1p hyper-excretors	82
Figure 3.4A. Fluorescence emission spectrum of pure GFP and control supernatants	83
Figure 3.4B-H. Fluorescence emission spectrum of pure GFP and background-corrected fluorescence of supernatants from wild type cells, true GFP-Sag1p hyper-excretors, and the GFP-Sag1p hypo-excretor <i>nsr1/nsr</i>	84-87
Figure 3.5. 3-phosphoGlycerate kinase (PGK) western blot	88
Figure 3.6. Determination of total protein excreted from true GFP-Sag1p hyper-excretors	89
Figure 3.7A. Regions within the genome complementary to primer pairs used for diagnostic PCR	90
Figure 3.7B-E. Confirmation of gene deletions by diagnostic PCR	91-93
Figure 3.8. Determination of cell surface fluorescence for GFP-Sag1p hyper-excretors <i>GPI13/gpi13</i> and <i>MCD4/mcd4</i> relative to wild type	97
Figure 3.9. Determination of cell surface fluorescence for GFP-Sag1p hyper-excretors <i>tdh3/tdh3</i> and <i>gda1/gda1</i> relative to wild type	98
Figure 4.1. Determination of the effect of pepstatin A on GFP-Sag1p excretion from cell wall mutants <i>dcw1/dcw1</i> and <i>dfg5/dfg5</i> by immunoblotting	116
Figure 4.2. Integrated GFP signal for GFP-Sag1p excretion from <i>dcw1/dcw1</i> and <i>dfg5/dfg5</i> in the presence of pepstatin A	117
Figure 4.3. Determination of the effect of pepstatin A, PMSF, and both protease inhibitors together on the levels of excreted cytosolic PGK from <i>dcw1/dcw1</i> and <i>dfg5/dfg5</i> relative to wild type	119

Figure 4.4. Effect of pepstatin A on cell viability in <i>dcw1/dcw1</i> and <i>dfg5/dfg5</i> cells relative to wild type	121
Figure 4.5. Effect of pepstatin A on growth rate of <i>dcw1/dcw1</i> cells relative to wild type	122
Figure 4.6. Effect of pepstatin A on growth rate of <i>dfg5/dfg5</i> cells relative to wild type	123
Figure 4.7. Determination of cell surface fluorescence in <i>dcw1/dcw1</i> and <i>dfg5/dfg5</i> relative to wild type	124

Tables

Table 2.1. Oligonucleotides used for the construction of pGFP-Sag1p	37
Table 3.1. Open reading frames 1-96 screened for their involvement in GPI-dependent anchoring of glycoproteins to the cell wall in <i>S. cerevisiae</i>	69
Table 3.2. Open reading frames 96-179 screened for their involvement in GPI-dependent anchoring of glycoproteins to the cell wall in <i>S. cerevisiae</i>	74
Table 3.3. Cell surface fluorescence in GFP-Sag1p hyper-excretors relative to wild type cells	99

Chapter 1

Introduction

1.1 On fungal infections and the need for new strategies to treat them

Fungal infections continue to be a problem of concern due to the lack of safe and effective antifungals that can withstand the emergence of resistant strains. An increase in the incidence of superficial and systemic opportunistic mycoses over the last two decades stems from the growing number of patients susceptible to infection due to severe illness and immunosuppression [1] and from the widespread use by clinicians of currently available antifungals. Specifically, empirical and prophylactic therapy as a preventive measure in high-risk patients promotes the emergence of resistant strains [2, 3]. In these patients, preventive measures usually result in positive outcomes. However, those who nonetheless fall victim to infection, often battle hard to treat and potentially life-threatening infections. A recent study shows that in contrast to the mostly harmless superficial infections, disseminated fungal infections involving resistant strains have a high mortality rate of > 40% [4]. An additional study compared critically ill patients receiving fluconazole as a preventive measure with patients who did not receive treatment and found a higher mortality rate (40% vs. 20%, respectively), longer stays in intensive care units, and overall longer hospital stays in treated than in the non-treated patients [2]. This group also had a higher rate of isolation of *Candida* species resistant to fluconazole. This is an unfortunate outcome considering that fluconazole is a preferred method of treatment for candidiasis due to its lower toxicity effects compared to the alternative choice, amphotericin B [5].

Advances in the medical field have led to an increase in the number of patients receiving hematopoietic stem cell transplantation, implantation of indwelling medical devices (stents, catheters, prostheses, etc.) and an increase in the number of patients receiving organ transplants. Many of these patients are subjected to prolonged empiric and prophylactic antifungal treatment accompanied by administration of immunosuppressive drugs to control host-vs-graft disease and predisposition to invasive mycoses. A rise in the frequency of preventive treatments is suspected to be the cause for an increase in the incidence of fungal pathogens that were previously uncommon such as *Candida krusei* and *Candida glabrata*, and for an increase in invasive mycelial infections other than *aspergillosis* [1]. For instance, at a bone marrow transplantation center, the incidence of aspergillosis and other mycelial infections increased from 18% in years before the use of fluconazole prophylaxis to 30% in the period after use of fluconazole prophylaxis became routine [6]. Because these less common pathogens tend to be unresponsive to currently available antifungals [1], it is evident that there is a critical need for more effective treatments. This need is heightened by the fact that the use of existing antifungals is limited due to low potency [7], poor solubility [8], narrow clinical spectrum, and toxicity effects that range from mild to severe [9, 10].

In recent years, a new class of antifungal compounds was introduced to the market with very promising results due to their relatively milder toxicity effects and rapid fungicidal activity against most isolates of *Candida* spp, *Aspergillus* spp, and *Pneumocystis carinii* [11]. These compounds, collectively recognized as “the echinocandins” work by inhibiting synthesis of the cell wall polysaccharide, β -1,3 glucan. The desirable characteristics of echinocandins are based on that these agents

disrupt a process that is unique to fungi, conserved across many fungal species and essential for cell viability. The success of cell wall-targeted antifungals makes it clear that efforts into developing novel antifungals should ideally concentrate on elaborating agents that target/damage the cell wall.

Some researchers believe that although prolonged prophylactic therapy in at-risk patients can be effective toward eradicating susceptible microorganisms, it may also be what later facilitates colonization and invasion from pathogens that are innately resistant to the antimicrobial agent used [1]. A potentially effective way to inhibit recurrence of infection with more aggressive, resistant strains would be to administer the patients with agents capable of blocking adhesion of the fungus to host cells as this is a prerequisite for colonization. Antifungals with this mechanism of action are currently not available to clinicians. The work described here seeks to indentify genetic elements that contribute to the adhesive properties of the fungal wall since these elements may serve as ideal targets for novel antifungal strategies. Interfering with the ability of the fungal cell to adhere to its substrate/host would be of great value because *i)* the inhibitor may not have to enter the cell to exert its function, thus toxicity would be minimized *ii)* adherence to substrate/host is a prerequisite for fungal cells to become infective, thus agents that inhibit this process would likely be of broad-spectrum application.

In addition to the increasing incidence of resistant fungal strains, effective treatments against fungal biofilms remains a challenge to clinicians because of their widespread tolerance to currently available antifungals. Biofilms are microbial “communities” that grow on biotic and abiotic surfaces (e.g. dental cavities, stents, catheters, prostheses and plastic surfaces) and are therefore a threat not only to affected

patient but also to food-processing companies where adherent fungi can form highly resistant biofilms in industrial installations [12]. These fungal communities often share substratum with bacterial agents and inevitably depend on the ability of fungal cells to adhere to each other and to a variety of other surfaces to retain the often multilayered structure of the biofilm [13]. Biofilms not only offer the cells protection from environmental assault but serve as a reservoir for infective cells that can later disseminate through the host's bloodstream to other organs for infection [12-14].

Because fungal cells depend on being able to adhere tightly to its host before becoming infectious, elucidation of the biosynthetic pathways that make the cells "adhesive" represent excellent drug targets.. One such process is the cross-linking of mannoproteins to cell wall polysaccharides through glycosylphosphatidyl inositol (GPI)-anchors. These glycoproteins, commonly referred to as GPI-proteins, play a variety of important cellular roles one of them being the role of adhesins that mediate attachment of fungal cells to host surfaces. Studies show that pathogenic fungi with reduced levels of GPI-CWPs at the wall are less virulent and more susceptible to the lytic actions of macrophages [15].

The work presented here describes the development and application of a genome-wide approach for screening the *S. cerevisiae* gene deletion library for genes required for anchorage of GPI-mannoprotein (GPI-CWPs) to the cell wall. The library was purchased from *Invitrogen* and a subset of 179 different gene deletion strains transformed in high throughput with a reporter GPI-CWP (GFP-Sag1p) and screened for deficiencies in anchoring the reporter protein to the cell wall. The reporter protein consists of the carboxyl end of the GPI-CWP α -agglutinin encoded by the SAG1 gene, N-terminally

fused to the green fluorescent protein (GFP). All 179 strains contain deletions in genes previously implicated in cell wall biogenesis. 10 of the 179 gene deletants harbor deletions in essential genes and are therefore heterozygote for the deletion. These mutants were assayed for GFP-Sag1p excretion into the growth medium relative to wild-type cells and those with interesting phenotypes were subjected to secondary screens to assess for cell-surface fluorescence, amount of cytosolic protein in the medium and total amount of excreted protein. Chapters 2 and 3 describe development and application of the screening approach, respectively. The cytosolic enzyme, 3-phosphoglycerate kinase (PGK), was used as a marker for intracellular protein. Controversy exists as to whether PGK is a true cytosolic marker since this enzyme has also been found in cell wall preparations from *S. cerevisiae* and *C. albicans* cells [16, 17]. However, a recent study suggests that the presence of PGK in cell wall preparations may simply be a consequence of the commonly used cell wall purification techniques, which require the use of plasma membrane disrupting agents that cause leakage of cytoplasmic components into the cell wall extracts. A novel cell wall fractionation approach has been proposed that yields cell wall fractions devoid of proteins of presumably cytosolic origin including PGK [18].

Application of the screen led to the identification of *MCD4* and *GPI13* (two putative essential genes thought to play a role in GPI-anchor biosynthesis), *GDA1* (a GDPase involved in GPI-protein O-mannosylation), and the glycolytic enzyme, *GAPDH/TDH3*, as required for GPI-CWP anchorage to the cell wall. The recently discovered homologs of bacterial mannosidases, Dcw1p and Dfg5p, are suspected of playing a direct role in the transferring of GPI-CWPs from the plasma membrane to cell-

wall glucan due to their combined glucosidase and transglycosidase activities. We present additional data that corroborates a role for these genes in this process (chapter 4).

1.2 Cell wall synthesis and assembly as targets for drug design

Fungal pathogens cause significant morbidity and mortality, especially among the immunosuppressed and the chronically ill. This makes fungal infections emerging diseases which is exemplified by findings that *Candida* infections are the fourth most common hospital-acquired disease and are rapidly rising to third [19].

However, the biological relatedness of fungi and animals has meant that many anti-fungal drugs are severely toxic to humans, so there are few clinically-approved antifungals available compared to anti-bacterials. New approaches and lead compounds for antifungal development are therefore a critical medical need. Because fungi have cell walls that animals lack, the walls are an obvious target for potential anti-fungal drugs. Many of the processes that assemble the cell walls occur exterior to the plasma membrane [20-25]. Therefore inhibitors of the assembly process would be active even if they did not reach the interior of the fungal cells.

Of the ~250,000 different species of fungi that populate the earth only a few hundred (400-500) are capable of infecting animals and humans [26]. The major cell wall components and molecular organization of the wall are generally shared across fungi although species-specific variations exist at the level of ratio of the components, how these components cross-link with each other, and their special distribution throughout the wall. Since the work presented here employs the fungus *Saccharomyces cerevisiae* as the model organism for studying cell wall biology, description of cell wall synthesis,

architecture, and function would primarily focus on this organism. The *S. cerevisiae* cell wall is a good studying model for inquiries into fungal wall biology because its general body plan and composition resembles that of other (dimorphic) ascomycetous yeasts such as the human pathogens *Candida* ssp. and *Exophiala dermatitidis*, the fission yeasts *Schizosaccharomyces pombe*, and mycelial pathogenic fungi such as *Aspergillus* spp. and *Fusarium oxysporum* (Klis et al. 2007).

1.2a Cell wall composition and organization

Like plant and bacterial cells, fungal cells are surrounded by a thick “woody” layer or cell wall. Fungal walls are approximately 100-200 nm wide and differ significantly from plant and bacterial walls in their structure and composition. In the budding yeast *S. cerevisiae*, the cell wall is a bi-layered structure primarily composed of polysaccharides and protein. The polysaccharide components in order of abundance consist of β -1,3 and β -1,6 linked glucose monomers and β -1,4 linked N-acetylglucosamine residues or chitin. In addition to these structural polysaccharides, elaborate O- and N-linked mannose side chains are added to many of the protein molecules that reside in the cell wall. Electron microscopy of potassium permanganate stained cell walls shows an electron dense outer layer emanating from a mostly translucent inner layer. The inner layer is in contact with the plasma membrane and consist of long (1000-1,500 glucose residues), spring-like chains of β -1,3 linked polymers that interconnect through hydrogen bonds to form the flexible framework onto which a densely populated outer layer of GPI-CWPs is covalently cross-linked. The majority of cell wall mannoproteins are cross-linked to the β -1,3 glucan network indirectly through shorter (300-500 glucose residues), more branched β -1,6 chains [27,

28]. Figure 1.1 shows a schematic of the fungal cell wall [28]. A smaller subgroup of glycoproteins, dubbed PIR proteins, “proteins with internal repeats”, is directly cross-linked to the β -1,3 glucan network through ester linkages between glutamine residues in the proteins’ repeat sequences and non-reducing ends of β -1,3 glucan chains [29]. PIR proteins may therefore contribute to strengthening the cell wall by cross-linking different β -1,3 glucan chains (Figure 1.1). Consistent with this view is that PIR proteins can be found throughout the cell wall. Mannoproteins cross-linked to β -1,3 through β -1,6 glucan chains are known as GPI-dependent proteins (GPI-CWPs) because it is through a trimmed version of the GPI anchor that they are covalently bound to the non-reducing ends of β -1,6 glucan chains. These proteins receive a preformed GPI anchor at the ER [30, 31] prior to being delivered to the cell surface via the secretory pathway. At the cell surface, the protein remains tethered to the plasma membrane through the lipid part of the GPI anchor which may or may not undergo further processing depending on the protein’s final cellular role. For details on GPI-CWP structure and function, see section 1.3.

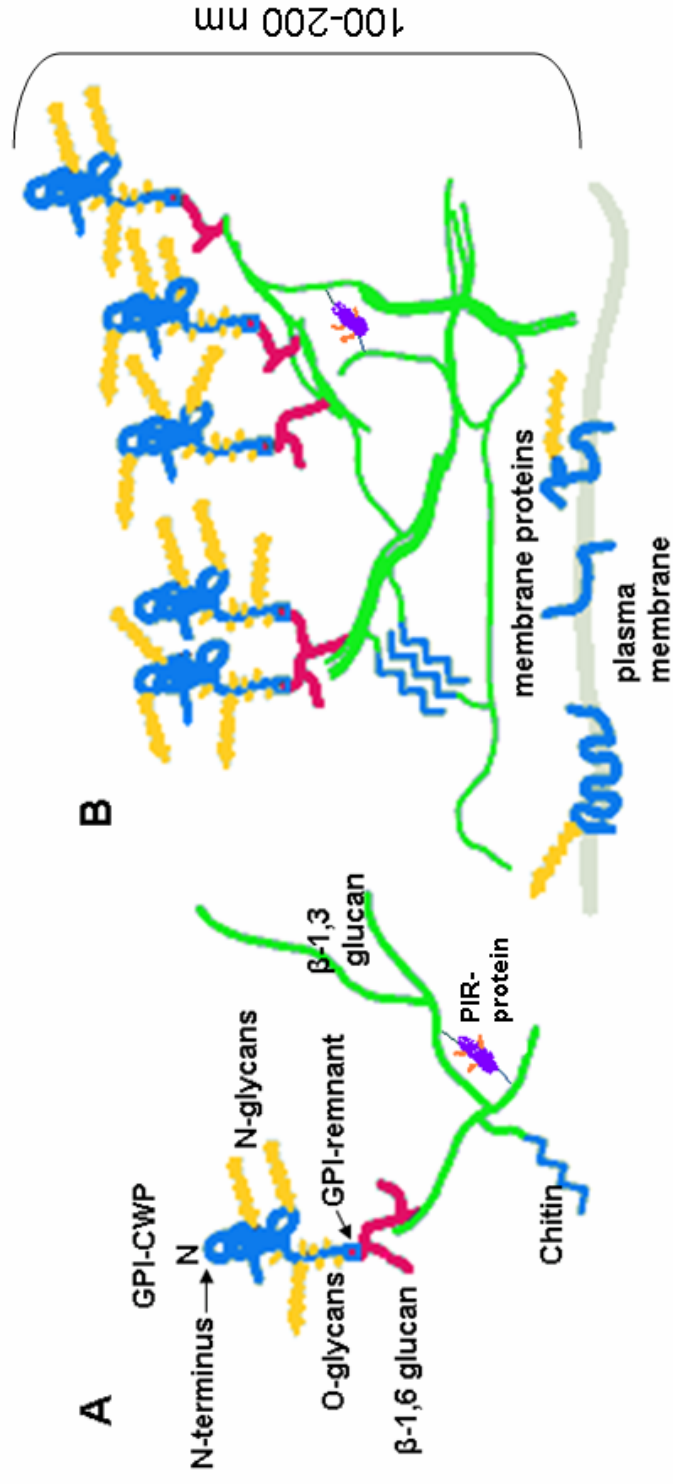


Figure 1.1. Schematic of the *S. cerevisiae* cell wall. A) cell wall module B) cell wall modules interconnect laterally through covalent and non-covalent interactions to form the cell wall (Lipke et al [28]).

1.2b Cell wall polysaccharide synthesis and processing

1.2b1 Chitin

Chitin is a minor but important component of the wall. It accounts for 1-3% of the total polysaccharide content of the wall and is mostly found at the primary septum that separates dividing cells [32]. The primary septum is later digested by chitinases to allow for cell separation following cytokinesis. A secondary septum consisting mostly of β -glucans and protein forms around the primary septum and serves as the foundation for daughter cell wall synthesis [33]. Chitin can also be found at bud scars in mother cells and sparingly throughout the cell wall serving as a linker between β -1,3 glucan chains [34]. It may also cross-link β -1,6 glucan chains and in this manner contribute to the mechanical strength and insolubility of the wall [20]. Cell-wall mutants often up-regulate their wall chitin content to compensate for cell wall debilitation [35-37]. Chitin synthesis takes place at the plasma membrane through the action of an enzymatic complex encoded by the *Chs* group of integral membrane proteins, known as Chs1p, Chs2p and Chs3p ([38, 39]. Chitin chains are extruded into the cell wall periplasmic space and assembled and cross-linked to other cell wall polymers by the GPI-CWPs, Crh1p and Crh2p [40]

1.2b2. Mannan

The mannan content of the wall is a consequence of extensive N- and O-mannosylation of GPI-CWPs, PIR, and other secreted glycoproteins at asparagine, and serine and threonine residues, respectively. Protein N- and O-mannosylation begins at the ER where the first mannosyl residues are added in a process highly conserved among eukaryotes. Subsequent elongation of the mannan chains is fungi-specific and proceeds at

the Golgi. The *PMT* and, *MNT* and *MNN*, families of mannosyltransferases carry-out protein glycosylation at the ER and Golgi, respectively [41-43]. These enzymes depend on Dolichol-Phosphate-mannose (Dol-P-mann) and GDP-mannose as the mannosyl donors for mannan synthesis [44], although the initial N- and O-mannosylation steps occurring at the ER depend on Dol-P-Mann only as the mannosyl donor [45]. Chain elongation occurring at the Golgi depends on the GDPase, Gda1p, to ensure a constant supply of GDP-mannose as the mannosyl donor [46]. In this study, *GDA1* was identified as required for anchorage of GPI-CWPs to the cell wall since *gdal/gdal* cells excrete larger than wild type amounts of the GPI-CWP reporter protein, GFP-Sag1p, and have lower levels of the reporter protein at the wall relative to wild-type cells. *gdal/gdal* Cells also appear to form large aggregates possibly because of cell separation defects (Chapter 2I).

Both *N*- and *O*-linked side-chains of CWPs may contain phosphodiester linkages. At most physiological pHs, these phosphodiester groups are negatively charged and are thus responsible for the numerous negative charges at the fungal cell surface. The mannan phosphate groups are added by members of the *MNN* gene family, *MNN4* and *MNN6* [47]. The fungal cell wall therefore acts a cation exchanger, thus allowing them to bind positively charged proteins, for example, proteins released from the cytosol, and explaining the stainability of many fungi with the positively charged dye Alcian blue [21]. Negative charges at the fungal cell surface may also be important for helping the cell adapt to environmental changes and changing conditions within the host, thus contributing to pathogenicity [48]. A recent review on mannoprotein glycans in fungi is provided in (Gonzalez *et al.*, 2008).

1.2b3. β -1,6 glucan

Among the various cell wall polysaccharides, β -1,6 glucan synthesis and processing remains the least understood. Whether the polysaccharide is synthesized inside the cell or at the cell surface prior to its incorporation into the wall and what enzymes process these reactions remains to be resolved. To date, no biosynthetic precursors for the glucan have been recovered from *S. cerevisiae* cell extracts devoid of cell walls, thus doubts as to an intracellular origin for the synthesis of the polymer remain. The same does not apply for *Schizosaccharomyces pombe* for which β -1,6 polymers have been detected in the Golgi [49]. Additional experiments with mutants exhibiting reduced levels of β -1,6 glucan at the wall show that many of the missing genes localize throughout the secretory pathway which implies that synthesis of the polymer may begin at the ER and proceed at the Golgi with the last processing steps taking place at the cell surface or periplasmic space through the action of proteins like Kre1p [50]. The GPI-dependent protein Kre1p, which resides both at the plasma membrane and the cell wall has been implicated in β -1,6 glucan branching and assembling [51, 52]. Additional enzymes in the *KRE* (killer toxin resistant) gene family appear to play a role in β -1,6 glucan synthesis although the implication is indirect. For instance, deletion of the *KRE5* gene results in reduced levels of β -1,6 glucan at the wall presumably because of its putative role as a ER chaperone that promotes folding of enzymes involved in synthesizing the polymer [53].

1.2b4. β -1,3 glucan

In the case of β -1,3 glucan, its synthesis, processing and assembly is better understood. The Fks1p and Fks2p gene products have been identified as the biosynthetic subunits [54, 55] whose activity is closely regulated by the GTP-binding protein Rho1p [56]. The Fks proteins are integral plasma membrane proteins whose association with Rho1p at the cell surface has been demonstrated by immunoprecipitation [56]. Rho1p acts a “switch” that can rapidly turn synthesis of the polymer on and off by interchanging between its GTP and GDP-bound forms, respectively. This mechanism would enable the cell to quickly respond to demands for changes in cell wall composition, shape and organization as the cell adapts to its environment. As the glucan chains are synthesized by the Fks1p-Rho1p complex, newly generated molecules are extruded into the wall space where members of the GAS family, such as the glucanosyltransferase GAS1p further process and assemble the chains into the flexible network that serves as foundation to which all other wall components are added. Gas1p acts by internally splitting a β -1,3 glucan molecule and transferring the newly generated reducing end to the non-reducing end of another β -1,3 glucan molecule. This results in the formation of a new β -1,3-linkage that elongates and cross-links the β -1,3 glucan chains [57]. The mechanical strength of the β -1,3 lattice is further fortified by cross-links to chitin and β -1,6 glucan [20].

1.2b5. GPI anchors

Mannoproteins with a carboxy-terminal signal peptide for GPI-anchoring receive a GPI-anchor in the lumen of the ER [58]. This step is mediated by a transamidase, which

cleaves the protein at about 20-30 amino acids from the C-terminus and adds a pre-assembled glycolipid anchor to the new carboxyterminal residue. In the transamidase reaction, an amide linkage is formed between the protein and the ethanolamine phosphate of the third mannose residue (Figure 1.2). GPI-anchoring ties a protein with its C-terminus to the membrane, allowing it to travel to the cell surface within the lumen of cellular vesicles. GPI-anchoring of mannoproteins is an essential function in ascomycetous yeasts but not, for example, in the clinical, filamentous fungus *Aspergillus fumigatus* [59]. The preassembled glycolipid anchor consists of a phosphatidylinositol group, a glucosamine residue (GlcN, obtained by deacetylation of GlcNAc), and four or five mannose residues (Figure 1.2). The first three mannose residues each receive an ethanolamine phosphate group added by three different enzymes of the Mcd4 family [60]. Modification of the GPI anchor has been reported to occur in the Golgi during the translocation of GPI-mannoproteins to the cell surface. In baker's yeast, about 50% of the GPI-protein molecules become covalently linked to the cell wall, the remainder being retained at the plasma membrane. Some GPI-proteins are known as typical cell wall resident proteins (*e.g.* ScCwp1, ScSag1, CaAls1, CaHwp1), and others as abundant plasma membrane proteins (ScEcm33, Sc Gas1); however, intermediate distributions also occur. The distribution between wall and plasma membrane depends on characteristics of the sequence immediately upstream of the GPI addition site. Consecutive basic residues in this region seem to stimulate plasma membrane retention; however, this may be overridden when they are preceded by long stretches of serine and/or threonine residues [61]. Cleavage of GPI anchors of proteins destined for wall incorporation occurs between glucosamine and the first mannose residue [62] (Figure 1.2). In the same or separate

reaction, the active sugar end of the trimmed anchor is cross linked to a non-reducing end of β -1,6-glucan [25, 63] (Figure 1.2). This positions the protein in the outermost layer of the cell while covalently linking it to the cell wall framework. Which protein or protein complex is responsible for anchor cleavage is still uncertain. Interesting candidates are the paralogs Dfg5p and Dcw1p, belonging to subfamily 76 according to the carbohydrate-active enzyme classification. Both are plasma membrane-localized GPI proteins and homologs of bacterial endomannosidases. Their coupled deletion leads to synthetic lethality in both *S. cerevisiae* and *C. albicans* [64]. In this study we find that null mutants of these genes hyper-excrete a GPI-CWP reporter protein (GFP-Sag1p) and localize reduced levels of the marker protein to the cell wall relative to wild-type cells.

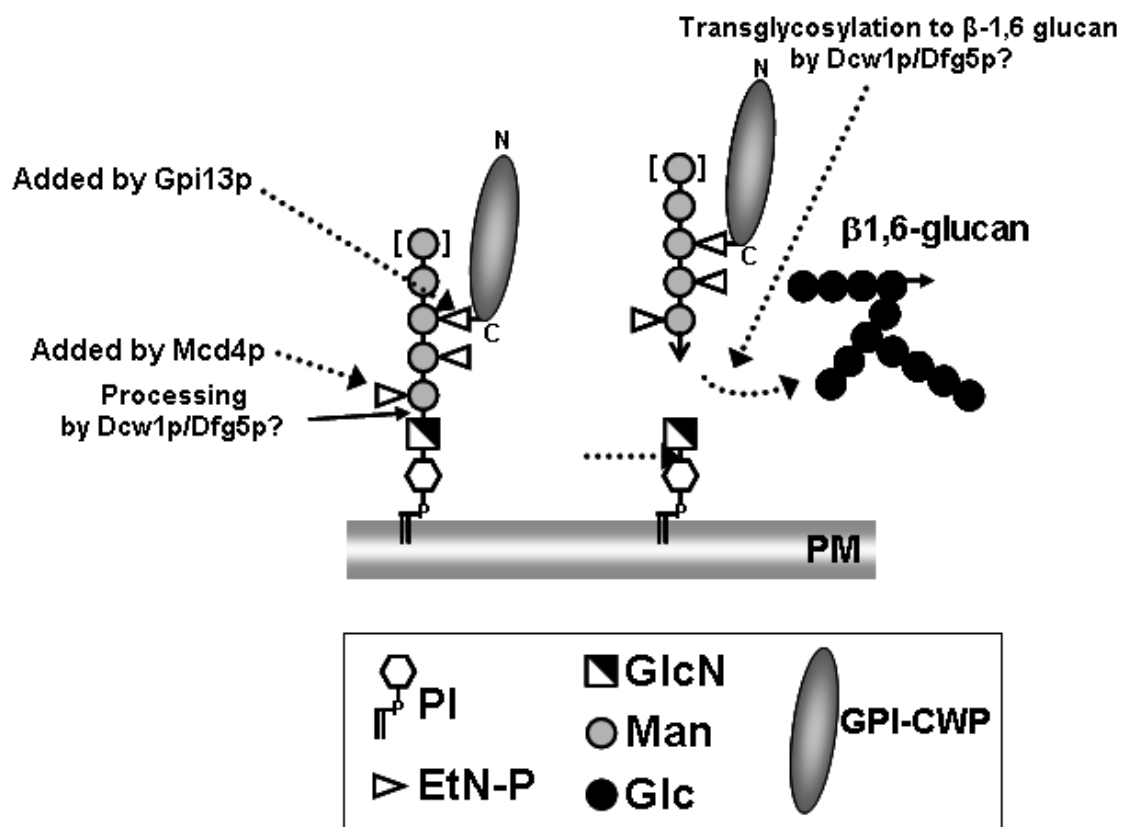


Figure 1.2. A model for anchorage of GPI-CWPs to the cell wall in fungi

1.2c. Additional cell wall components

Additional cell wall components are important for ensuring the cell wall's role as a protective and selectively permeable barrier. Many proteins reside at the wall as soluble proteins that can be extracted with reducing agents such as β -mercaptoethanol and dithiothreitol or in the presence of hot SDS. In contrast, release of proteins covalently bound to cell-wall glucan requires chemical treatment (e.i, boiling in 30 mM NaOH) or digesting with β -glucanases. Other proteins are linked to the wall via disulfide bonds to other cell wall glycoproteins or through ionic interactions. Additionally, a number of glycolytic enzymes such as PGK and the Tdh proteins, traditionally thought of as cytosolic proteins, are increasingly being detected at the cell wall [65]. Their presence at the wall is mysterious as these proteins lack secretion signals and are not glycosylated. Among the many ideas postulated for how these proteins might make it to the wall are: via a non-classical secretory pathway, yet to be elucidated, as "hitch-hikers" of secretory vesicles, or they may just be by-products from lysed cells that latch on to hydrophobic surfaces on the wall. Most recently, the proteins are described as probable intracellular contaminants resulting from the cell wall purification techniques used [66]. Interestingly, we identify the glycolytic enzyme, Glyceraldehyde-3-phosphate dehydrogenase, isozyme 3 (*TDH3*) as required for normal anchoring of GPI-CWPs to the cell wall since null mutants of this enzyme exhibit reduced levels of the GPI-CWP reporter protein (GFP-Sag1p) at the wall and excrete more of the fluorescent protein into the growth media than wild-type cells (Chapter 2I).

1.2d. Fungal cell wall function

The fungal wall is an essential organelle that comprises 20-30% of the dry weight of the cell [67]. Its essentiality stems from the cell's dependence on the wall for protection against environmental assault, for maintaining internal osmolarity, and for attaining the morphogenetic changes that most take place during cell division, cell-cell contact, cell mating, and transitioning from a non-infectious to an infectious state, in the case of pathogenic fungi.

The cell wall acts as a selectively permeable barrier that allows passage of essential nutrients and metabolites into the cell while protecting it from extracellular cell wall digesting enzymes from other organisms [68]. The wall also stores soluble proteins that are important for cell-wall function. Despite its strong mechanical strength, the wall is not rigid but rather flexible and dynamic in nature. The plasticity of the wall is critical for preserving cell wall integrity and stability through the various morphological changes that a cell goes through throughout its life cycle. The cell wall serves as the reservoir for a multitude of proteins and enzymes that inform the cell of its environment and help it coordinate the appropriate response to a particular environmental stimulus. For example, when cells of opposite mating type come into proximity, the cells release specific pheromones (*a* and α factor from *a* and α cells, respectively) that promote the synthesis and display at the wall of unique mating adhesins that mediate contact between the cells. These GPI-CWPs are known as *a* and α agglutinins and are displayed on the surface of *a* and α cells, respectively. Contact between agglutinins of opposite mating type promotes the formation of a mating structure known as a "smooch" that mediates fusion of the haploid cells into a diploid organism [69].

As the cell's first point of contact with the environment, the cell wall is at constant risk of [70] damage and must therefore be equipped with a myriad of biosynthetic and remodeling enzymes that rapidly repair it and restore its integrity and prevent cell lysis. The important role that the cell wall plays during pathogenicity also depends on the proteins that reside within it, most of which are cross-linked to the wall via GPI anchors. In their role as adhesins, GPI-proteins help the fungus bind tightly to its host as the primary and required step for initiation and establishment of infection [12, 70]. Cell wall GPI-proteins also help the fungus survive within the host by protecting it from the host's innate immune response [12, 71, 72]. In this particular role, GPI-CWPs mask underlying cell-wall glucans that can be recognized by host cells as immunogens to mount an immune response. Other GPI-proteins may act as hydrolytic enzymes of host tissue that help the fungus "dig" for new binding sites thus helping in the dissemination of infection [73]. Clearly, cell wall formation, integrity and function tightly depend on the proteins and enzymes that built and remodel the wall as well as on those proteins that keep it in contact with the extracellular environment. The majority of these enzymes/proteins are anchored to the cell wall via GPI-anchors. Enzymes required for the incorporation of these proteins at the wall represent excellent targets for antifungal drug-design.

1.3 Cell wall GPI-mannoproteins (GPI-CWPs)

1.3a. Synthesis and structure

GPI-CWPs account for close to 1% of the total eukaryotic cell proteome [58]. The proteins consist of multiple domains with distinct functions *i)* a hydrophobic N-terminal

secretion signal that targets the protein to the ER for further synthesis, *ii*) a N-terminal region that harbors the catalytic or functional domain of the protein *iii*) a central region rich in tandem stretches of serine/threonine repeats that serve as sites for multiple N- and O-glycosylation and *iv*) a mostly hydrophobic C-terminal region that signals addition of a GPI anchor [74]. The GPI anchor addition signal which for most GPI proteins consists of the last 30-40 C-terminal amino acids residues, harbors a putative cell wall targeting signal and the amino acid residue or ω -site at which the protein is cleaved and subsequently linked to a GPI anchor [75, 76]. The presence of a dibasic amino acid motif upstream of the ω -site has been postulated to act as a plasma membrane retention signal while absence of these residues appears to favor cell wall localization. Additional studies suggest that the absence of a dibasic motif N-terminal to the ω site is not a definitive signal for cell wall localization and that it may be overridden by long serine/threonine rich stretches in the central region of the protein [77, 78]. For example, a protein may have the dibasic motif but a long enough ser/thr repeat region would target the protein to the cell wall.

GPI-protein synthesis begins in the cytoplasm where signal recognition particles (SRPs) bind the secretion signal and target it to the ER membrane where protein synthesis resumes as the protein is translocated into the lumen of the ER. A transamidase enzyme complex at the ER membrane recognizes the protein's ω site, cleaves at this residue and replaces the GPI anchor additional signal for a preassembled GPI-anchor. GPI-anchor biosynthesis takes place at the ER membrane where as many as 20-30 different enzymes participate in a stepwise chain of events that gradually incorporate each component of the GPI anchor. Each step is carried out by a multi-subunit enzymatic

complex. Many of these enzymes have been identified through complementation experiments in mammalian cells, and their homologs found throughout most eukaryotic organisms implying that the GPI-anchor biosynthetic pathway is evolutionarily conserved. Although the core structure of the GPI anchor is shared amongst most eukaryotes, differences exist at the level of side chain elaborations and the number of mannose residues attached. For instance, fungal GPI anchors require the addition of four mannose residues whereas many GPI-anchors of mammalian cells do not have a fourth mannose and addition of this residue may be tissue-specific. In yeast, addition of the fourth mannose is a pre-requisite for incorporation of a phosphoethanolamine (EtNP) group to the third mannose residue of the GPI anchor. EtNPs are added to mannoses one, two and three by the ethanolamine transferases *MCD4*, *LAS21/GPI7* and *GPI13*, respectively (Figure 1.2). It is through the ethanolamine group added by Gpi13p to the hydroxyl group on carbon 6 of the third mannose of the GPI anchor, that the anchor is linked to the protein's carboxyl end via an amide bond [60]. In this study we identify *GPI13* and *MCD4* as required for GPI-dependent anchoring of mannoprotein to the cell wall since heterozygote deletants of these genes hyper-excrete GFP-Sag1p, relative to wild-type cells. *MCD4/mcd4* and *GPI13/gpi13* cells appear to up-regulate expression of the reporter protein (likely to compensate for deficits in GPI-anchor attachment to GPI-CWPs) since they show ~2-fold more GFP-Sag1p at the cell surface than wild-type cells. Although the phenotypes we observe are not surprising considering the essential roles of *MCD4* and *GPI13* in GPI-anchor biosynthesis, we are the first to show that the genes are haploinsufficient and that heterozygote deletants hyper-excrete GPI-CWPs, have altered levels of GPI-CWPs at the wall and in the case of *GPI13/gpi13* deletions, the cells fail to

separate following cytokinesis (chapter 3). Important to note is that although Gpi13p and Mcd4p are essential for cell viability in fungi, their activities are dispensable in mammals and may thus represent ideal targets for antifungal drug design.

Following addition of the GPI anchor and of precursor groups for N- and O-glycosylation at the ER, pre-GPI-proteins are packaged into specialized COPII-coated vesicles for transport to the Golgi, where the N- and O-linked carbohydrate chains and the GPI-anchor are extended and modified [79]. Mature GPI-proteins are then delivered to the cell surface via secretory vesicles where they remain tethered to the outer leaflet of the plasma membrane through the lipid part of the GPI anchor. At the cell surface, some GPI-mannoproteins function as integral plasma membrane proteins, while many others are released from the membrane to become cross-linked to wall polysaccharides. This transitioning from the cell membrane to the wall is believed to be mediated by glucosidases and transglycosylases that in principle would cleave the GPI anchor and subsequently cross-link the GPI anchor-protein remnant to β -1,6 glucan acceptor molecules in the wall. Evidence that such enzymatic reactions occur is provided by the elegant experiments performed by Lu et al [25, 63].

GPI anchors are cleaved at their glycan part likely in between the glucosamine and first mannose residue in a reaction that leads to loss of the glucosamine and phosphoinositol groups from the GPI anchor (Figure 1.2). A glycosidic bond is believed to form between mannose one of the trimmed GPI-anchor-protein remnant and the non-reducing end of a β -1,6 glucan acceptor molecule, thus covalently linking the GPI-protein to the wall. Recently, evidence has amounted for a direct role of the mannosidase

homologs Dcw1p and Dfg5p in cleaving the GPI anchor and mediating transglycosylation of the GPI-protein remnant to wall polysaccharides.

1.3b. Functional roles of GPI-CWPs as structural, biosynthetic and virulent components of the cell wall.

The fungal cell wall accounts for 15-30% of the cell dry weight of the cell of which 1-3% is constituted by GPI-CWPs [23, 67]. Genome-wide *in-silico* studies have identified as many as 70 different GPI-protein encoding genes, of which more than a half encode proteins that localize to the cell wall [80]. Despite the abundant amount of GPI-encoding genes, only 15-20 of them may be expressed at the cell wall at any given time. For example, when cell walls purified from actively growing cells are treated with hot SDS to remove soluble proteins and subjected to hydrolysis with β -1,3 glucanases. Western blotting of the digests with anti- β -1,6 -glucan antibodies, revealed ~ 20 proteins of differing molecular weights [81]. Likewise, mass spectrometric analysis of log-phase SDS-extracted cell walls treated with proteinases, identified peptides from ~20 different putative GPI-cell wall proteins [82]. This was not surprising considering the high level of redundancy in the fungal genome and the dependence of fungal cells on the cell wall proteome to adjust to continuously changing environments outside and within a host. Many studies show that cells vary the composition of their cell wall proteome according to growth conditions, growth stage, nutrient availability and their infectious-state (example, yeast vs hyphal form). Moreover, a number of structural and biosynthetic GPI-proteins are up-regulated in response to cell wall stress or damage [83, 84]. Our recent reviews (Gonzalez et al. 2008, and Gonzalez et al. 2009) provide up to date information on GPI-CWP structure and function.

1.4. The *S. cerevisiae* gene deletion library as a tool for studying GPI-CWP anchorage to the fungal cell wall.

Systematic mutation and subsequent phenotypic analysis of every predicted gene offers the potential to assess all genes for a role in a particular biological process. For *S. cerevisiae*, the availability of a complete genome sequence made possible the construction of a gene deletion library encompassing all ~ 6200 predicted genes in the genome [85]. The library was generated through the combined efforts of research teams around the world, using PCR-based homologous recombination and is now commercially available [86, 87]. Targeted deletion of each gene was achieved using deletion cassettes consisting of the *kanMX4* selection marker flanked by unique 20 bp “barcodes”, dubbed, uptags and downtags. Additional 45 bp oligonucleotides flank the ends of the deletion cassettes and are homologous to the 5’ and 3’ ends of the gene targeted for deletion [86]. The 20 bp barcodes marking the deleted gene serve as strain identifiers that allow simultaneous analysis of large numbers of deletants. For instance, the growth fitness (under various environmental conditions) for all 6200 deletion strains has been simultaneously determined by growing the strains in a single culture, removing small culture aliquots at various times, and isolating genomic DNA for each sample. Isolated DNA was subjected to PCR using 2 pairs of universal primers designed to amplify the 20 bp uptag and downtag sequences of each of the strains present at the start of the experiment. Amplified tags were hybridized to high-density microarray chips bearing complementary sequences for the barcodes. The abundance of each strain was assessed based on the intensity of the hybridization signal; the brighter the signal for a particular strain, the more that strain must be represented in the culture [88]. It then

follows that strains showing weak hybridization signals must be missing a gene that is required for normal growth under a specified condition.

Development of the library led to the identification of ~1105 essential genes which are present as heterozygotes in diploid libraries. The mutant collections can be obtained in either pool or microtiter plate format. The entire viable collection is available in 54 96-well plates in which each well stores a single gene deletant. Diploid heterozygote essentials can be obtained in a single pool that contains all 1105 deletants represented equally at a concentration of 10^7 cells/mL. The strength of this approach relative to conventional methods (genetic footprinting, random mutagenesis) through which genetic saturation is seldom achieved, has been demonstrated by several phenotypic screens of all 5100 viable mutants. Such screens have successfully determined alterations in drug sensitivity [89], defects in cell size and morphology [90], and cell surface function, bud site selection and vacuolar protein sorting [91].

This study describes the development and application of a functional genomics approach to search for genes required for anchorage of GPI-CWPs to the fungal cell wall. 178 gene deletion strains, each missing a gene previously implicated in cell wall biogenesis were transformed with a GPI-CWP reporter gene (GFP-Sag1p) and the transformants screened for deficiencies in anchoring the reporter protein to the cell wall. Of the 178 ORFs, 4 genes: *MCD4*, *GPI13*, *GDA1* and *TDH3* were identified as required for GPI-CWP anchorage to the cell wall based on their ability to hyper-excrete the reporter protein. Additional findings and known functions of these genes are discussed in Chapter 2I. Development and validation of the approach to identify mutants defective in GPI-CWP anchorage to the wall are described in Chapter 2.

Chapter 2

High expression yield and control of expression noise of a GFP-labeled cell wall GPI-CWP in *Saccharomyces cerevisiae*

2.1. Introduction

The use of green fluorescent protein (GFP) to visualize the expression and localization patterns of a protein of interest is common in biological research [92-94]. Unlike alternative reporters (β -galacturonidase, β -glucuronidase, chloramphenicol acetyltransferase, and firefly luciferase), which rely on cofactors or substrates for activity, in vivo observation of GFP expression is possible with individual cells, with cell populations, or in whole organisms in real time by simply illuminating the GFP-expressing organism with UV light /blue light in the presence of molecular oxygen. GFP and chimeric proteins consisting of other protein domains fused to GFP are often successfully expressed in both prokaryotic and eukaryotic organisms. Red-shifted GFPs that can be excited by blue light have lessened the problem of UV-induced toxicity and photobleaching, thus fusions to these GFP are usually well tolerated or non-toxic to the cells [95]. Moreover, protein domains fused to red-shifted GFPs often retain the ability to properly fold and be processed by the cell's machinery, ensuring their cellular activity and expected cellular localization. Visualization and quantification of GFP on cells and tissues is generally accomplished by laser scanning confocal microscopy and conventional epifluorescence microscopy. Data gathered by either method can be analyzed with image analysis software. Spear et al. provide an excellent review on methods for visualizing and quantifying GFP [96]. Reviews detailing GFP applications

are prevalent in the literature and are summarized by Zimmer et al. in a comprehensive review of the chemistry and functional properties of GFP [97]. GFP applications in cell biology and biotechnology are thoroughly reviewed in [98].

GFP is a 238-amino acid, 27-Kda protein which absorbs light at maxima of 395 or 488 nm in the case of GFP enhanced for fluorescence, and emits light at a maximum of 508 nm. GFP variants enhanced for fluorescence harbor amino acid substitutions in the region of the chromophore. These amino acid changes contribute to the protein's stability at higher temperatures, and increase the protein's solubility and resistance to photobleaching [99-101]. Despite its important advantages over alternative reporter genes, common obstacles encountered when using GFP in yeast and other eukaryotic systems include *i*) low signal to noise ratios [102, 103] *ii*) poor yields that require optimization of expression conditions before detectable signal can be obtained [103-106] and *iii*) variation (noise) in signal levels across expectedly comparable or clone samples [107, 108]. The low signal to noise ratios often result from the cumulative effects of interference fluorescence from cellular metabolites and low protein expression yields. Among the substances identified to contribute to background fluorescence are: oxidized flavins and NADH, which have emission maxima that overlap with that of GFP, the amino acids tyrosine, tryptophan and phenylalanine, as well as reduced nicotinamides and the poorly characterized group of chemicals called lipofuscins, all of which emit at a range of 280-490 nm [109]. To improve GFP expression yields in yeast, the proteins are often expressed from strong promoters in multi-copy episomal plasmids. Strong GFP signals can be achieved under these conditions in intracellular compartments and at the cell surface that allow for efficient GFP detection and quantification. The use of a GFP as

a reporter has however remained primarily for tracking events within the cell, and only a few studies describe the use of GFP as a reporter of protein secretion into the growth medium [106, 110]. The scarcity of this type of approach may reflect the difficulties posed by extracellular interference fluorescence and the commonly low yields of soluble protein due to protein aggregation [97] and degradation by extracellular proteases [106]. In a study where a fusion of GFP to the extracellular enzyme, glucoamylase, was expressed in *Aspergillus niger*, the protein could be recovered from culture filtrates only when the cells were grown in medium containing protease inhibitors. Furthermore, concentration of the culture filtrates was required to obtain detectable GFP levels and the signal was observed to decline with culture age, presumably because of cumulative protein degradation [106].

Variability in protein levels (noise) among clonal populations of cells presents a problem when a study depends on reproducibility of phenotype for each clone, relative to a genetically different cell population. However, few studies have been done to identify the source/s of noise in gene expression [108, 111-113]. Interestingly, the consensus findings appear to be that extrinsic factors, most of which are deterministic and therefore possibly controllable, contribute to the majority of noise in gene expression [108, 114]. Extrinsic factors of a deterministic nature result from fluctuating environmental variables, whereas those which are stochastic or unavoidable stem from variations in the elements of the protein transcriptional machinery [112]. Intrinsic sources of variability, on the other hand, are believed to originate from the small number of regulatory molecules (example, gene promoters and transcription factors), that participate in the inherently noisy biochemical reactions leading to gene expression, and may therefore be minimized

by increasing the number of molecules involved in mediating gene expression [112, 115]. Consistent with this prediction is the finding that expression variability is minimal for highly expressed genes or genes under regulation of strong, constitutively active promoters like those of genes essential for cell viability. For instance, when the expression levels of GFP fusions of ten highly expressed *S. cerevisiae* proteins were compared, near-constant level of expression variability was observed among all construct fusions [108]. A different experiment demonstrates the larger contribution of deterministic, experimentally controllable elements, to gene expression variability. Using the native *GALI* promoter from *S. cerevisiae*, and enhanced GFP as a quantifiable marker, five different yeast strains, engineered to differ in the number of GFP copies integrated into the *GALI-10* locus, were assessed for GFP expression upon induction of *GALI* with galactose. Researchers observed increases in expression variability when *GALI* was poorly induced. For example, more noise in GFP signal was observed among clone populations induced with 0.1% galactose than with 2% galactose. Another factor these researchers took into account was the effect of population dynamics in expression noise. A larger than 50% reduction in GFP signal noise was observed when cell populations were made as similar as possible in terms of growth stage and cell size. Mathematical analysis of expression data from this *GALI* system led to the conclusions that each promoter-gene pair transcribes at the same mean rate and that extrinsic sources dominate the observed variations in gene expression [108].

In this study, high expression yields with minimal expression variability among clonal populations of cells was accomplished for a fusion of the carboxyl end of the cell wall GPI-mannoprotein α -agglutinin to GFP to generate, GFP-Sag1p. The protein was

engineered to test the idea that it could be used as a reporter for deficiencies in GPI-CWP anchorage to the cell wall in *S. cerevisiae*. The protein was expressed from the promoter of the *S. cerevisiae* gene, glycerol 3-phosphate dehydrogenase, (*GPD1*) which is constitutively expressed. Cells transformed with the reporter gene were grown to similar cell concentrations under conditions determined to increase GFP yield (1M sorbitol, lower temperature, and non-lethal amounts of the aspartyl protease inhibitor, pepstatin A). When the reporter protein was expressed in *S. cerevisiae* cell-wall mutants previously identified as hyper-excretors of GPI-CWPs, more than wild type levels of excreted GFP could be detected in these mutants in as low as 40 μ l of cell-free supernatant from 3 mL cultures grown to mid-log phase. The specific phenotype was reproducible for each tested strain. Supernatant GFP was visualized by immunoblotting and the signal remained within linear range at volumes of 40-150 μ l. In this study yeast enhanced GFP (yEGFP), Mut3-GFP which contains a serine-to-glycine substitution at amino acid 65 (S65G), and a serine to alanine substitution at amino acid 72 (S72A) and has excitation and emission maxima of 488 and 512 nm, respectively, was fused to the carboxyl of the GPI cell wall protein α -agglutinin encoded by the *SAG1* gene.

The achievable high expression yields and low expression noise among clonal cultures for excreted GFP-Sag1p made possible the scaling-up of assays designed to identify mutants unable to properly anchor the reporter protein to the cell wall. Chapters III and IV describe the development, application and findings of a high-throughput approach for screening the commercially available *S. cerevisiae* gene deletion library for genes required for anchorage of GPI-CWPs to the cell wall.

2.2. Materials and Methods

2.2a. Strains, Media and Reagents

Homozygous and heterozygote diploid deletion strains in the BY4743 background (13), isogenic to the sequenced strain S288c, were used for viable and lethal deletions, respectively. All of the yeast strains were constructed during the EUROFAN project and obtained from the *Invitrogen* collection. Yeast was grown in either YPD medium (1% yeast extract, 2% peptone, 2% glucose) or defined medium (0.2% yeast nitrogen base without amino acids, 0.5% ammonium sulfate, 2% glucose, and 0.08% complete synthetic media (CSM) lacking uracyl), containing 1 M sorbitol and buffered to pH 6.5 with 50 mM MOPS, supplemented with 200 μ M geneticin (Sigma Co.). For growth in the presence of pepstatin A, 1 mM pepstatin A stock solutions were prepared in methanol and stored at -20 $^{\circ}$ C for no more than 9.0 months. 1 μ M pepstatin A concentrations were used during cell growth. *Escherichia coli* strains DH5 α and XL10-Gold (Stratagene) were used as hosts for recombinant DNA manipulation. *E. coli* were grown in LB medium (1% tryptone, 0.5% yeast extract, 0.5% sodium chloride, 0.1% glucose, 0.01% ampicillin). Methylene blue stain was obtained from Sigma Chemical Co.

2.2b. Construction of reporter plasmid, pGFP-Sag1p and yeast transformation

Plasmid pGFP-Sag1p was constructed as follows: An EcoRI-BglIII fragment of the yeast enhanced GFP (yEGFP) gene from *Aequorea victoria* was prepared by PCR using pMut3-yEGFP as the PCR template (pMut3 was provided by Dr. T. Hughes, Yale Univ. USA). A BglIII-XhoI fragment encoding the last 300 residues at the C-terminus of the cell wall glycoprotein α -agglutinin was similarly prepared using pH27 as the PCR template [116]. A SpeI-EcoRI fragment encoding the invertase secretion signal and

cleavage site was synthesized using overlapping oligomers of 51 and 53 base pairs each. Extension of the non-overlapping regions was achieved using DNA polymerase I Large Fragment (Klenow) (New England BioLabs). Table 2.1 lists all the oligonucleotides used in this work. Each fragment was subjected to restriction digestion with the indicated enzymes. Restriction fragments were subjected to agarose gel electrophoresis and recovered from the gel using *QIAquick Gel Extraction Kits (Fisher Scientific)*. A four-fold ligation reaction involving all 3 restriction fragments described above and vector p416GPD1 (ATCC, Manassas, VA, USA) bearing SpeI-Xho1 sticky ends was performed using T4 DNA Ligase (New England BioLabs). Constructs were verified by restriction analysis in 1.0% agarose gels and sequenced to exclude possible PCR artifacts. No mutations were found that would affect the amino acid sequence of the fusion constructs. The resulting plasmids were propagated in and purified from *E. coli* using a *Qiagen* plasmid purification kit according to the instructions of the manufacturer. The plasmids were transformed into yeast strains by the lithium acetate method¹⁰.

2.2c. Fluorescence Microscopy

Yeast strains transformed with pGFP-Sag1p plasmid and control samples transformed with plasmid lacking the reporter gene were grown in CSM-URA medium at pH 6.5 at 18 °C to an OD₆₆₀ between 0.4-0.6. A fluorescence microscope (Olympus ??) was used to visualize GFP with a fluorescein isothiocyanate (FITC) filter (excitation at 470 nm, emission at 530 nm) and a 60X immersion objective with a numerical aperture of 1.2. Prior to observing for cell-surface fluorescence, cell samples were washed two times in distilled water and incubated in 10 mM Tris-HCL, pH 7.5 for 2 hours to promote

maximal GFP folding. For visualization of cell-surface fluorescence of cell-wall mutants, 1 M sorbitol was added to the Tris buffer to prevent cell bursting.

2.2d. Cell wall extraction

For cell wall purifications, 50 mL of a cell suspension at 10^8 cell/mL was washed 3 times in Tris-PMSF buffer (10 mM Tris-HCL, 1 mM PMSF pH 7.8) at 4 °C. After washing, the cells were resuspended in the same buffer (Tris-PMSF) containing glass beads (diameter 0.45 mm) at a ratio of 1:1:1 (cell:buffer:glass beads, v/v/v). The cells were then homogenized by vortexing 10 times (each 1 min) with 1 min cooling intervals on iced water. The cell lysate was separated from the beads by repeated washings with 1 M NaCl (pH 7.5). The lysate was centrifuged at 3000x g for 10 minutes. The cell wall fraction recovered as insoluble material after centrifugation was washed twice with 1M NaCl. This fraction was then treated with 1% SDS for 20 minutes at room temperature, rather than with heat, to prevent denaturation of the GFP protein. The surfactants were removed by repeated washings with 1 M NaCl followed by 3 washings with Tris-PMSF buffer (10 min each). The cell wall fractions were stored in 1 mM PMSF (pH 7.5) at 0.1g cell wall/mL at -20 °C if not immediately analyzed for fluorescence by fluorescence microscopy. Cell wall fractions from control cells not expressing GFP-Sag1p were similarly prepared.

2.2e. Immunoelectron microscopy

To confirm cross-linking of the GFP-Sag1p to cell wall polysaccharides, immunoelectron micrographs were prepared from wild-type cells as follows: cells were grown to mid-log phase, washed twice with 1% SDS and twice with 50 mM Tris-

chloride, pH 7.5. Following, a 3-4 mm cell pellet was incubated overnight in 30 mL of a 1:500 monoclonal mouse anti-GFP solution. The cells were then washed 3 times for 10 minutes in 1X PBS, 0.5 % twin 20 and incubated overnight in 1:2000 gold-labeled Goat anti-mouse antibody. Following antibody labeling, the cells were fixed in 5% formaldehyde and brought to Dr. Ron Gordon's lab in Mount Sinai Medical School for preparation of the electron micrographs.

2.2f. Dot blotting

Yeast supernatants were recovered by high-speed centrifugation that ensured removal of all yeast prior to dot blotting. Supernatants were applied to nitrocellulose membranes using a 96-well BioRad dot blotter/protein concentrator as recommended by the manufacturer. Supernatants from cultures grown to mid-log phase (OD_{660} 0.5-0.6) were applied to individual wells in 100 microliter volumes. Membranes were allowed to dry overnight and assayed for GFP levels using mouse anti-GFP and HRP-labeled goat anti-mouse as follows: incubate membrane in blocking buffer (1X PBS, 2% BSA, 0.5% tween-20) for 2 hours at room temperature or at 4 °C overnight, with mild shaking. Incubate in primary antibody (mouse anti-GFP, prepared in blocking buffer at 1:500 dilution) for 1 hour at room temperature or 4 °C overnight. Wash in 1X PBS, 0.5% tween-20, 1X for 5 minutes, 1X for 20 minutes and 3X for 10 minutes each. Incubate in secondary antibody (HRP-labeled goat anti-mouse at a 1:2000 dilution). Repeat washing as above and develop for chemiluminescence using PIERCE-ECL western blotting substrate. Working solutions of the substrates were prepared as recommended by the manufacturer and added to the blots for 1 minute. The membranes were removed from

the substrates and placed in plastic sheet protectors. Each membrane was exposed to CL-XPposure Film for periods of 30 seconds to 5 minutes.

2.2g. Methylene blue exclusion assay for estimating effect of pepstatin A on cell viability

Six 3 mL cultures of wild-type cells were grown at 18 °C in CSM-URA, 1 M sorbitol (pH 6.5) to early log phase (OD₆₆₀ 0.2-0.3). Three of the cultures were supplemented with 3 µl of a 1 mM stock solution of pepstatin A prepared in methanol, to give a final concentration of 1 µM. The other 3 cultures were supplemented with 3 µl of methanol only. The cultures were put back to grow with shaking at 200 rpm and cell samples collected immediately after addition of pepstatin A (time=0 hrs), and two more times at 6 hrs and 2 hrs. For each culture sample collected, percent cell death was determined by methylene blue staining, as follows: the medium was centrifuged at 10000 g for 5 min, and the yeast pellets re-suspended in a pH 7.2 phosphate buffer saline solution (PBS; 0.13 M NaCl in 10 mM Na₂HPO₄). The methylene blue solution, which contained 0.01% Methylene Blue and 2% (w/v) sodium citrate dihydrate in PBS, was mixed with an equal volume of yeast solution for 10 min. The stained cells in the mixture were quantified using a light microscope and a hemocytometer. For each of the six cultures, a total of 1000 cells were counted three times for each time point collected. Percentage cell death was estimated by taking the ratio of stained (blue) cells over total number of cells counted and multiplying by 100. Average percent death for each time point was calculated from percent cell death averages from three independent clone cultures. The latter values were plotted with their corresponding standard errors.

2.3. Results

2.3a. Construction of the cell wall GPI reporter protein GFP-Sag1p

A reporter cell wall GPI-mannoprotein was engineered to test the hypothesis that mutants defective in GPI-mannoprotein anchorage to cell wall can be identified based on their ability to hypo or hyper-excrete the reporter protein relative to wild type levels. The reporter construct was created by fusing a fungi-optimized GFP cDNA upstream of the last 900 base pairs of the *S. cerevisiae SAG1* cDNA. *SAG1* encodes the cell wall GPI-mannoprotein α -agglutinin. The signal sequence and cleavage site of the cell surface enzyme, invertase, was generated using overlapping oligomers and inserted upstream of the GFP cDNA. The resulting recombinant gene was inserted in front of the *GPD1* promoter in *CEN* plasmid p416*GPD1*. The authenticity of the construct was confirmed by DNA restriction analysis as shown in figure 2.1B and by sequencing. The arrangement of individual components of the reporter gene is shown in figure 2.1A.

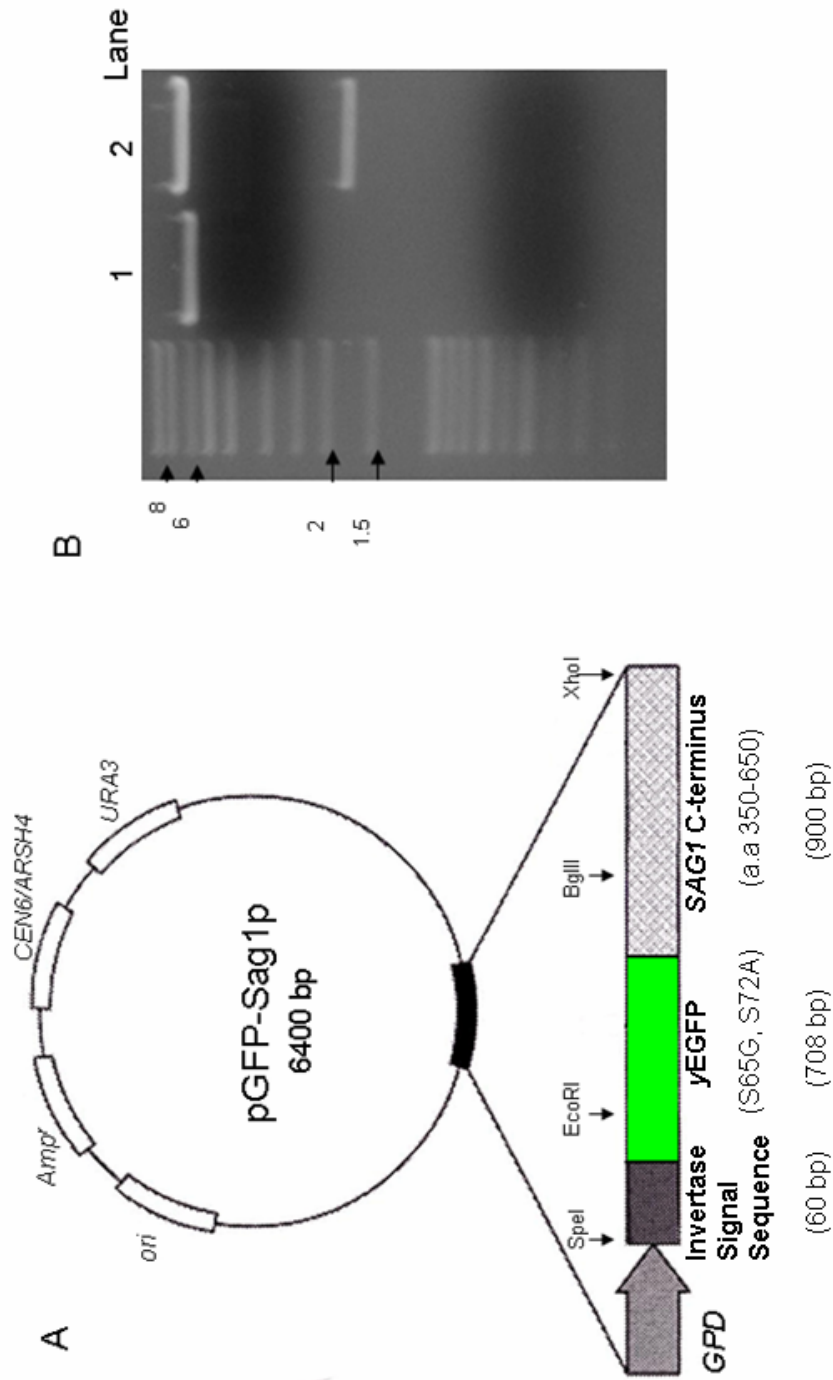


Figure 2.1. Schematic of pGFP-Sag1p reporter construct (A) and restriction analysis of empty plasmid (lane 1) and pGFP-Sag1p (lane 2) with SpeI and XhoI (B). Expected product sizes: 6.4 kb (lane 1) and 6.4 and 1.7 kb (lane 2).

Table 2.1. Oligonucleotides used for the construction of GFP-Sag1p.

Primer	Length	Sequence (5'--3')	Remarks
InvP1	51	<u>GCGCCGACTAGTATGCTTTTGCAAGCTTTCCTTTTCCTTTTGGC</u> <u>TGGTTT</u>	Underlined SpeI and overlapping region
InvP2	53	<u>CGCCGGGAATTCATGCTGATATTTAGCTGCAAAACCAGCC</u> <u>AAAAGGAAA</u>	Underlined ECORI and overlapping region
GFPP1	30	<u>GCGCCGGAATTCAGTAAAGGAGAAGAACTT</u>	Forward Primer, Underlined ECORI
GFPP2	30	<u>CGCCGCAGATCTGTATAGTTCATCCATGCC</u>	Reverse Primer, Underlined BglII
α -aggGPIP1*	30	<u>GCGCCGAGATCTAGTGCGTATTCACACTGGA</u>	Forward Primer, Underlined BglII
α -aggGPIP2	30	<u>CGCCGCCCTCGAGTTA</u> <u>GAA</u> <u>TAGCAGGTACGA</u>	Reverse Primer, Underlined XhoI and stop codon

2.3b. Fluorescence and immunoelectron microscopy show expression and localization of GFP-Sag1p to the cell wall

Cells transformed with the reporter construct were assayed for GFP expression by fluorescence microscopy. Because irreversible damage to the GFP fluorophore occurs at pH levels below 3.0 and *S. cerevisiae* cultures can quickly reach pH levels below 3 due to acidifying waste products, cells were grown in media buffered to pH 6.5 with 50 mM MOPS and titrating to desired pH with Tris-base. Visualization of GFP fluorescence at the cell surface confirmed that the reporter protein was successfully expressed and processed as a cell surface protein (Figure 2.2 A and B). As a negative control, cells were independently transformed with vector lacking the reporter gene. These cells did not show cell-surface fluorescence (Figure 2.2C). Cell-surface fluorescence was significantly less prominent in cells grown in unbuffered media (data not shown).

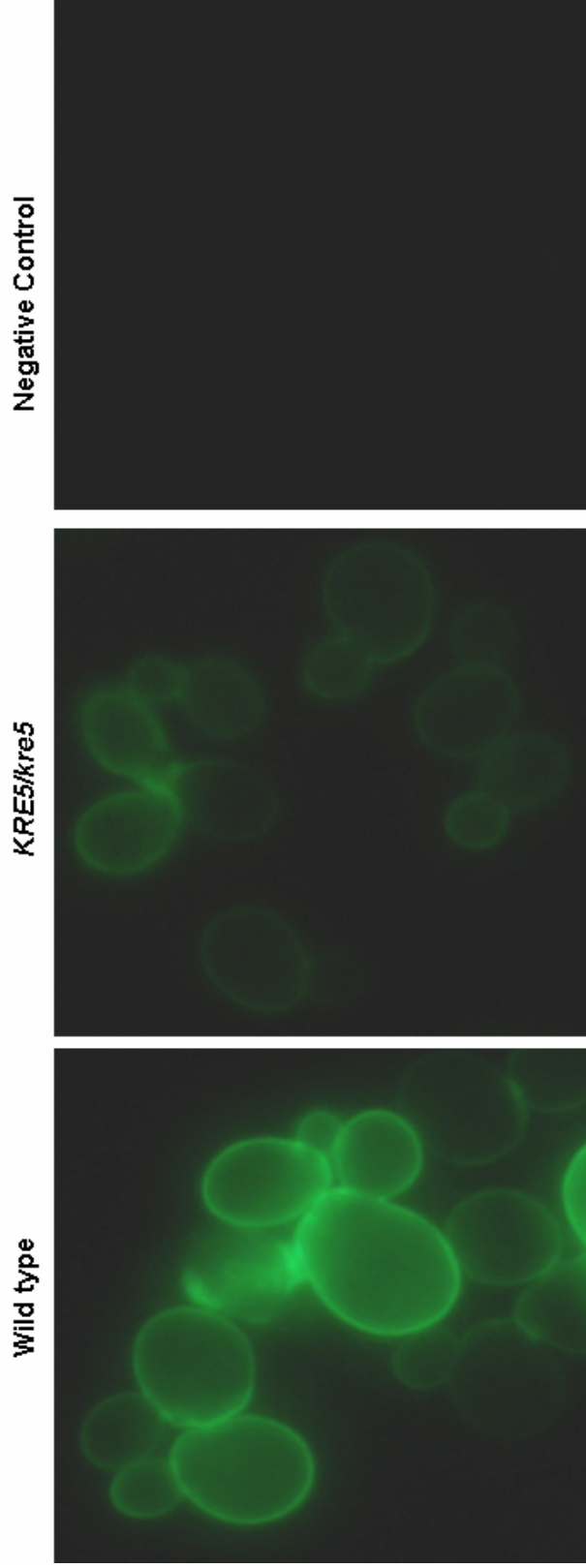


Figure 2.2. Visualization of cell surface fluorescence by fluorescence microscopy reveals significantly less GFP-Sag1p in KRE5/kre5 cells than in wild type cells . Cells were grown to early log phase (OD₆₆₀ 0.3-0.4) at 18 °C in CSM-URA containing 1 M sorbitol and buffered to pH 6.5 with 50mM MOPS. Cells were harvested , washed with dh20 and re-suspended in 10 mM Tris-HCL pH 7.5 prior to fluorescence analysis. Images were captured at exposure times of 1/2 of a second. Controls cells are wild type cells transformed with empty plasmid.

Fluorescence microscopy indicated expression of the reporter protein at the cell surface but was not sufficient to prove cell wall localization. To establish cell wall localization, cell walls were purified following a procedure that would remove soluble protein from the wall without disrupting GFP fluorescence [66]. Cell walls were also purified from cells transformed with empty plasmid. Figure 2.3C shows that isolated cell walls purified in this manner retain GFP suggesting that the protein localizes to the cell wall and is not present as a soluble protein.

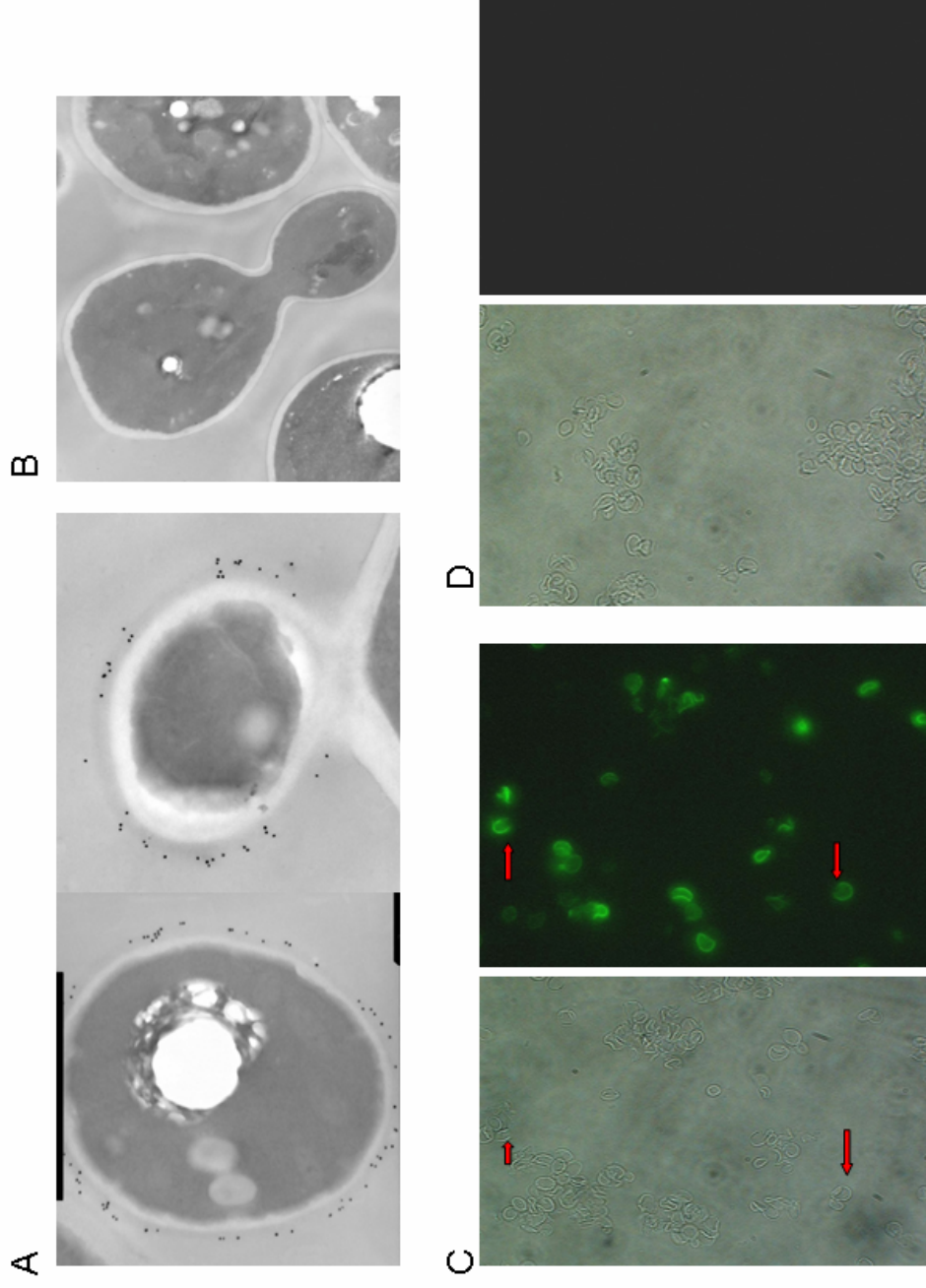


Figure 2.3. Immunoelectron and fluorescence microscopy show localization of GFP-Sag1p to the cell wall in wild type cells. A) Immunoelectron micrographs of wild type cells expressing GFP-Sag1p labeled with mouse monoclonal anti-GFP as primary antibody and gold labeled goat anti-mouse as secondary antibody. B) Control wild type cells expressing GFP-Sag1p not labeled with anti-GFP and incubated with gold-labeled secondary antibody. C) Cell wall extracts from wild type cells expressing GFP-Sag1p and treated to remove soluble protein remained fluorescent. D) Control cell wall extracts from wild type cells not expressing GFP-Sag1p.

Cell walls from cells transformed with empty plasmid did not show any fluorescence (Figure 2.3D). Covalent attachment of the GFP-fusion protein to cell-wall glucan was further confirmed by immunoelectron microscopy. Figures 2.3A and 2.3B show electron micrographs of wild-type cells expressing GFP-Sag1p and of wild-type cells not expressing the fusion protein, respectively. For preparation of electron micrographs, intact cells were labeled with monoclonal mouse anti-GFP antibodies as the primary antibody and gold-labeled goat anti-mouse as the secondary antibody as described in Materials and Methods.

2.3c. 1M sorbitol and 1 μ M pepstatin A increase yields of excreted GFP-Sag1p.

The cell-wall mutants, *cwp1/cwp1*, *kre1/kre1* and *KRE5/kre5*, previously shown to hyper-excrete GPI-CWPs were transformed with the reporter construct (pGFP-Sag1p) and assayed for GFP levels in cell-free supernatants relative to wild-type cells. 20 mL cultures of GFP-Sag1p-expressing cells were grown (in duplicate) to log phase at 30 °C in defined media lacking uracil for selection of the transforming plasmid. An identical set of duplicate cultures were similarly grown with the exception that 1 M sorbitol was added to the growth medium to provide osmotic support. Following growth to mid-log phase (OD₆₆₀ 0.5-0.6), 200 μ l of cell-free supernatants were assayed for GFP levels by dot blotting. Surprisingly, GFP could be detected in supernatants from cultures grown in the presence of 1 M sorbitol and not in those from cultures grown without sorbitol (Figure 2.4A). Furthermore, in contrast to expectations, more GFP was detected in supernatants from wild-type cells than in supernatants from *cwp1/cwp1* and *kre1/kre1* cells (Figure 2.4 A).

The lower levels of excreted GFP in *cwp1/cwp1* and *kre1/kre1* is likely due to GFP degradation by secreted extracellular proteases since when the cells were grown in the presence of the aspartyl protease inhibitor, pepstatin A, significantly more GFP is found in the supernatants from *cwp1/cwp1* and *kre1/kre1* cells than in those from wild-type cells (Figure 2.5). At the concentration used of 1 μ M, pepstatin A did not affect growth rate (Figure 2.7A) or lead to losses in cell viability (Figure 2.7B) in wild-type cells. These observations were further confirmed in the cell-wall mutants *dcw1/dcw1* and *dfg5/dfg5* (Chapter 1V).

As expected for *KRE5/kre5* cells, more GFP was detected in cell-free supernatants from these cells than in those from wild type (Figure 2.4B). *KRE5/kre5* cells have been previously shown to excrete more than wild type levels of GPI-CWPs into the growth medium presumably because of diminished levels of β -1,6 glucan at the wall, which acts as anchoring sites for the proteins [50, 52]. For this experiment, 3 mL cultures of wild type and *KRE5/kre5* cells were grown in triplicates to mid-log phase, in sorbitol-containing media. The cells were pelleted and 100 μ l of cultures supernatant assayed for GFP-Sag1 levels by immunoblotting. Figure 2.4B shows that under these growth conditions, GFP signal is detectable and consistent among clonal cultures grown from independent transformants of these strain with the reporter plasmid, pGFP-Sag1p. Furthermore, in wild-type cells, GFP signal could be detected in dot blots from 80 μ l of cell-free supernatant from 3 mL cultures and the signal increased with increasing volume in the range of 40 to 140 microliters (Figure 2.4D). Based on these results, 100 microliters was chosen as the volume to use in subsequent blotting experiments for all

tested strains. *KRE5/kre5* cells also show significantly less cell-surface fluorescence than wild-type cells (Figure 2.2B)

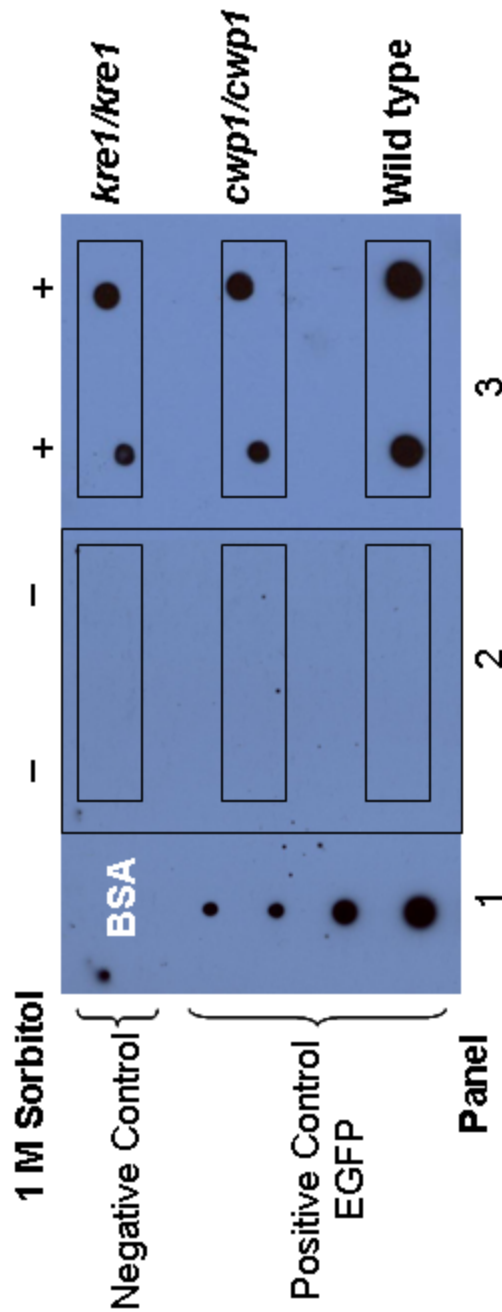


Figure 2.4 A. Growth in the presence of 1 M sorbitol increases GFP-Sag1p expression yields. Panel 1. negative control (1 μ g BSA) and positive control (pure GFP (Clontech) at 1, 2, 4 and 8 ng from top to bottom. **Panel 2.** Duplicate subclone cultures of the cell wall mutants *kre1/kre1* and *cwp1/cwp1* and the corresponding parental strain were grown to late-log phase in CSM-URA at 30 °C and 200 μ l of their cell-free supernatant applied to nitrocellulose membranes using a BioRad dot blotter/protein concentrator. **Panel 3.** An identical set of duplicate cultures were grown as in panel 2, with the exception that 1 M sorbitol was added to the medium. Dot blots were probed with mouse monoclonal anti-GFP and HRP-labeled goat anti-mouse. Subclone cultures are boxed.

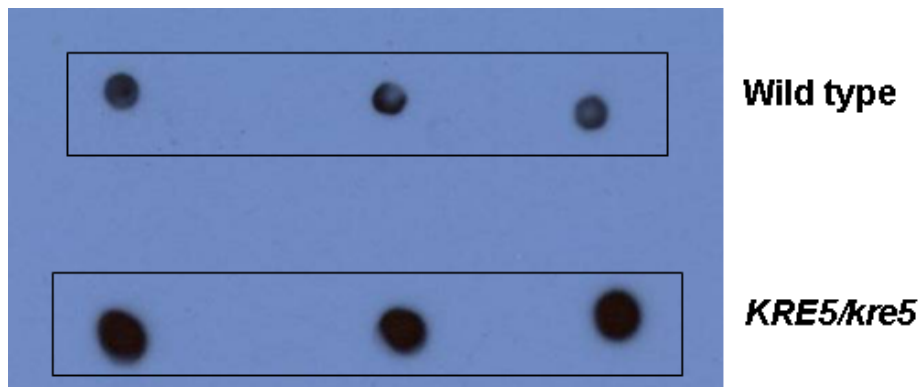


Figure 2.A B . Immunoblot analysis shows hyper-excretion of GFP-Sag1p in *KRE5/kre5* cells relative to wild type cells. Clonal cultures were grown in triplicates to late-log phase at 30 °C in CSM-URA containing 1 M sorbitol, without pepstatin A, and 100 μ l of cell-free supernatants assayed for GFP levels using mouse anti-GFP as primary antibody and HRP-labeled goat anti-mouse.

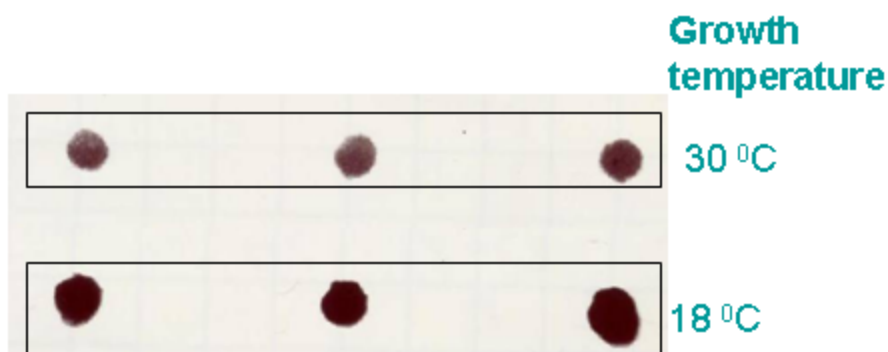


Figure 2.AC. Growth at lower temperature increases GFP-Sag1p yields. Clonal cultures of wild type cells were grown in triplicate to mid-log phase in CSM-URA containing 1M sorbitol and without pepstatin A at 18 °C and 30 °C. 100 μ l of their corresponding cell-free supernatants were assayed for GFP levels by immunoblotting.

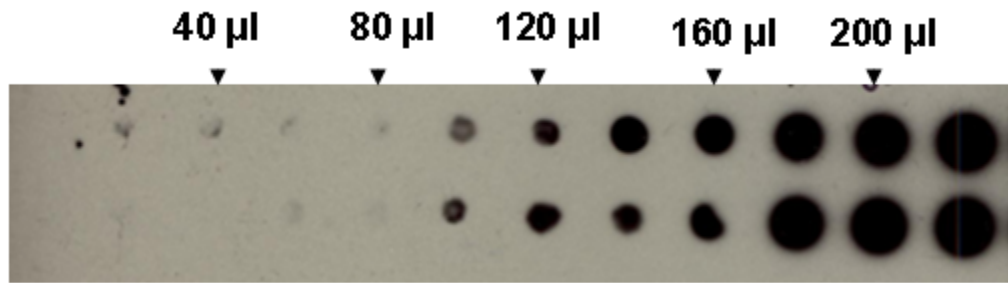


Figure 2.4D. Determination of linear range for GFP-Sag1p excretion from wild type cells by dot blot immunnoanalysis. Duplicate subclone cultures were grown to mid-log phase at 18 °C in CSM-URA containing 1 M sorbitol. Supernatant volumes of 20-220 µl were blotted to nitrocellulose using a *BioRad* dot blotter/protein concentrator.

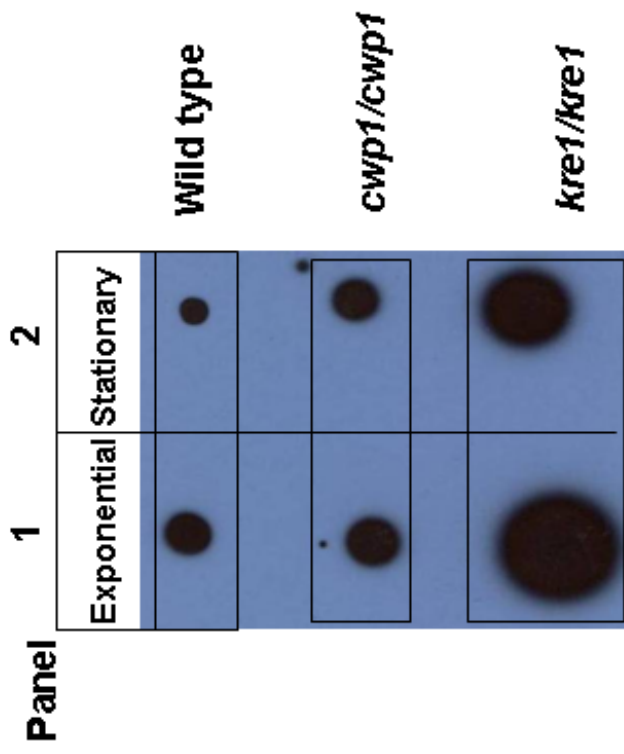


Figure 2.5. Growth in the presence of pepstatin A increases GFP-Sag1p yields. Cultures were grown in CSM-URA, 1 M sorbitol at 18 °C prior to adding pepstatin A to 1 μM. Cultures were allowed to continue to grow to mid-log phase (panel 1) and stationary phase (Panel 2). 100 μl of cell-free supernatants were assayed for GFP-levels by immunoblotting. The expected GPI-CWP hyper-excretion phenotype for *cwp1/cwp1* and *kre1/kre1* cells, relative to wild type cells, is observed when the cells are grown under these conditions. In the absence of pepstatin A, *cwp1/cwp1* and *kre1/kre1* cells are hypo-excretors of GFP-Sag1p (figure 2.4 A).

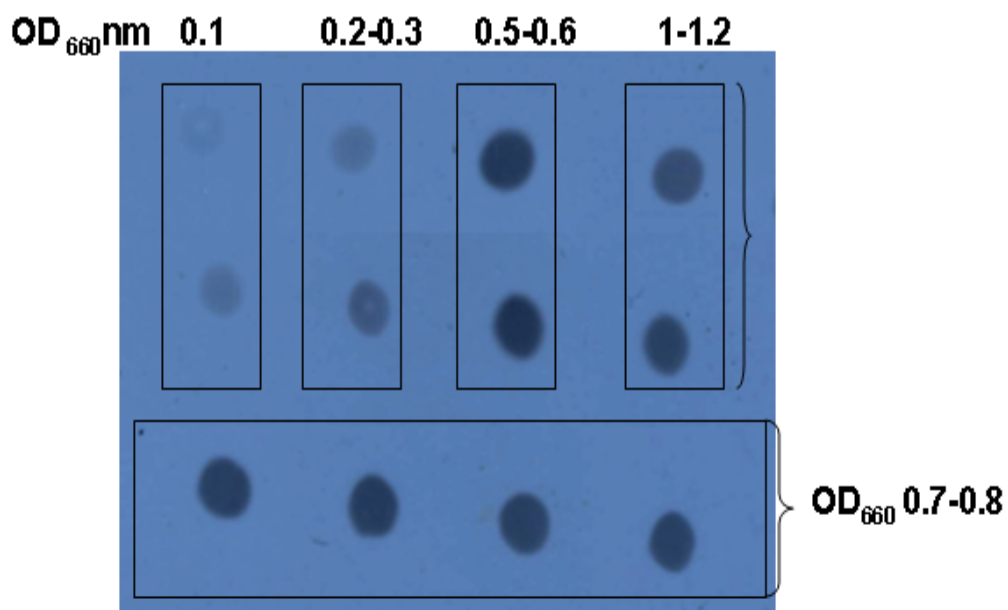


Figure 2.6. Subclone cultures grown to similar cell concentrations excrete similar amounts of GFP-Sag1p. Wild type cells were grown as 3 ml cultures in CSM-URA containing 1 M sorbitol, to specified ODs. All cultures were grown at 18 °C. GFP was detected by immunoblotting. Subclone cultures are boxed.

2.3d. Growth at lower temperature further increases yields of excreted GFP-Sag1p

To test the effect of growth temperature on GFP-Sag1p yields, separate sets of 3 mL cultures were grown at 18 °C and 30 °C to mid log (OD₆₆₀ 0.5-0.6). The cultures were grown in triplicate in 13x100 borosilicate test tubes. Following, 100 µl samples of culture supernatant were assayed for GFP levels by immunoblotting. As can be observed from figure 2.4 C, similar GFP levels were observed among clone cultures at each growth temperature used. Significantly more GFP was detected in supernatants from cultures

grown at 18 °C. Due to the elevated expression levels at 18 °C, this temperature was used in subsequent GFP-Sag1p expression experiments.

2.3e. Expression variability/noise of excreted GFP-Sag1p is minimal among clonal cultures grown to similar cell concentrations.

An experiment was done to determine the level of noise in expression of secreted GFP-Sag1p. Wild type cultures were grown in duplicate and the level of GFP released into the growth medium determined by immunoblotting at various culturing times. The cultures were grown at 18 °C as 3 mL cultures in sorbitol-containing medium, and samples were collected at approximate optical density values of 0.15, 0.3, 0.6 and 1.2 at 660 nm (O.D₆₆₀). When grown under these conditions, cultures do not reach O.D values beyond 1.2 and the transition to stationary phase lies between O.D values of 0.8-1.2. To assay for GFP levels at the various growth stages, 200 microliters of culture would be removed from the 3 mL cultures and centrifuged at high speed to remove the cells. Supernatant were then transferred to silicon-coated microcentrifuge tubes and stored at -80 °C in the presence of protease inhibitor cocktail to inhibit extracellular proteolytic activity. Remaining cultures were put back to grow and sample collection continued for the rest of O.D values, as just described, until all desired samples were collected. The supernatants were then removed from the -80 °C freezer and allowed to thaw in ice for immunoblotting. As can be observed from figure 2.6, GFP excretion peaked at O.D values of close to 0.6 and diminished thereafter, whereas the signal was barely detectable at earlier cell concentrations. Importantly, the amount of excreted GFP seems consistent among cultures grown to similar cell concentrations and differs greatly among cultures at different cell concentrations.

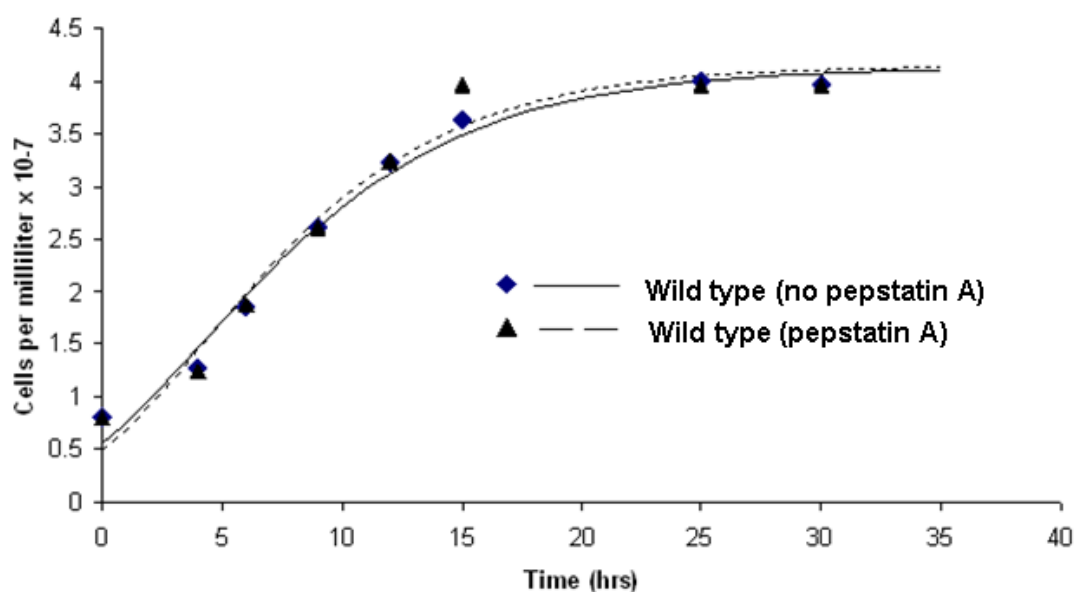


Fig. 2.7A. *Pepstatin A does not affect growth rate.* Wild type cells were grown to early log (OD_{660} 0.2) at 18 °C in CSM-URA, 1 M sorbitol and added 1 μ M pepstatin A (▲) and solvent alone (◆). OD_{660} measurements were taken at t=0 (immediately after addition of pepstatin A) and t=4, t=6, t=9, t=12, t=15, t=25 and t=30 hours after addition of pepstatin A.

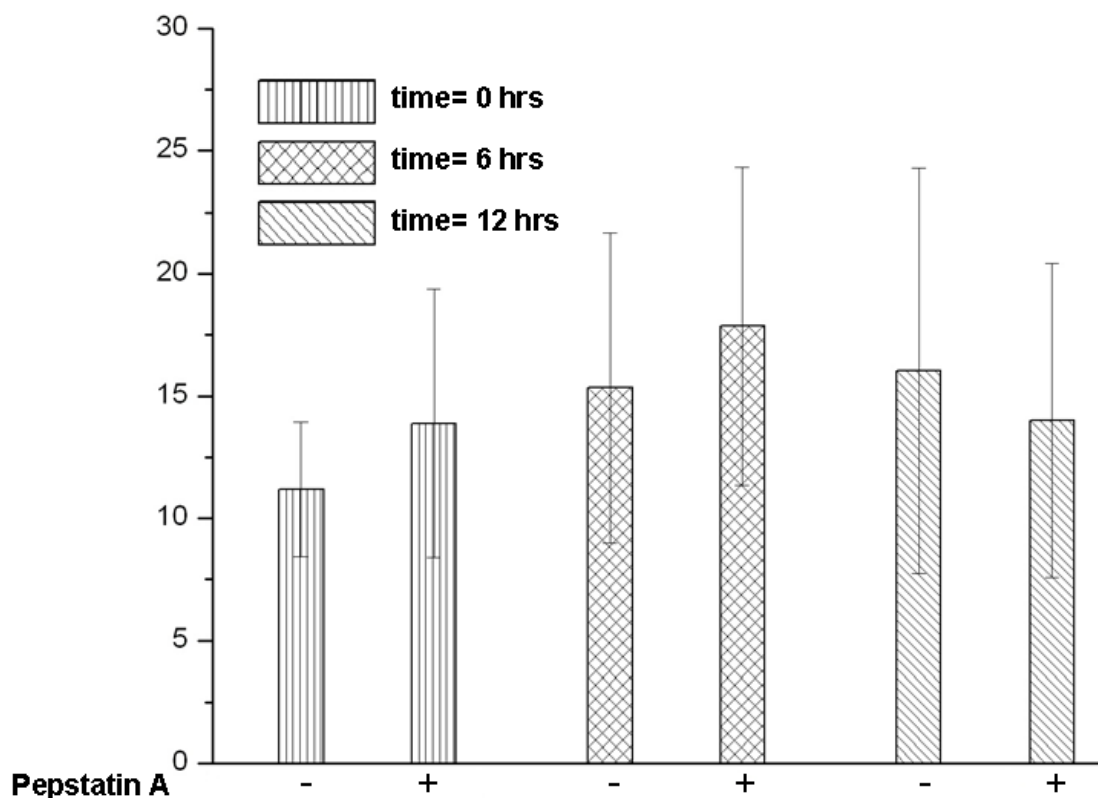


Figure 2.7B. *Pepstatin A* does not significantly affect cell viability. Percent cell death for wild type cells was determined by the methylene blue exclusion assay. Cells were grown to early log (OD_{680} 0.2) at 18 °C in CSM-URA, 1 M sorbitol and added 1 μ M pepstatin A (+) and solvent (-). Cell samples for staining with methylene blue were collected at 0 hrs, 6 hrs and 12 hrs after addition of pepstatin A.

2.4. Discussion and Conclusions

2.4a. The effect of pepstatin A in increasing GFP-Sag1p yields.

To screen for deficiencies in GPI-CWP anchorage to the cell wall, a reporter GPI-protein was built by fusing GFP to the carboxyl end of the GPI-mannoprotein adhesin, α -agglutinin. The reporter protein was expressed in yeast cells to confirm processing and cell wall localization. Fluorescence microscopy, preparation of cell extracts devoid of

soluble protein, and immunoelectron microscopy of cells expressing the reporter protein confirmed proper folding and localization of the reporter protein to the cell wall. The reporter protein was also expressed in the cell-wall mutants *cwp1/cwp1* and *kre1/kre1*. These mutants have been shown in previous studies to excrete more than wild type levels of the GPI-CWPs Cwp2p [117, 118] and Sag1p and were thus chosen as positive controls for deficiencies in cell wall anchorage of GPI-CWPs. Surprisingly, it was necessary to grow these mutants in the presence of non-lethal amounts of the aspartyl protease inhibitor, pepstatin A to see the expected hyper-excretion phenotype. A possible reason for this is that without the addition of Pepstatin A, proteolytic activity in the medium leads to destruction of GFP. The inhibitors are apparently not necessary for detection of excreted Cwp2p. Unlike GFP, Cwp2p has many glycan side chains that limit the access of proteases to the peptide chain and thus protect it from degradation [119, 120]. However, it was possible to detect GFP-Sag1p hyper-excretion from a different cell wall mutant without a need for adding pepstatin A. This cell wall mutant harbors a *KRE5/kre5* deletion, has reduced levels of β -1,6 glucan at the wall and has been previously shown to excrete more the wild type levels of the GPI-CWP, Cwp2p [118, 121]. Since β -1,6 glucan chains act as acceptor molecules for GPI-mannoproteins, their shortage at the wall leads to secretion of GPI-proteins unable to find cross-linking sites. In this mutant, the extent to which the reporter protein is hyper-excreted is apparently large enough to permit detection of the hyper-excretion phenotype even on the face of GFP proteolysis.

In *S. cerevisiae* and *Candida spp*, a class of aspartyl proteases known as yapsins have been found to reside at the plasma membrane and anchored to the wall via trimmed GPI-anchors [122, 123]. Evidence exists for a possible yapsin activity as “sheddas” of

GPI-CWPs to promote GPI-CWP turn-over at the wall [122, 124, 125]. Since yapsins are GPI-CWPs themselves, their activity at the wall would presumably cause their own cleavage from the cell surface into the growth media. Growth in the presence of pepstatin A may act to enhance the sensitivity of GFP-Sag1p as a reporter by preventing shedding of aspartyl proteases from the wall and thus lowering proteolytic activity in the media and by inhibiting aspartyl proteases in the medium. This effect of pepstatin A would help explain our observation that in some cell-wall mutants known to hyper-excrete GPI-CWPs, GFP-Sag1p hyper-excretion is detectable only in the presence of the inhibitor. It would also help explain why less GFP-Sag1p is excreted from wild-type cells grown in the presence of pepstatin A than without, since only but a small fraction of GFP-Sag1p is expected to be excreted from wild-type cells. Inhibition of GPI-CWPs shedding from the wall should further decrease the number of GFP-Sag1p molecules released from the wall in wild-type cells.

2.4b. 1 M sorbitol improves soluble GFP-Sag1p expression yields by promoting protein folding and enhancing expression from the GPD1 promoter

All cultures were grown in the presence of 1 M sorbitol to provide osmotic support for cells with weakened cell walls. Studies show that osmotically stable media minimizes cell lysis due to cell wall damage and may even remediate cell wall defects [126, 127]. Surprisingly, significantly higher yields of soluble excreted GFP-Sag1p were observed in supernatants from cells grown in the presence of 1 M sorbitol than in those from cells grown without sorbitol. This effect may be attributable to observations that in *S. cerevisiae*, high osmolarity in the surrounding medium leads to activation of the HOG (high osmolarity glycerol) pathway, which in turn up-regulates expression of genes

involved in glycerol biosynthesis and genes encoding heat shock proteins [128-131]. For instance, a study shows that increased salinity in the growth medium leads to a 30-40% increase in the specific activity of glycerol-3-phosphate dehydrogenase which in conjunction with a phosphatase catalyzes the production of cytoplasmic glycerol [132]. A different study shows close to eightfold increase in the specific activity of this enzyme in *gpd1Δ* cells transformed with an episomal plasmid encoding a healthy copy of the *GPD1* gene. The increase in enzyme activity was observed after exposing the cells to 1.8 M sucrose for 4 hours [133].

Glycerol has been shown to act as a protein folding aid by contributing to protein solubility and inhibiting the formation of protein aggregates that can hinder protein folding and lead to significant losses in protein yield [134, 135]. As mentioned above, 1 M sorbitol, through activation of the HOG pathway, can also induce expression of heat shock proteins which can further help in stabilizing proteins by assisting in their proper folding. 1 M sorbitol would therefore enhance soluble GFP-Sag1p yields by *i*) increasing transcription from the *GPD1* promoter *ii*) increasing protein solubility through the action of glycerol (soluble protein molecules are more likely to be properly folded and processed by the cell) and by *iii*) further enhancing protein folding through the action of chaperones. In a study, GFP was found to associate with molecular chaperones in *E. coli* [136] while different GFP folding rates observed in mammalian and bacterial cells imply differential associations with the protein folding machinery in these organisms [137]. It is therefore conceivable that manipulation of the yeast cell folding environment also has the potential to elevate GFP and GFP-protein fusion expression yields.

2.4c. Temperature dependence of GFP-Sag1p secretion

The secretion level of GFP-Sag1p was highest at the lowest growth temperature tested (18 °C). This dependence could be due to the intrinsic characteristics of the GFP protein given that GFP originates from the cold water *Aequorea victoria* jellyfish species [97]. Similar temperature dependence results were found for cytoplasmic GFP expression in *S. cerevisiae* [138] and mammalian cells [139]. Since GFP has exposed hydrophobic patches on its surface that can promote dimerization [97], it is possible that lower temperature enhances excretion yields by diminishing aggregation effects. Similar temperature dependency has been observed for aggregation-prone single-chain antibodies [140] and T-cell receptors [141] as well as for excreted GPI-less α -agglutinin (our lab, unpublished results). At higher growth temperatures, the aggregation effect may also contribute to loss of promoter robustness by saturating the cell's protein quality control apparatus to create an overall decline in protein expression yields.

Because cross-linking of GPI-CWPs to the cell wall is shared across various fungi including those capable of infecting animals and plants, the GFP-reporting system described here can be extended to these organisms as well. Since previous attempts to screen for deficiencies in GPI-CWP anchorage to the wall have depended on the use of non-commercially available antibodies which are difficult to have access to at the quantities required for large-scale studies, an additional value to the use of GFP as a reporter is that both GFP and GFP-antisera are commercially available.

Chapter 3

Large-scale screening for new yeast mutants affected in anchorage of GPI-mannoproteins to the cell wall

3.1. Introduction

The cell walls of fungi are rich in glycoproteins essential for cell wall formation and function. Of the glycoprotein subfamilies that reside at the wall, those anchored to cell wall polysaccharides through trimmed GPI anchors (GPI-CWPs) are the most abundant. GPI-CWPs serve as structural and biosynthetic components of the wall, in addition to providing the cell with its adhesive properties. In pathogenic fungi such as *Candida spp*, GPI-CWPs play an essential role in pathogenesis by mediating adhesion of the fungal cell to its host which is a prerequisite for the initiation and establishment of infection. Because the cellular processes that mediate GPI-CWPs processing at the cell wall are unique to fungi and highly conserved throughout the fungal kingdom, enzymes that carry out these processes represent excellent targets for novel antifungal drug design.

A number of studies have used collections of *S. cerevisiae* gene deletion mutants to screen for genes involved in cell wall biogenesis [51, 84, 142, 143]. The most comprehensive screen of this type interrogates ~ five % of the genome and leaves the remaining 15 % of the approximately 1200 genes implicated in cell wall biogenesis, open to question as to their specific role in cell wall formation and function [144]. New genomic approaches to investigate the specific function of genes implicated in cell wall biogenesis are needed to advance on the understanding of how the fungal cell builds and uses its cell wall. One such study screened a collection of 620 gene deletants of non-

essential ORFs for cell wall deficiencies. Of the 620 gene deletants, 145 were found to exhibit cell wall damage and were screened further using assays of higher specificity to discriminate between mutants related to different aspects of cell wall formation and mutants that presented a more general phenotype. After secondary screens, 56 cell-wall mutants were chosen to be screened for deficiencies in GPI-mannoprotein anchorage to the wall. Three genes (*(gpi7Δ, ydl231c Δ and ecm33 Δ)*) were identified as required for this process. The 56 strains were screened for levels of GPI-mannoproteins in culture supernatants by dot-blot immunoanalysis using antibodies against the *S. cerevisiae* GPI-CWPs, Cwp1p and Ssr1p [144]. For this assay the researchers report too low protein yields to allow for detection of mutants showing less than wild type levels of GPI-CWPs in the culture supernatant. To our knowledge, this is the only mechanistically based genomic screen performed so far to search for genes required for GPI-CWP anchorage to the wall. Novel approaches that offer increased sensitivity and that have the potential to be applied to any fungus of interest would be of great value. The current study describes the development of a genomic screen with the potential to address these needs.

To screen for genes involved in cross-linking GPI-proteins to the cell wall, we designed a reporter GPI-cell wall protein tagged with GFP (GFP-Sag1p), and tested the idea that mutants missing genes required for anchoring GPI-proteins to the wall would either retain the reporter protein inside the cell or at the plasma membrane (hypo-excretors) or fail to anchor the reporter to the wall and excrete it into the growth media (hyper-excretors). GFP was selected as the reporter protein for this screen for three reasons: *i)* fluorescence levels in culture supernatants would be conveniently and systematically measured using a microplate-reading fluorimeter *ii)* gene deletants could

be assessed for levels of the reporter protein at the cell surface by fluorescence microscopy *iii*) we did not have access to antisera to GPI-CWPs used in previous studies. The reporter protein was expressed in cell-wall mutants previously identified to hyper-excrete GPI-CWPs to validate the idea that mutants of this type could be identified using our approach. The screened was performed using conditions that significantly increase GFP-sag1p yields (Chapter 2). Growth in the presence of non-lethal amounts of the aspartyl protease inhibitor Pepstatin A was required in some mutants to see the expected GFP-Sag1p hyper-excretion phenotype, presumably because of increased extracellular protease activity in these mutants that leads to destruction of the GFP.

In this study, 178 *S. cerevisiae* gene deletion strains from the EUROFAN collection were selected for screening for deficiencies in GPI-CWP anchorage to the cell wall. The selected ORFs were chosen because of their previous implication in cell wall biogenesis. Among the screened ORFs, 60 were identified in a previous *in-silico* study as putative GPI-CWP-encoding genes [74, 80, 145, 146] on the basis that. the ORF would contains i) an N-terminal signal peptide, ii) a serine/threonine rich central domain, and iii) a hydrophobic C-terminal GPI-anchor addition signal. The remaining 118 ORFs were selected from the list of genes listed on the *S. cerevisiae* Genome Database (SGD) website as required for cell wall biogenesis. Most of these genes were found to confer sensitivities to cell wall disrupting agents when deleted, which suggests that their function is important for cell wall biogenesis and integrity.

Using the proposed approach we identified four genes (*MCD4*, *GPI13*, *TDH3* and *GDA1*) as required for GPI-CWP anchorage since deletants of these genes excreted more than wild type levels of the reporter GPI-CWP, GFP-Sag1p. The genomic screen

was performed without the use of pepstatin A, which implies that these mutants excrete large enough amounts of the reporter protein to allow detection of the hyper-excretion phenotype, relative to wild type levels, even in the presence of GFP degradation by extracellular proteases.

Recent studies strongly suggest a role for the cell wall genes *DCWI* and *DFG5* in the transitioning of GPI-CWPs from the plasma membrane to the cell wall likely by cleaving the GPI anchor and cross-linking the GPI-remnant-protein to cell-wall glucan [64, 147, 148]. We find that null mutants of these genes hyper-excreted our reporter protein when grown in the presence of pepstatin A and had reduced levels of the reporter protein at the wall (see Chapter IV for details).

3.2. Materials and Methods

3.2a. Strains and Media

Homozygous and heterozygote diploid deletion strains in the BY4743 background (13), isogenic to the sequenced strain S288c, were used for viable and lethal deletions, respectively. All yeast strains used in this study were constructed during the EUROFAN project and obtained from the *Invitrogen* collection. All strains, apart from the deleted gene share the genotype; MATa/ α his3 Δ 1/his3 Δ 1, leu2 Δ /leu2 Δ , lys2 Δ /LYS2, MET15/met15 Δ , ura3 Δ /ura3 Δ . Tables 3.1 and 3.2 list the 178 gene deletants used in this study. Yeast was grown in either YPD medium (1% yeast extract, 2% peptone, 2% glucose) or defined medium (0.2% yeast nitrogen base without amino acids, 0.5% ammonium sulfate, 2% glucose, and 0.08% complete synthetic media (CSM) lacking

uracyl), containing 1 M sorbitol and buffered to pH 6.5 with 165 mM MOPS and supplemented with 200 μ M geneticin (*Sigma Co.*)

3.2b. High-throughput transformation and growth of gene deletion strains

High-throughput transformation of gene deletants was accomplished using the *bio101 EZ-yeast transformation kit* designed for large scale transformation of yeast. 100 transformations were done simultaneously in about 3 hrs where preparation of competent cells was not required. Cells to be transformed were obtained from fresh growth patches in sterile 127.8 x 85.5 mm rectangular Petri dishes (*Fisher Sci. Co.*). Approximately 2-3 mm cell clumps were picked for each individual strain using sterile wood sticks and transferred to 125 μ l of *transformation mix buffer*, previously added to wells of a sterile 96-well microtiter plate. Following, 2 micrograms of transforming/plasmid DNA (pGFP-Sag1p) and 5 μ ls of *EZ-yeast* carrier DNA were added to cell suspensions in the wells. The 96-well micro plate was gently shaken and incubated at 30 $^{\circ}$ C for 30 min. Following incubation, the entire content of each well was plated in 10 cm x 10 cm Petri plates in plasmid selective media containing geneticin to which gene deletants are resistant. Cell spreading on transformant-selection plates was done by adding a few sterile 5 mm glass beads into the plate and swirling the plates either by hand or by putting them in a rotating platform. The glass beads were recycled for next use.

3 mL cultures of transformed colonies (of similar size) were grown at 18 $^{\circ}$ C in 13x100 mm borosilicate tubes in plasmid-selective medium containing 1 M sorbitol. Growth in small test tubes permits easy monitoring of cell growth by taking OD readings from the tubes directly. We have in the lab a set up that allows the growth of up to 100 3

mL cultures simultaneously. The cultures were grown using the same parameters under which GPI-Sag1p hyper-excretion was observed for cell-wall mutants used as positive controls (*cwp1/cwp1*, *kre1/kre1* and *KRE5/kre5*) with the exception that no pepstatin A was added to the growth media (Chapter 2). To account for differences in growth rate among the mutants, OD readings were taken regularly. Cultures at the desired OD₆₆₀ (0.5-0.6) were centrifuged and 500 µl of their cell-free supernatant stored at -80 °C in silicon-coated tubes in the presence of fungi-specific protease inhibitor cocktail (*Sigma*), a condition we found leads to least protein loss (data not shown). Stored supernatants were then thawed on ice and assayed for GFP fluorescence by single-wavelength fluorescence spectroscopy using a 96-well microtiter plate suitable for fluorescence measurements.

3.2c. High-throughput quantification of GFP levels in mutant and wild type supernatants by fluorescence spectroscopy and dot blot immunoanalysis

GFP cell wall marker protein levels in supernatants of 178 cell-wall mutants and corresponding wild type parental strains were determined by single-wavelength fluorescence spectroscopy using a *FLUOstar Optima* microplate-reading fluorimeter from *BMG labtechnologies*. Triplicates of each mutant were grown to similar cell concentrations, the supernatants collected and their fluorescence measured in black 96-well microtiter plates. Having replicate trials allowed estimation of the mean fluorescence and variance. These values were ranked and plotted, comparing to the values for wild type parental cells.

To quantify the amount of excreted GFP by multi-wavelength fluorescence spectroscopy, complete fluorescence spectra were collected from supernatants of samples

of interest. All spectra including that of wild-type cells were found to contain a background spectrum that was easily distinguished from pure GFP fluorescence based upon the wavelength of the peaks and their width at half height. The pure GFP fluorescence can be seen as a peak centered somewhere between 509 nm-520 nm with a width at half height of 56 nm (1200 cm^{-1}). The background spectrum consists of a single broad peak centered at 536 nm (18657 cm^{-1}) with a width at half height of 90 nm (3500 cm^{-1}). Spectra obtained from supernatants from wild-type cells transformed with empty plasmid were used as the representative data of this background spectrum since it is identical to each of the mutants except that it does not contain GFP. This background spectrum was interactively subtracted from each experimental spectrum to obtain spectra reflecting only the fluorescence from GFP. In other words, the corrected spectra were calculated as the difference,

$$\text{Corrected Fluorescence Spectrum} = \text{Experimental Spectrum} - \text{Constant} * \text{Background}$$

for many different values of the constant. The criterion for the *best* value of the constant was to produce a corrected spectrum that matched as closely as possible to the spectrum of the pure GFP from *Clontech*. In order to match the two spectra, the spectrum of pure GFP was shifted 0-15 nm to move its maximum to the same wavelength as the maxima in the corrected spectrum of the GFP-containing supernatants (pure GFP has fluorescence maximum at 509 nm, and inclusion in a fusion protein is expected to cause a shift in the fluorescence maxima). In most cases it was possible to have the corrected spectra almost perfectly overlay that of pure GFP. The only exception was mutant *GPI13/gpi13*. The corrected spectrum produced had a shoulder at 552 nm that is larger than that seen in the spectra of pure GFP. The size of this shoulder has been observed to be variable in GFP

mutants designed for enhanced for fluorescence [149]. Despite the difference in relative intensity of this shoulder to the maximum for this mutant, the spectrum clearly reflects fluorescence from GFP, since the wavelength of both this shoulder and the maximum peak fall in the range previously observed from GFP proteins enhanced for fluorescence [149].

The relative fluorescence for each sample was taken as the height at the maximum point in the corrected spectrum (Figure 3.4G). In the case of the *GPI13/gpi13* this clearly underestimates the fluorescence, since this mutant emits more from the peak at 552 nm than other mutants. This suggests a simple explanation for why this mutant appears to be a much stronger secretor by anti-body measurements than by direct fluorescence. This mutant is most likely the most prominent secretor of the GFP-cell wall fusion protein, but some of its fluorescence intensity is shifted into this shoulder leading to an underestimation by direct fluorescence measurements. Determination of GFP levels by immunoblotting was carried out as described in Chapter 2.

3.2d. Western Blotting

Specificity of mouse anti-PGK (*Molecular Probes*) for yeast PGK was confirmed by western blotting of yeast extracts prepared from parental strains. Yeast extracts for SDS-PAGE were prepared as described in *Methods of Yeast Genetics* (Cold spring Harbor 2005). 4-20 % Tris-Glycine gradient gels were used for SDS-PAGE and the gels run using the *SE 280 Tall Mighty Small Slab Gel Electrophoresis Unit* from *Amersham Biosciences* as specified by the manufacturer. 1X Tris-Glycine-SDS was used as the running buffer. Protein blotting onto nitrocellulose membrane was carried out using the

TE 22 Mighty Small Transphor Tank Transfer Unit from *Amersham Biosciences* following standard western blotting techniques. *BenchMark Pre-Stained* from *Invitrogen* was used as the protein standard. Following protein transfer to nitrocellulose membrane, the membrane was allowed to dry and then probed with mouse anti-PGK primary antibody and HRP-labeled goat anti-mouse secondary antibody. An optimal concentration range of 0.1µg/mL-0.3µg/mL was determined for anti-PGK solutions. A titer of 1:2000 was used for secondary antibody. Pure PGK from *Sigma* was used as a positive control. Membrane blocking, washing, antibody probing and developing was carried-out as described in Chapter 2.

3.2e. Total protein assay

5 mL cultures were grown to mid-log phase (OD_{660} 0.6-0.8), centrifuged at high speed to remove cells and the resultant 5 mL supernatant frozen at -80°C overnight. The following day, the samples were freeze-dried (lyophilized) overnight for concentration since several attempts to measure total protein from non-concentrated supernatants failed to give any signal due to extremely dilute samples and low protein yields. Dehydrated samples were then reconstituted in 400 µl sterile dH_2O prior to assaying for total protein using the *Coomassie Plus-The Better Bradford Assay Reagent* from *Pierce* (catalog number 23238). This reagent was chosen since unlike the BSA and Lowry assays for total protein determination it did not react with the growth medium and offered superior sensitivity. Each 400 µl sample was assayed for total protein in triplicates of 50 µl each as instructed by the manufacturer. Three independent 5 mL cultures were grown for each tested strain (wild type and select mutants) thus, 9 independent total protein assays were

performed for each strain. BSA standard curves were prepared for extrapolation of protein concentration of unknowns.

To determine total protein secreted into the medium per cell, the following was done: Average protein concentration for each unknown was divided by the concentration factor 12.5 (example; 5 mL supernatant samples were concentrated to 400 μ L, thus each sample was concentrated by 12.5 fold) to estimate protein concentration in micrograms per/mL for original 5 mL non-concentrated supernatants. Total protein amount in micrograms was determined by multiplying each average concentration (μ g/mL) by 5 mL. Amount of protein released into the medium per cell was determined by dividing total protein mass in micrograms by total number of cells in the original 5 mL culture. Cell numbers were estimated from OD₆₆₀ measurements using the conversion factor of 10^7 cells/mL*0.3 O.D⁻¹.

3.2f. Deletion strain confirmation by diagnostic PCR

Diagnostic PCRs to confirm gene deletions in strains of interest were carried out using unique primer sequences (A-KanB or D-KanC) recommended at the *S. cerevisiae* genome deletion project website: (www-sequence.stanford.edu/group/yeast_deletion_project) for each individual gene deletants. Figure 3.7A shows the primer complementary sequences within the genome. PCR reactions for were performed as follows: for a source of genomic DNA, a small amount of cells was mixed with 70 μ L of a Zymolyase solution (*Molecular Probes Inc.*) at 0.06 units/ μ L in a standard PCR tube, and the mixture incubated at 37 °C for 30 minutes. This was followed by a 10 minute incubation at 95 °C to disrupt the cell walls. This step was carried out in a PCR thermal cycler. 10 μ L of

Zymolyase-treated cells were used in standard PCR reactions containing 1x Taq DNA polymerase buffer, 0.2 mM dNTPs each, 0.2 μ M forward primers (A or D) and reverse primers (KanA or KanC) and 2.5 units Taq DNA polymerase. Since all primers were designed to have similar melting temperatures and the expected PCR products are of similar size, all PCR reactions were run simultaneously using the following parameters for 35 cycles of amplification: 3 min, 94 °C (initial denaturation), 15 sec, 94 °C (further denaturation), 15 sec, 57 °C (primer annealing), 60 sec, 72 °C (chain extension) and 3 min, 72 °C (final elongation). Resultant PCR products were analyzed by DNA gel electrophoresis using 1.0 % agarose gels and 1 kb DNA ladders from *New England Biolabs*.

3.3. Results

GFP cell wall marker protein levels in supernatants of 178 cell-wall mutants and corresponding wild type parental strains, were determined by single-wavelength fluorescence spectroscopy using a microplate-reading fluorimeter. Triplicates of each mutant were grown to similar cell concentrations using growth parameters defined in Chapter 2 to increase GFP-Sag1p expression yields. Cell-free supernatants were collected and their relative fluorescence measured in 96-well black microtiter plates relative to reference wells containing known amounts of pure GFP (clonotech). Having replicate trials allowed estimation of the mean fluorescence and variance. These values were ranked and plotted, comparing to the values for wild type parental cells. Figures 3.1A and 3.1B display the average relative supernatant fluorescence and variance for all tested strains. Screened ORFs represented in figures 3.1A and 3.1B are listed in tables 3.1 and

3.2, respectively. 17 gene deletants were identified as hyper-excretors of the GFP-Sag1p reporter protein of which seven (*YGR192CΔ* (*tdh3/tdh3*), *YMR006CΔ* (*plb2Δ*), *YLL031CΔ* (*GPI13/gpi13*), *YKL165CΔ* (*MCD4/mcd4*), *YGR159CΔ* (*nsr1/nsr1*), *YGR020CΔ* (*vma7/vma7*), and *YEL042WΔ* (*gda1/gda1*) show statistically validated differences from wild type. All 17 potential hyper-excretors were selected based on their mean fluorescence appearing higher than (above) the error bar for wild type. Approximately 66 of the 178 gene deletants excreted significantly less GFP-Sag1p than wild-type cells.

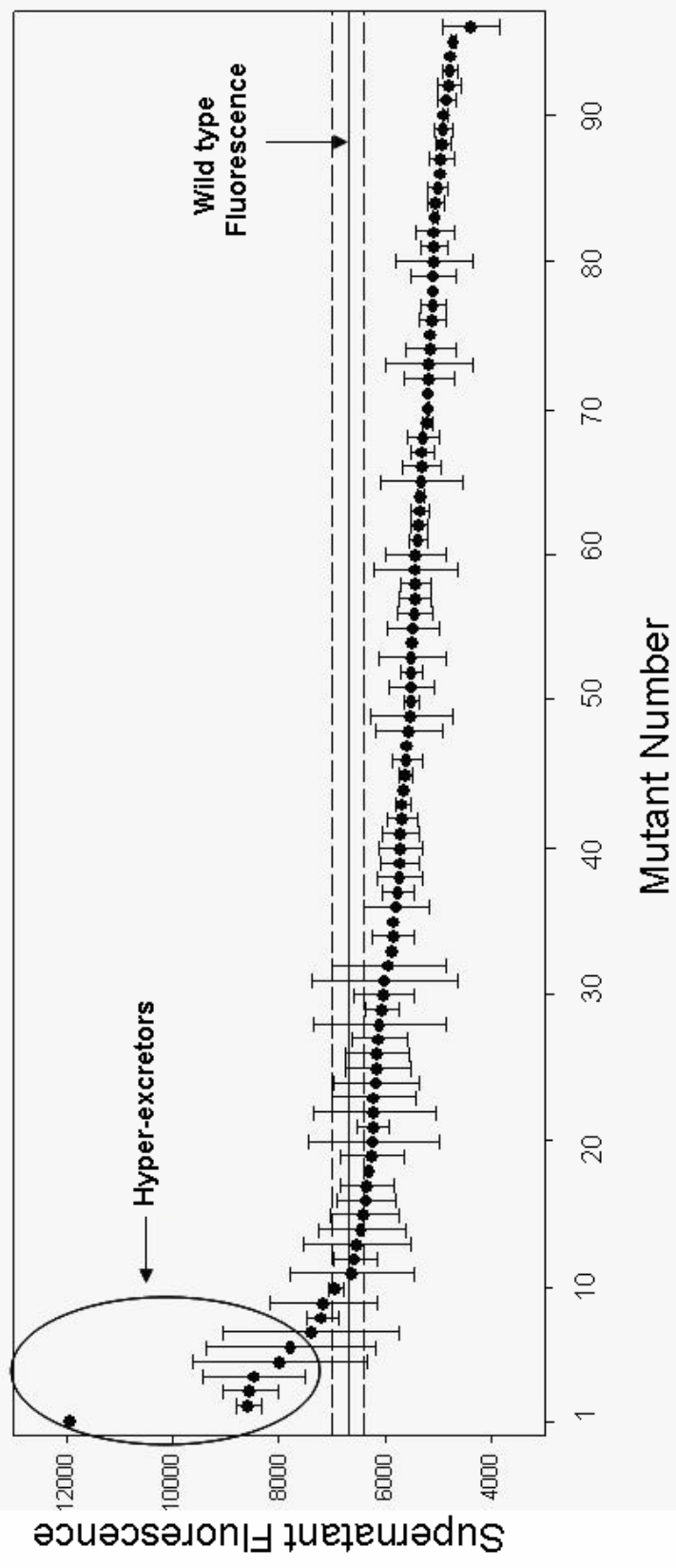


Figure 3.1 A. Amount of excreted fluorescence for cell wall mutants 1-96 listed in Table 3.1. Mean and s.e.m are plotted for each cell wall mutant. Data without error bars were not replicated. The mean \pm s.e.m. values for the wild type parental strain are shown as horizontal lines. Cultures were grown as 3 ml cultures in CSM-URA containing 1 M sorbitol to mid-log phase (OD660 0.5-0.6) at 18 °C and 200 μ l of corresponding cell-free supernatant assayed for fluorescence using a 96-well microplate reading-fluorimeter. Excitation and emission wavelengths were set at 488 and 520 nm, respectively.

Table 3.1. Genes 1-96 screened for their involvement in GPI-CWP anchorage to the cell wall in *S. cerevisiae*. Genes are listed in the order that they appear in figure 3.1 A from left to right

Mutant Number	ORF	Gene Name	Excretion of GFP-Sag1p relative to Wild Type (WT) Cells
1	<i>YGR159C</i>	<i>NSR1/SHE5*</i>	Hypo
2	<i>YGR192C</i>	<i>TDH3</i>	Hyper
3	<i>YMR006C</i>	<i>PLB2*</i>	Hypo
4	<i>YGR020C</i>	<i>VMA7*</i>	Hypo
5	<i>YLL043W</i>	<i>FPS1</i>	Like WT
6	<i>YHR156C</i>	<i>LIN1</i>	Like WT
7	<i>YLL024C</i>	<i>SSA2</i>	Like WT
8	<i>YHR143W</i>	<i>DSE2</i>	Like WT
9	<i>YGL228W</i>	<i>SHE10</i>	Like WT
10	<i>YHR204W</i>	<i>MNL1</i>	Like WT
11	<i>YJL186W</i>	<i>MNN5</i>	Like WT
12	<i>YNL160W</i>	<i>YGP1</i>	Like WT
13	<i>YCL051W</i>	<i>LRE1</i>	Like WT
14	<i>YKR042W</i>	<i>UTH1</i>	Like WT
15	<i>YPL154C</i>	<i>PEP4</i>	Like WT
16	<i>YGL027C</i>	<i>CWH4</i>	Like WT
17	<i>YOL030W</i>	<i>GAS5</i>	Like WT
18	<i>YOR214C</i>	<i>Undetermined</i>	Like WT
19	<i>YDR297W</i>	<i>SUR2</i>	Like WT
20	<i>YMR307W</i>	<i>GAS1</i>	Like WT
21	<i>YLR213C</i>	<i>CRR1</i>	Like WT

22	<i>YJL159W</i>	<i>HSP150/PIR2</i>	Like WT
23	<i>YEL049W</i>	<i>PAU2</i>	Like WT
24	<i>YNL322C</i>	<i>KRE1</i>	Like WT
25	<i>YLR144C</i>	<i>ACF2</i>	Like WT
26	<i>YKR013W</i>	<i>PRY2</i>	Like WT
27	<i>YGL027C</i>	<i>CWH41</i>	Like WT
28	<i>YHR126C</i>	<i>Undetermined</i>	Like WT
29	<i>YNL327W</i>	<i>EGT2</i>	Like WT
30	<i>YLR042C</i>	<i>Undetermined</i>	Like WT
31	<i>YMR244W</i>	<i>Undetermined</i>	Like WT
32	<i>YEL040W</i>	<i>UTR2</i>	Like WT
33	<i>YJL171C</i>	<i>Undetermined</i>	Like WT
34	<i>YGR279C</i>	<i>SCW4</i>	Like WT
35	<i>YLR040C</i>	<i>Undetermined</i>	Like WT
36	<i>YLR120C</i>	<i>YPS1/YAP3</i>	Like WT
37	<i>YJL158C</i>	<i>CIS3</i>	Like WT
38	<i>YLL025W</i>	<i>PAU17</i>	Like WT
39	<i>YPL163C</i>	<i>SVS1</i>	Like WT
40	<i>YNL190W</i>	<i>Undetermined</i>	Like WT
41	<i>YIL015W</i>	<i>BAR1</i>	Like WT
42	<i>YDR349C</i>	<i>YPS7</i>	Hypo
43	<i>YOR190W</i>	<i>SPR1</i>	Like WT
44	<i>YFL051C</i>	<i>Undetermined</i>	Like WT
45	<i>YGL032C</i>	<i>AGA2</i>	Hypo
46	<i>YKL096W</i>	<i>CWP1</i>	Hypo

47	<i>YIR019C</i>	<i>MUC1/FLO11/ STA4</i>	Like WT
48	<i>YER044C</i>	<i>ERG28</i>	Hypo
49	<i>YMR251W-A</i>	<i>HOR7</i>	Like WT
50	<i>YOR010C</i>	<i>TIR2</i>	Hypo
51	<i>YKL163W</i>	<i>PIR3</i>	Hypo
52	<i>YIR039C</i>	<i>YPS6</i>	Like WT
53	<i>YAL035W</i>	<i>FUN12</i>	Hypo
54	<i>YBR229C</i>	<i>ROT2</i>	Like WT
55	<i>YGR189C</i>	<i>CRH1</i>	Like WT
56	<i>YGL028C</i>	<i>SCW11</i>	Like WT
57	<i>YLR194C</i>	<i>Undetermined</i>	Like WT
58	<i>YDR134C</i>	<i>pseudogene</i>	Like WT
59	<i>YOR383C</i>	<i>FIT3</i>	Hypo
60	<i>YDR261C</i>	<i>EXG2</i>	Hypo
61	<i>YGL259W</i>	<i>YPS5</i>	Hypo
62	<i>YDR077W</i>	<i>SED1</i>	Hypo
63	<i>YMR008C</i>	<i>PLB1</i>	Hypo
64	<i>YAL068C</i>	<i>PAU8</i>	Hypo
65	<i>YMR215W</i>	<i>GAS3</i>	Like WT
66	<i>YOR382W</i>	<i>FIT2</i>	Hypo
67	<i>YOR247W</i>	<i>SRL1</i>	Hypo
68	<i>YOR002W</i>	<i>ALG6</i>	Like WT
69	<i>YAL005C</i>	<i>SSA1</i>	Hypo
70	<i>YKR073C</i>	<i>dubious ORF</i>	Hypo
71	<i>YMR305C</i>	<i>SCW10</i>	Hypo

72	<i>YLR037C</i>	<i>DAN2</i>	Hypo
73	<i>YOR009W</i>	<i>TIR4</i>	Hypo
74	<i>YFL020C</i>	<i>PAU5</i>	Hypo
75	<i>YLR121C</i>	<i>YPS3/YPS4</i>	Like WT
76	<i>YCL048W</i>	<i>SPS22</i>	Hypo
77	<i>YKL164C</i>	<i>PIR1</i>	Hypo
78	<i>YAL065C</i>	<i>Undetermined</i>	Like WT
79	<i>YOL011W</i>	<i>PLB3</i>	Hypo
80	<i>YBL075C</i>	<i>SSA3</i>	Hypo
81	<i>YLR300W</i>	<i>EXG1</i>	Hypo
82	<i>YPL106C</i>	<i>SSE1</i>	Hypo
83	<i>YPL130W</i>	<i>SPO19</i>	Hypo
84	<i>YAR020C</i>	<i>PAU7</i>	Hypo
85	<i>YOL132W</i>	<i>GAS4</i>	Hypo
86	<i>YGL261C</i>	<i>PAU11</i>	Like WT
87	<i>YEL030W</i>	<i>ECM10</i>	Hypo
88	<i>YER011W</i>	<i>TIR1</i>	Hypo
89	<i>YER020W</i>	<i>GPA2</i>	Hypo
90	<i>YDR055W</i>	<i>PST1</i>	Hypo
91	<i>YGR282C</i>	<i>BGL2</i>	Hypo
92	<i>YKL073W</i>	<i>LHS1</i>	Hypo
93	<i>YIL011W</i>	<i>TIR3</i>	Hypo
94	<i>YDR144C</i>	<i>MKC7</i>	Hypo
95	<i>YKL046C</i>	<i>DCW1</i>	Hypo

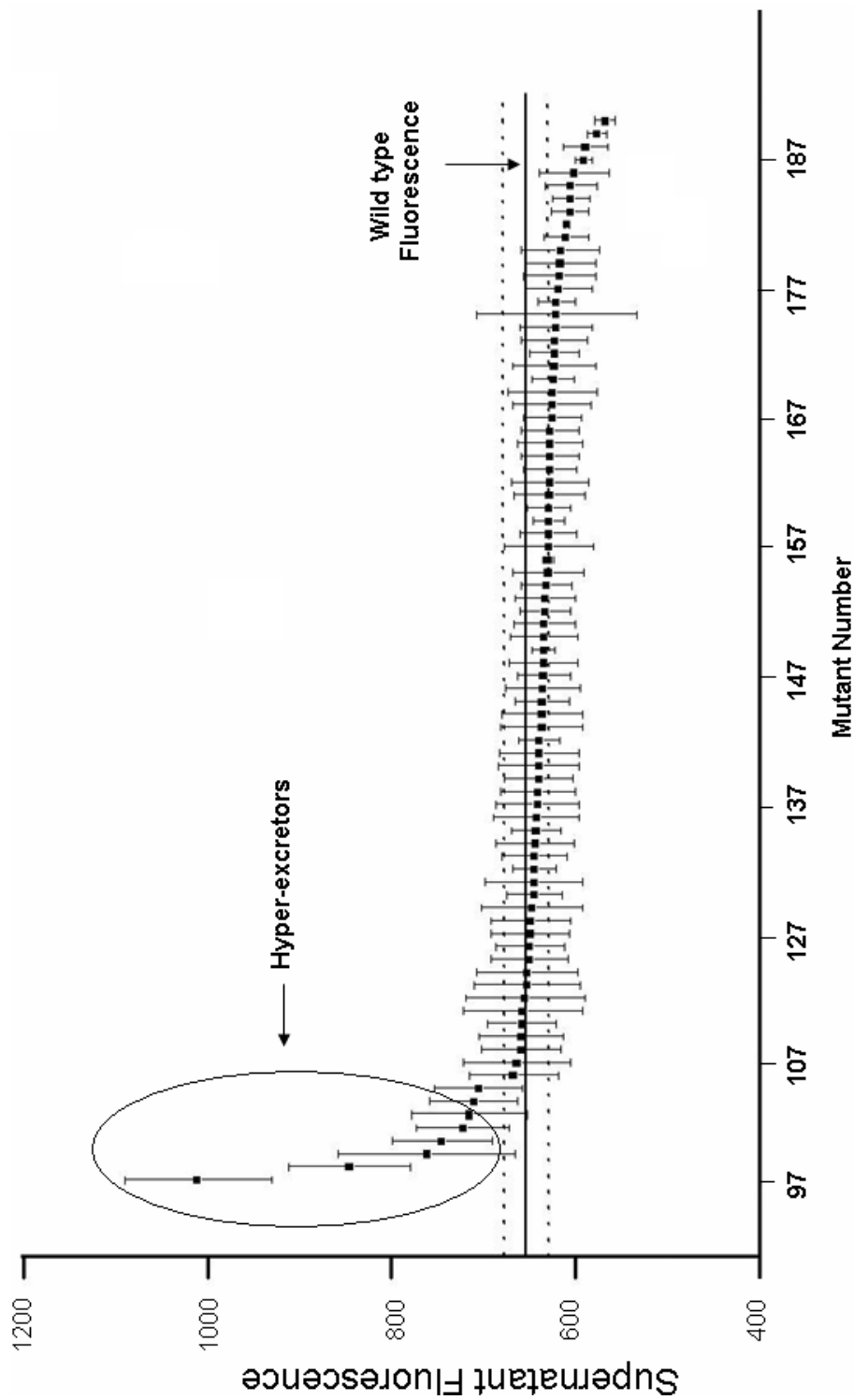


Figure 3.1 B. Amount of excreted fluorescence for cell wall mutants 97-179 listed in Table 3.2. Mean and s.e.m are plotted for each cell wall mutant. Data without error bars were not replicated. The mean \pm s.e.m. values for the wild type parental strain are shown as horizontal lines. Cultures were grown as 3 ml cultures in CSM-URA containing 1 M sorbitol to mid-log phase (OD660 0.5-0.6) at 18 °C and 200 μ l of corresponding cell-free supernatant assayed for fluorescence using a 96-well microplate reading-fluorimeter. Excitation and emission wavelengths were set at 488 and 520 nm, respectively.

Table 3.2. Genes 97-179 screened for their involvement in GPI-CWP anchorage to the cell wall in *S. cerevisiae*. Genes are listed in the order that they appear in figure 3.1 B from left to right

Mutant Number	ORF	Gene Name	Excretion of GFP-Sag1p relative to Wild Type (WT) Cells
97	<i>YKL165C</i>	<i>MCD4</i>	Hyper
98	<i>YBR078W</i>	<i>ECM33</i>	Like WT
99	<i>YLL031C</i>	<i>GPI13</i>	Hyper
100	<i>YBR282W</i>	<i>MRPL27</i>	Like WT
101	<i>YDR522C</i>	<i>SPS2</i>	Like WT
102	<i>YLR337C</i>	<i>VRP1</i>	Like WT
103	<i>YPR163C</i>	<i>TIF3</i>	Like WT
104	<i>YBR162C</i>	<i>TOS1</i>	Like WT
105	<i>YFL039C</i>	<i>ACT1</i>	Like WT
106	<i>YPR186C</i>	<i>PZF1</i>	Like WT
107	<i>YOR275C</i>	<i>RIM20</i>	Like WT
108	<i>YDL055C</i>	<i>PSA1</i>	Like WT
109	<i>YDR528W</i>	<i>HLR1</i>	Like WT
110	<i>YJL174W</i>	<i>KRE9</i>	Like WT
111	<i>YKL104C</i>	<i>GFA1</i>	Like WT
112	<i>YLR286C</i>	<i>CTS1</i>	Like WT
113	<i>YBR092C</i>	<i>PHO3</i>	Like WT

114	<i>YKL035W</i>	<i>UGP1</i>	Like WT
115	<i>YDR446W</i>	<i>ECM11</i>	Like WT
116	<i>YBR040W</i>	<i>FIG1</i>	Like WT
117	<i>YBR067C</i>	<i>TIP1</i>	Like WT
118	<i>YNL066W</i>	<i>SUN4</i>	Like WT
119	<i>YFL020C</i>	<i>PAU5</i>	Like WT
120	<i>YDR245W</i>	<i>MNN10</i>	Like WT
121	<i>YMR200W</i>	<i>ROT1</i>	Like WT
122	<i>YDL143W</i>	<i>CCT4</i>	Like WT
123	<i>YBR301W</i>	<i>DAN3</i>	Like WT
124	<i>YJL062W</i>	<i>LAS21/GPI7</i>	Like WT
125	<i>YNL012W</i>	<i>SPO1</i>	Like WT
126	<i>YBL105C</i>	<i>PKC1</i>	Like WT
127	<i>YDR534C</i>	<i>FIT1</i>	Like WT
128	<i>YKL096W-A</i>	<i>CWP2</i>	Like WT
129	<i>YBR023C</i>	<i>CHS3</i>	Like WT
130	<i>YDR483W</i>	<i>KRE2</i>	Like WT
131	<i>YHR101C</i>	<i>BIG1</i>	Like WT
132	<i>YBR093C</i>	<i>PHO5</i>	Like WT
133	<i>YFR039C</i>	<i>Uncharacterized</i>	Like WT
134	<i>YJL116C</i>	<i>NCA3</i>	Like WT

135	<i>YAL017W</i>	<i>PSK1</i>	Like WT
136	<i>YJR009C</i>	<i>TDH2</i>	Like WT
137	<i>YBL061C</i>	<i>SKT5</i>	Like WT
138	<i>YJL079C</i>	<i>PRY1</i>	Like WT
139	<i>YLR390W-A</i>	<i>CCW14</i>	Like WT
140	<i>YCR089W</i>	<i>FIG2</i>	Like WT
141	<i>YDL049C</i>	<i>KNH1</i>	Like WT
142	<i>YKR102W</i>	<i>FLO10</i>	Like WT
143	<i>YER150W</i>	<i>SPI1</i>	Like WT
144	<i>YLL043W</i>	<i>FPS1</i>	Like WT
145	<i>YDL037C</i>	<i>BSC1</i>	Like WT
146	<i>YJR150C</i>	<i>DAN1</i>	Like WT
147	<i>YBR169C</i>	<i>SSE2</i>	Like WT
148	<i>YGR282C</i>	<i>BGL2</i>	Like WT
149	<i>YJR004C</i>	<i>SAG1</i>	Like WT
150	<i>YJL117W</i>	<i>PHO86</i>	Like WT
151	<i>YIL123W</i>	<i>SIM1</i>	Like WT
152	<i>YOL155C</i>	<i>HPF1</i>	Like WT
153	<i>YIR019C</i>	<i>MUC1/FLO11/STA4</i>	Like WT
154	<i>YDL229W</i>	<i>SSB1</i>	Like WT
155	<i>YLR461W</i>	<i>PAU4</i>	Like WT

156	YAR050W	FLO1	Like WT
157	YMR082C	Dubious	Like WT
158	YAL064C-A	Uncharacterized	Like WT
159	YGR279C	SCW4	Like WT
160	YJR153W	PGU1	Like WT
161	YJL078C	PRY3	Like WT
162	YJL160C	ORF, Uncharacterized	Like WT
163	YLR110C	CCW12	Like WT
164	YER177W	BMH1	Like WT
165	YER103W	SSA4	Like WT
167	YJR045C	SSC1	Like WT
168	YDL222C	FMP45	Like WT
169	YNR067C	DSE4/ ENG1	Like WT
170	YLR343W	GAS2	Like WT
171	YFL051C	ORF, Uncharacterized	Hypo
172	YDL024C	DIA3	Hypo
173	YLR040C	ORF, Uncharacterized	Like WT
174	YJL052W	TDH1	Like WT
175	YLR037C	DAN2	Like WT
176	YER125W	RSP5	Hypo
177	YIR039C	YPS6	Hypo

178	<i>YMR103C</i>	<i>ORF, Dubious</i>	Hypo
179	<i>YOL132W</i>	<i>GAS4</i>	Hypo

The hyper-excretion phenotype was corroborated for all seven mutants on a second round of screening by single-wavelength fluorescence spectroscopy (Figure 3.2). To further confirm the hyper-excretion phenotype of all seven gene deletants, their supernatants were assayed for GFP levels, relative to those in wild type supernatants by dot-blot immunoanalysis. Five independent subcultures of each mutant and of wild-type cells were grown to similar cell concentrations for this analysis (Figure 3.3A). Analysis of dot blot in figure 3.3A is illustrated in figure 3.3B. Of the 7 hyper-excretors, three: *YMR006CΔ* (*plb2/plb2*), *YGR159CΔ* (*nsr1/nsr1*) and *YGR020CΔ* (*vma7/vma7*), excreted less than wild type by immunoblotting. Hyper-excretors confirmed by dot blot analysis ((*YGR192CΔ* (*tdh3/tdh3*), *YLL031CΔ* (*GPI13/gpi13*), *YKL165CΔ* (*MCD4/mcd4*) and *YEL042WΔ* (*gda1/gda1*)) were further corroborated by continuous-wavelength fluorescence spectroscopy. For these four mutants and for hypo-excretor *nsr1/nsr1*, complete fluorescence spectra of their respective cell-free supernatants were collected and corrected for background fluorescence (Figure 3.4C-G) as described in Materials and Methods. After subtraction of background fluorescence, a fluorescence peak remained at the expected emission wavelength for pure GFP (Figure 3.4A) for all four hyper-excretors that was larger than the observed for wild type supernatants (Figure 3.4 B-F). In accordance with what was observed by immunoblot analysis, background-corrected fluorescence spectra from *nsr1/nsr1* cells showed a fluorescence peak substantially lower than the observed for wild-type cells (Figure 3.4G). The relative fluorescence for each

sample was taken as the height at the maximum point in the corrected spectrum (Figure 3.4H).

In the case of *GPI13/gpi13*, this clearly underestimates the fluorescence, since this mutant emits more from the peak at 552 nm than other mutants. This suggests a simple explanation for why this mutant appears to be a stronger excretor by dot blot immunoanalysis (Figure 3.3A) than by direct fluorescence. This mutant is most likely the most prominent excretor of the GPI-CWP reporter protein, but some of its fluorescence intensity is shifted into this shoulder leading to an underestimation by direct fluorescence measurements.

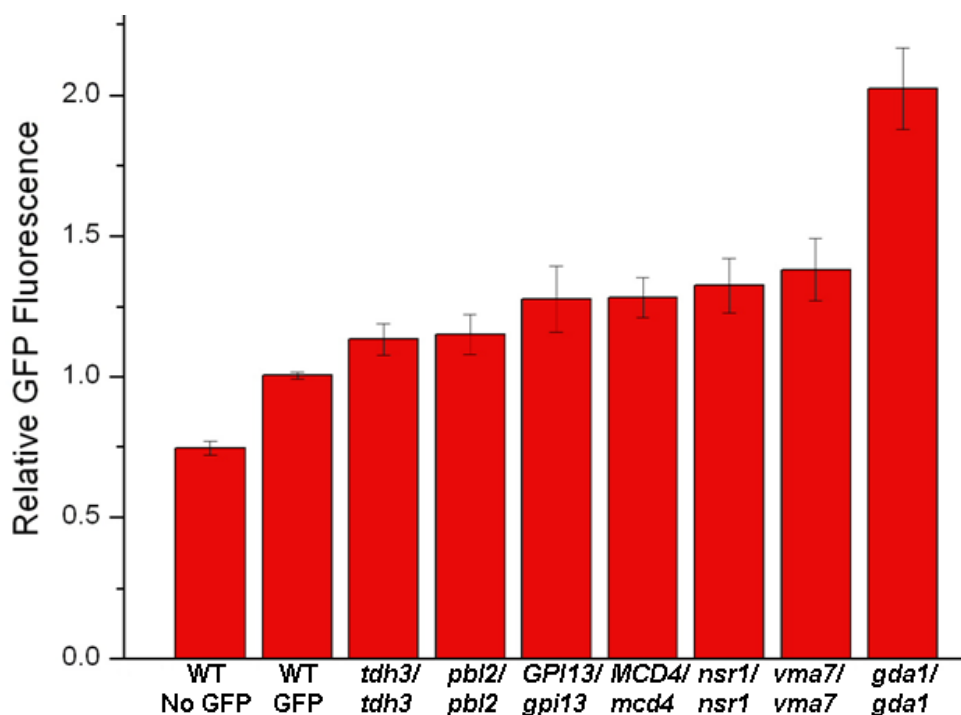


Figure 3.2. Confirmation of GFP-Sag1p hyper-excretion for all seven mutants identified as hyper-excretors in primary screens (see Figures 3.1 A and 3.1B). Cultures were grown as 3 ml cultures in CSM-URA containing 1 M sorbitol to mid-log phase (OD660 0.5-0.6) at 18 °C. 200 µl of corresponding cell-free supernatant were assayed for fluorescence using a 96-well microplate reading-fluorimeter. Excitation and emission wavelengths were set at 488 and 520 nm, respectively.

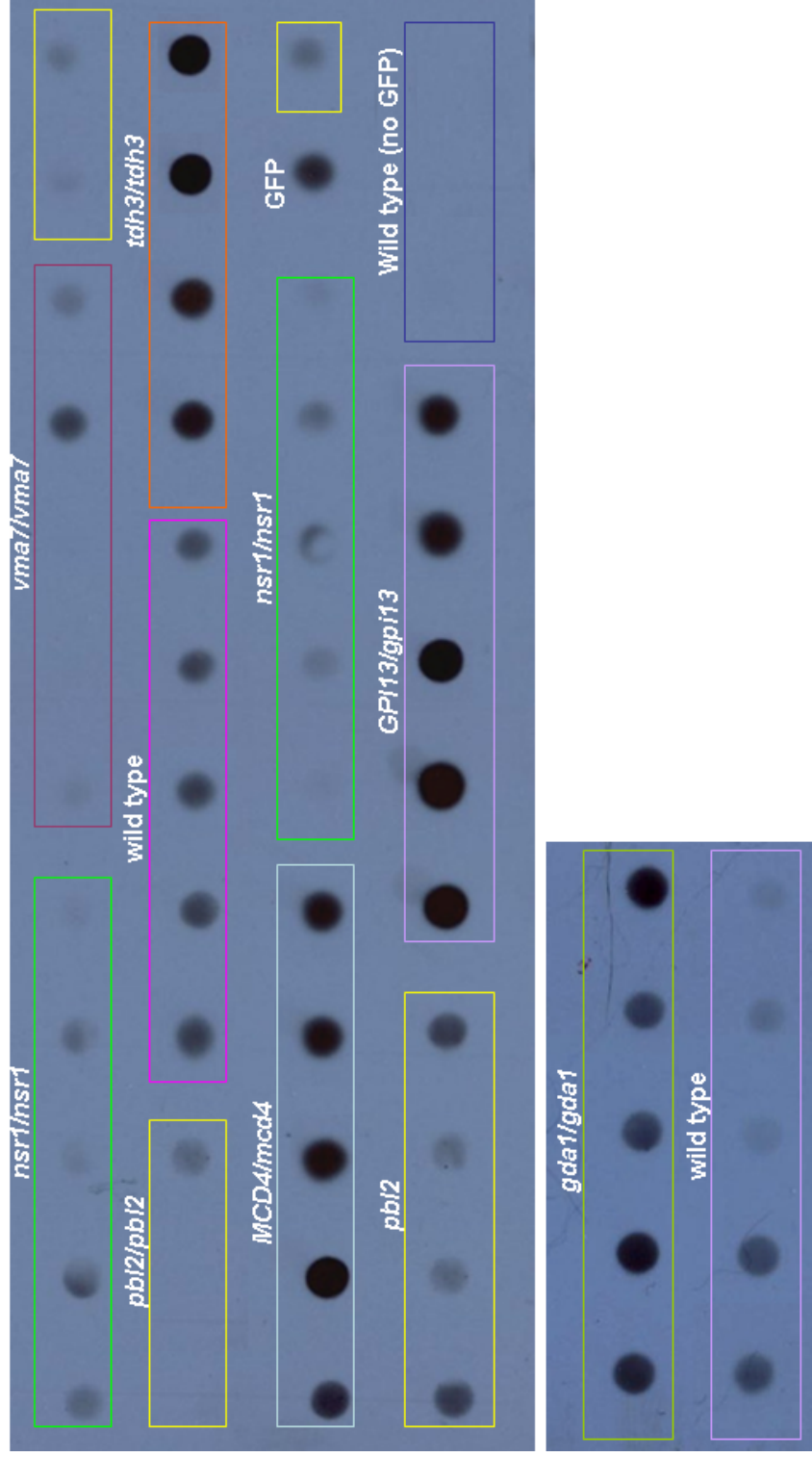


Figure 3.3A. Immunoblot analysis of excreted GFP-Sag1p in seven mutants identified by single wavelength fluorescence spectroscopy as hyper-excretors of GFP-Sag1p. Of the seven mutants identified, four are confirmed as true hyper-excretors by dot blot analysis: *tdh3/tdh3*, *MCD4/mcd4*, *GPI13/gpi13* and *gda1/gda1*. Subclone cultures are boxed. All cultures were grown at 18 °C in CSM-URA containing 1 M sorbitol. No pestatin A was added to the medium. 3 ml Cultures were grown to mid-log phase (OD₆₀₀ 0.5-0.6) and 100 µl of cell-free supernatants applied to nitrocellulose membrane using a BioRad dot blotter/protein concentrator. Blots were probed with mouse anti-GFP as primary antibody and HRP-labeled goat anti-mouse as the secondary antibody.

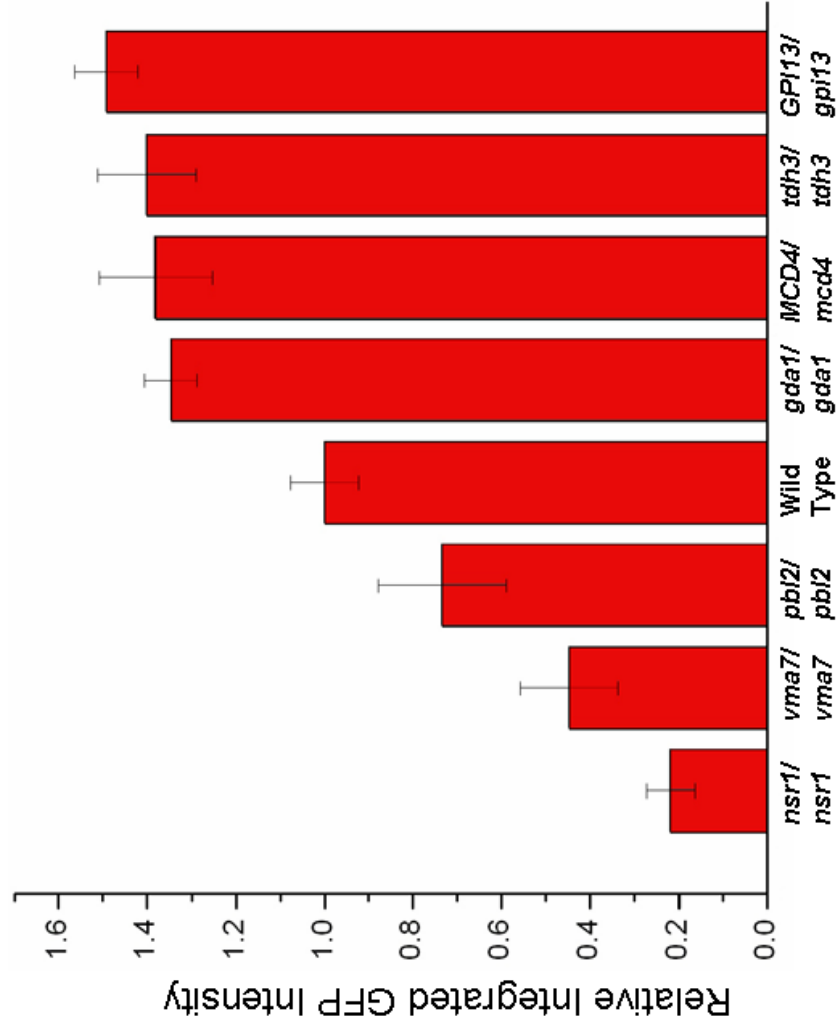


Figure 3.3 B. Quantification of excreted GFP-Sag1p from dot blot in figure 3.3 A using ImageJ software. Integrated measures of the intensity and size (absolute intensity) were determined for each spot and their relative intensities determined using the absolute intensity of wild type cells as the standard or common point of comparison. That is, the absolute intensity of each spot was divided by the absolute intensity of the spot from wild type cells to determine relative intensities. Spots with relative intensities lower than 1 have less protein than the standard and those with relative intensities larger than 1 have more protein than the standard. The relative intensities are unitless values.

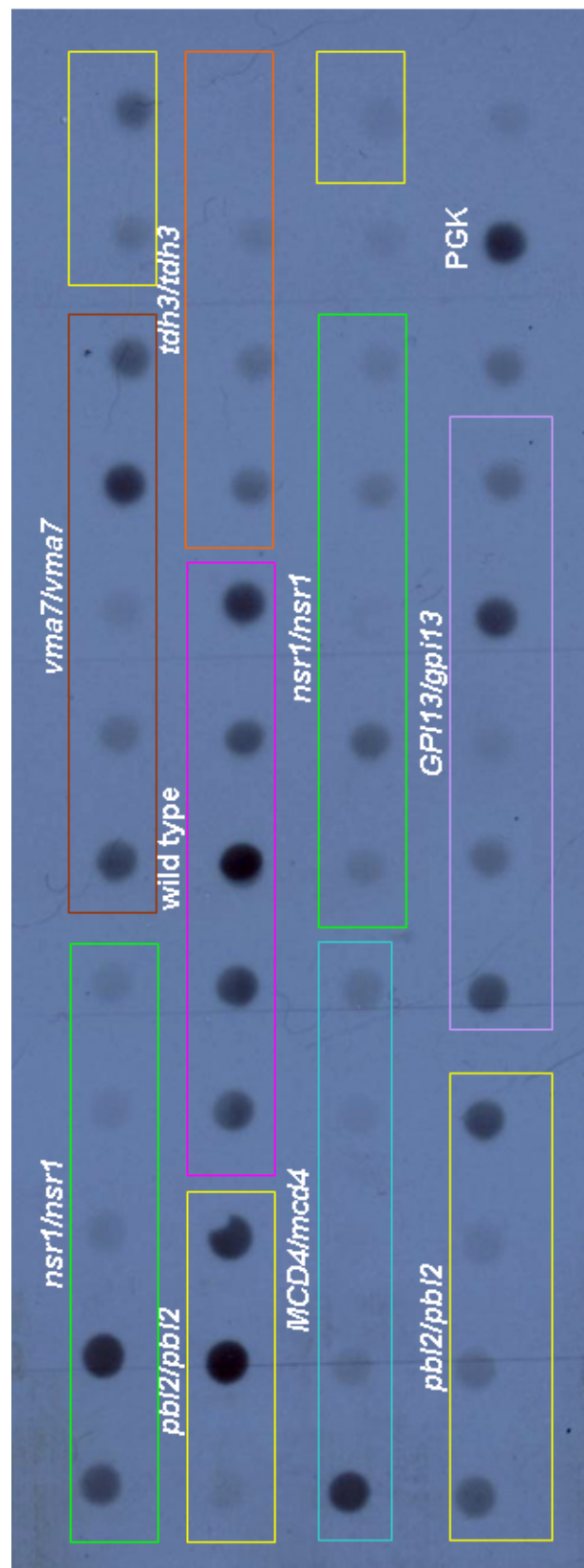


Figure 3.3C. Immunoblot analysis of excreted cytosolic phosphoglycerate kinase (PGK) in seven hyper-excretors of GFP-Sag1p. More PGK is excreted into the growth media by wild type cells than any of the seven mutants. Cultures were grown at 18 °C in CSM-URA containing 1 M sorbitol to mid-log phase. Pepstatin A was not added to the growth medium. 150 µl of cell-free supernatants were applied to nitrocellulose membrane using a BioRad dot blotter/protein concentrator. Dot blots were probed with mouse anti-PGK as primary antibody and HRP-labeled goat anti-mouse.

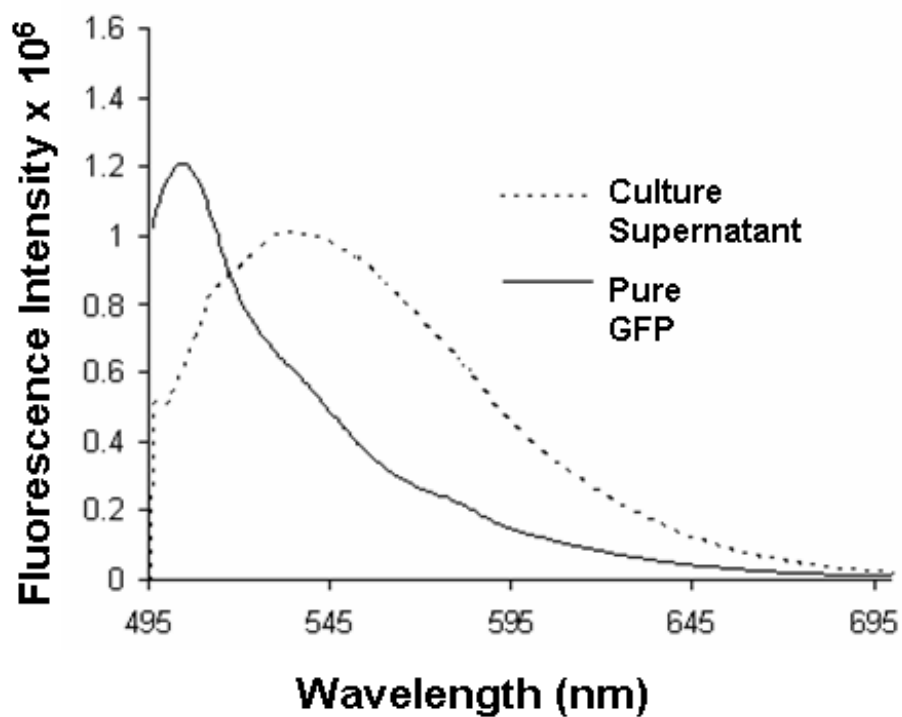
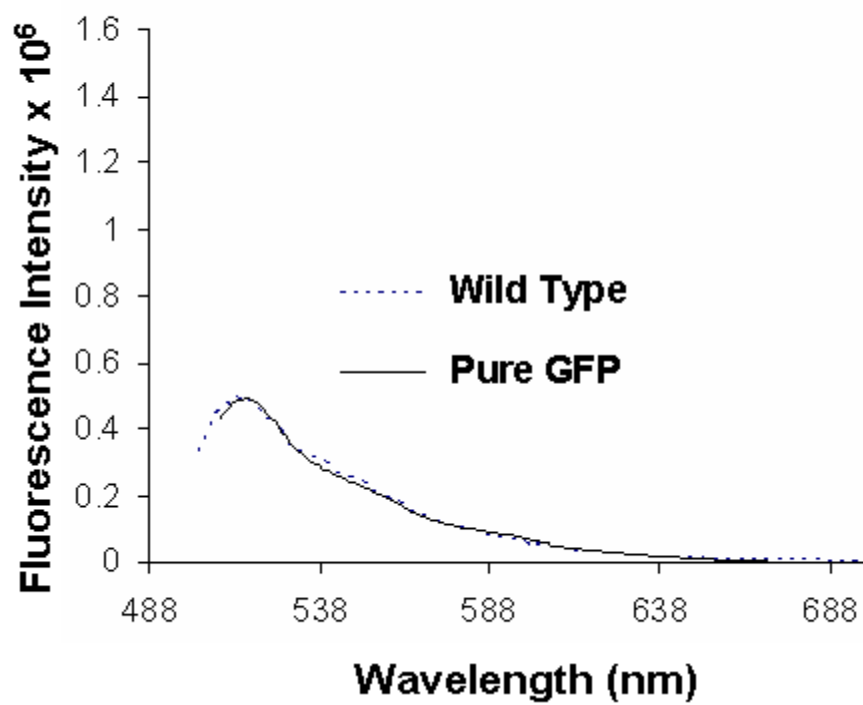
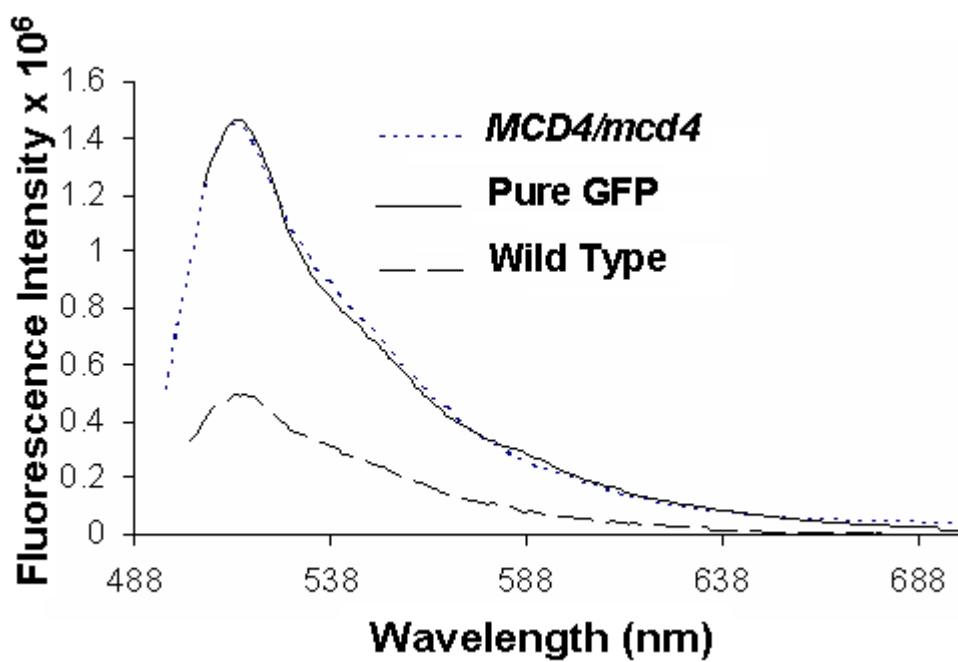
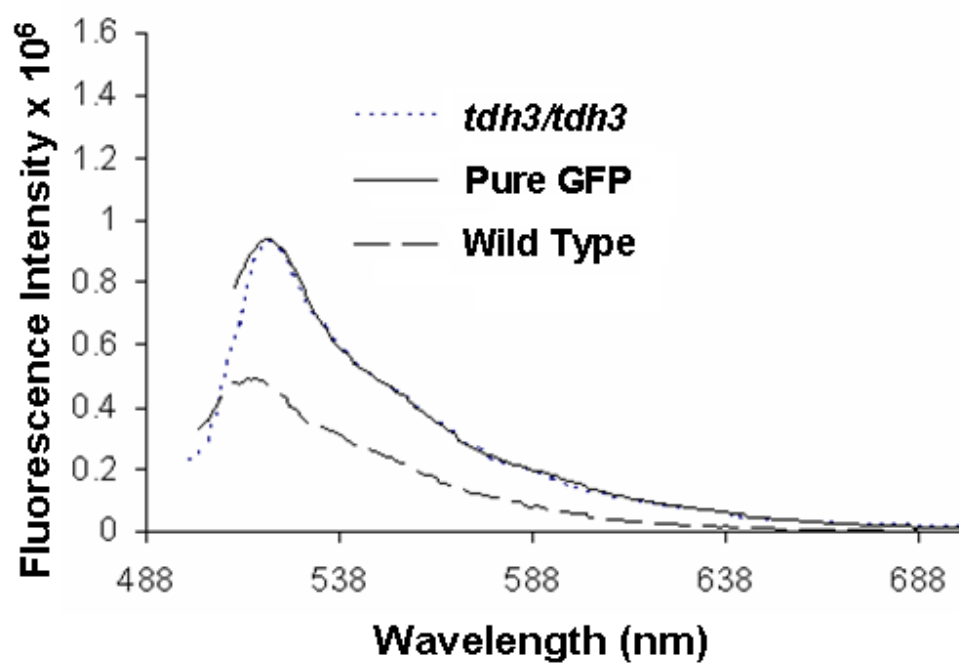
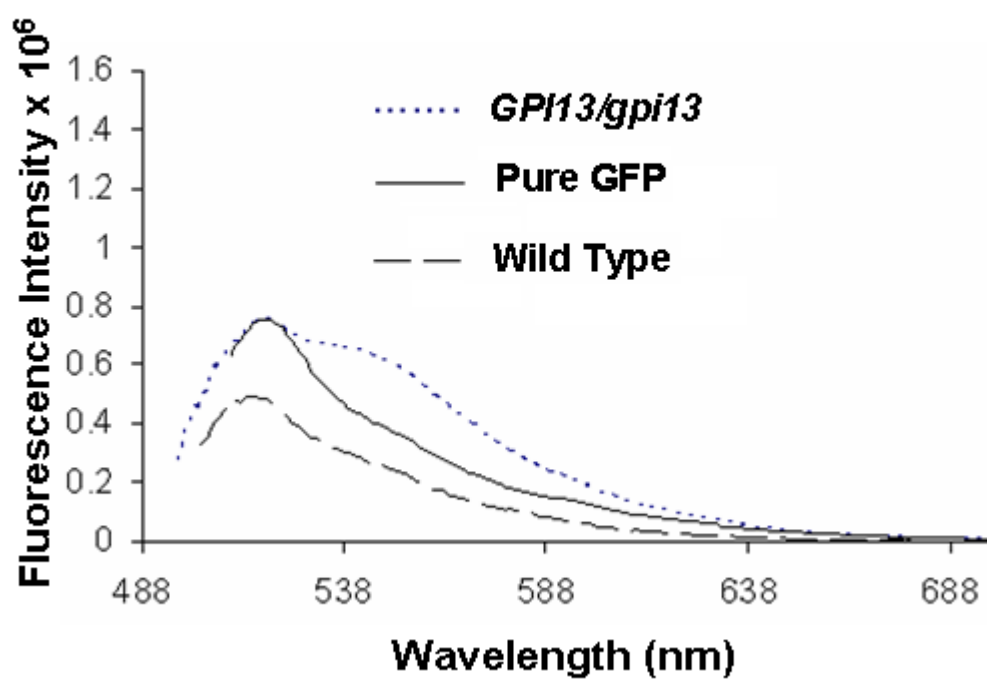
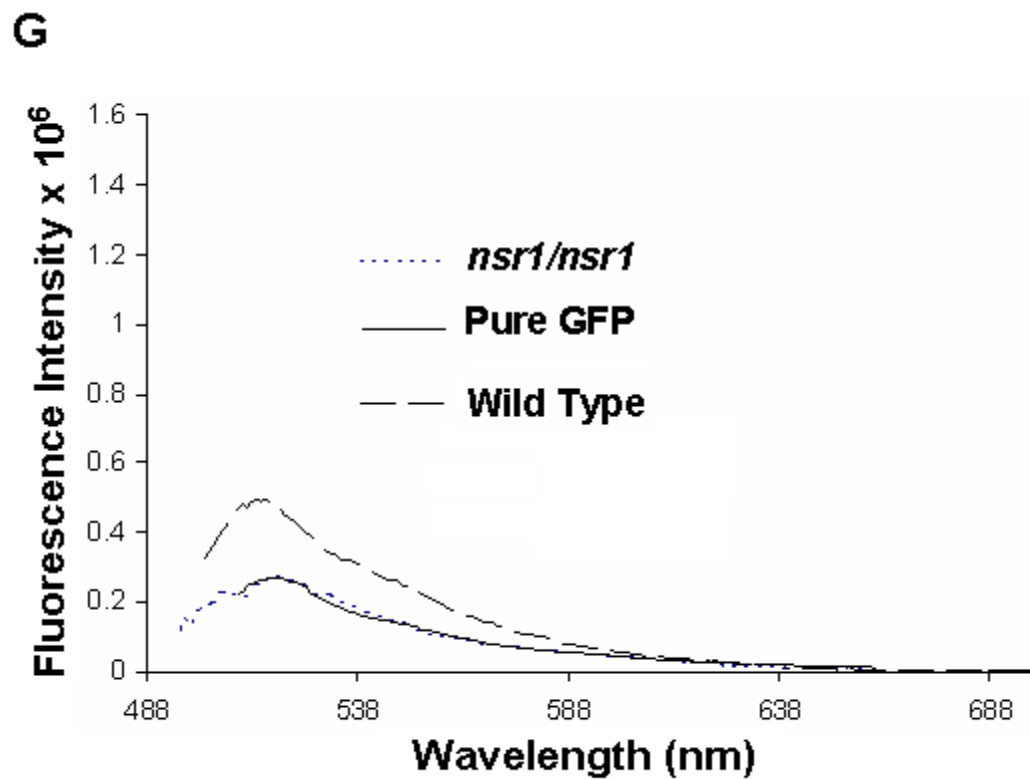
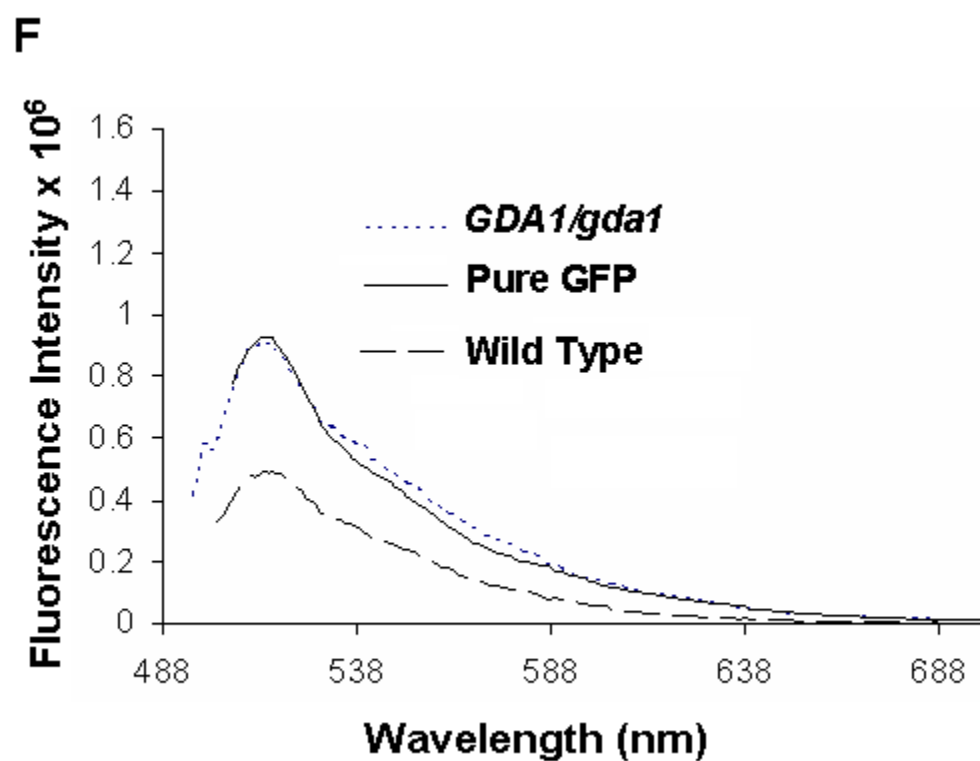


Figure 3.4A. Emission spectra from 1.0 nanogram of pure GFP (*Clontech*) and from supernatant from wild type cells transformed with empty plasmid, thus not expressing GFP.

B**C**

D**E**



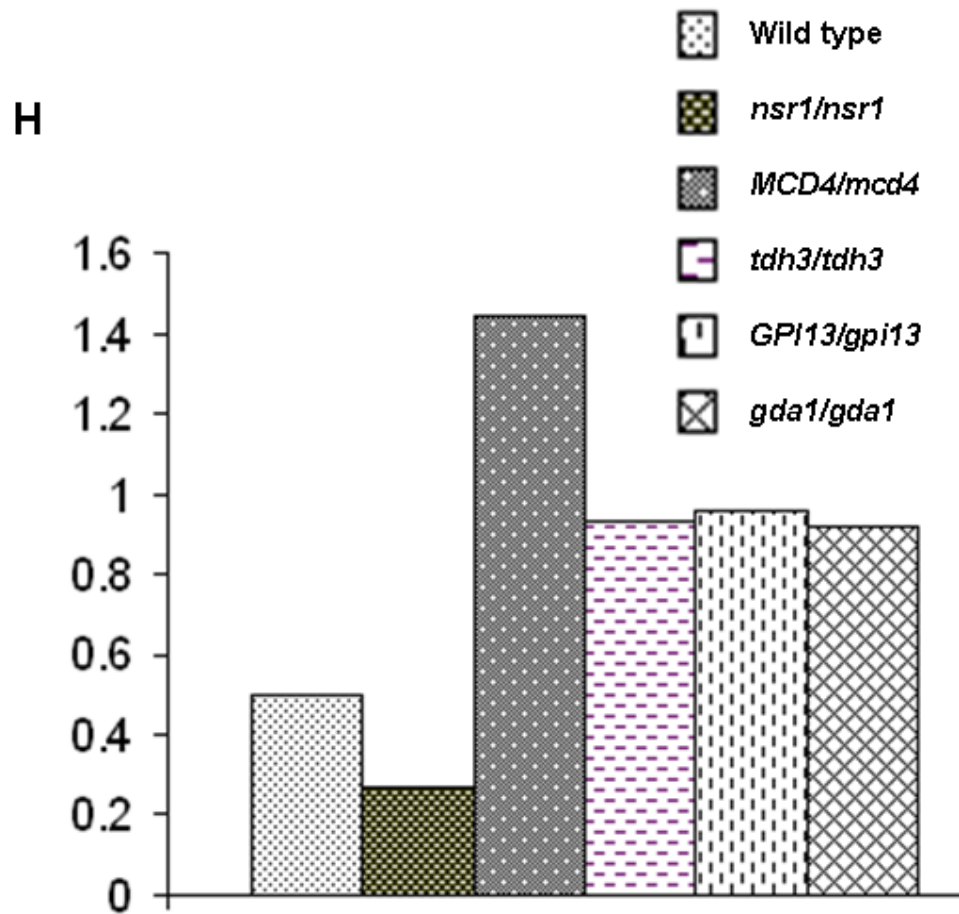


Figure 3.4 B-H. Fluorescence spectrum of pure GFP and background-corrected fluorescence for supernatants of wild type cells (B) mutants confirmed as true hyper-excretors (C-F) and for hypo-excretor *nsr1/nsr1* (G) of GFP-Sag1p, by dot blot immuno-analysis. All mutants that showed more GFP excretion by dot blotting also have spectra of higher fluorescence intensity than that of wild type cells. As observed by immunoblotting *nsr1/nsr1* cells show very little GFP in culture supernatants. The relative fluorescence for each sample was taken as the height at the maximum point in the corrected spectrum (H).

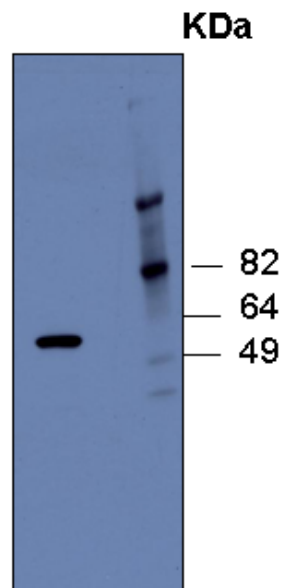


Figure 3.5. Immunodetection of 3-PhosphoGlycerate Kinase (PGK) protein by western blotting of cell extracts from wild type *S. cerevisiae* cells. PGK has an apparent molecular size of 55 KDa.

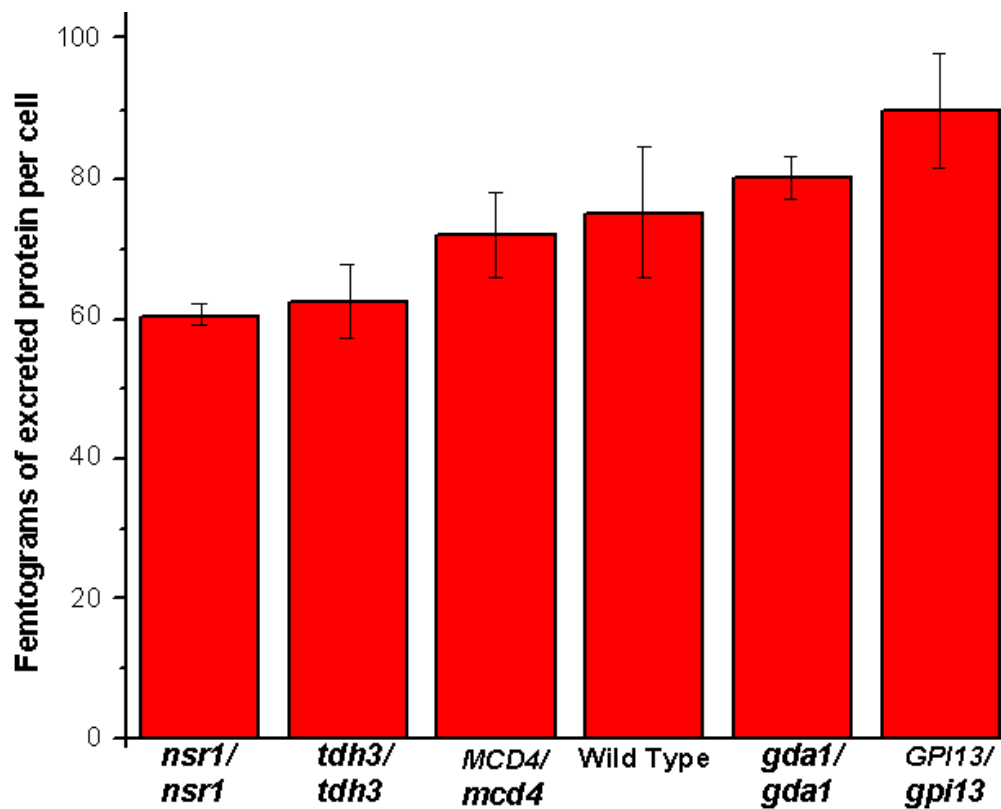


Figure 3.6. Total amount of protein excreted into the growth medium is similar among true GFP-Sag1p hyper-excretors and wild type cells. Total protein in cell-free supernatants was estimated by the *Bradford* method.

(a) Unsuccessful Deletion, ORF still present



(b) Successful Deletion, kanMX4 module replaces ORF

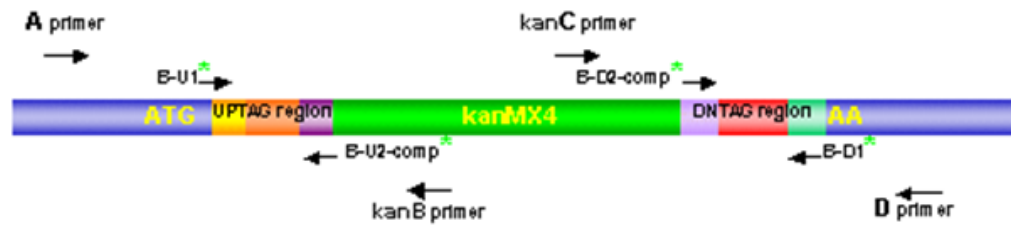
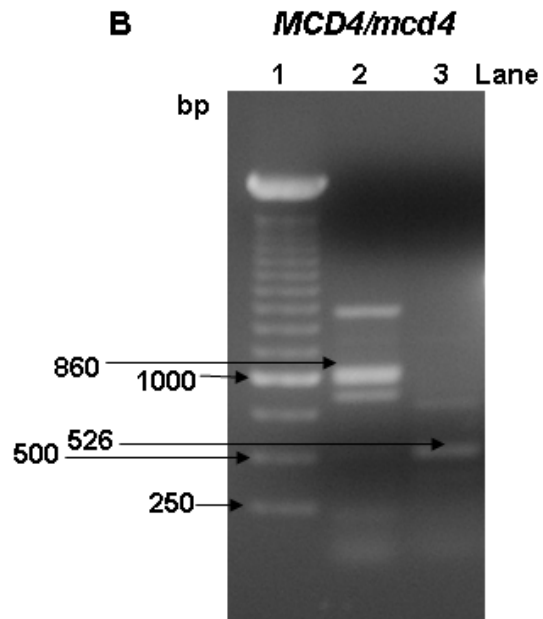


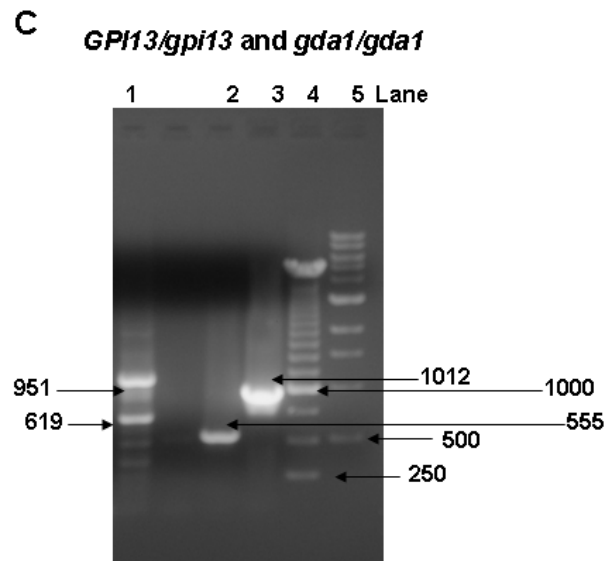
Figure 3.7A. Regions within the genome complementary to primer pairs used for diagnostic PCR. Primer pairs A-KanB and D-KanC were used to confirm deletion junctions. PCR products of the expected size were obtained for all checked strains



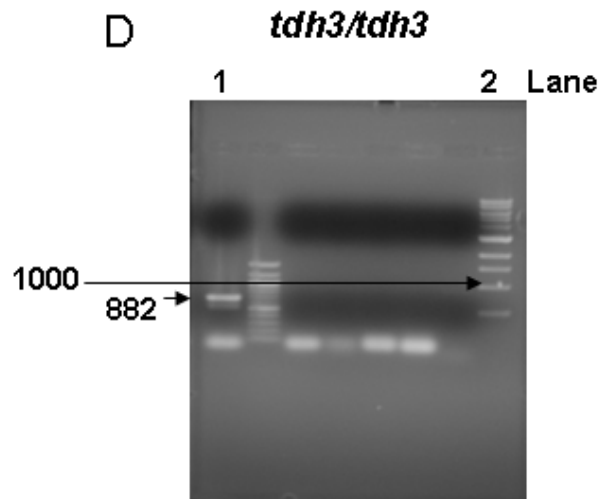
Lane 1: 1 kb DNA ladder

Lane 2: Expected PCR product when using primer pair D-KanC (860 bp).

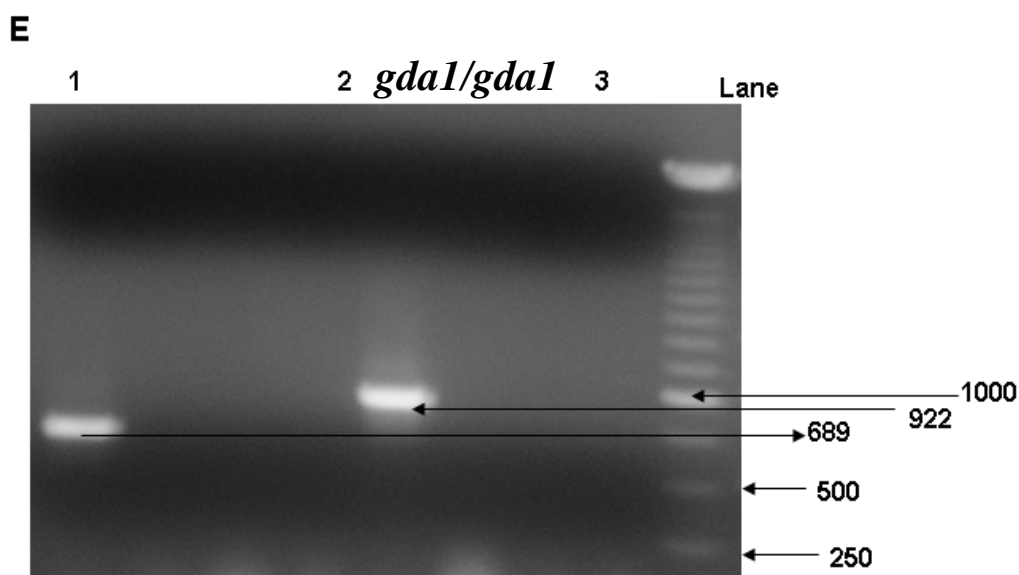
Lane 3: Expected PCR product when using primer pair A-KanB (526 bp).



- Lane 1.** Expected PCR product when using primer pair A-KanB (619 bp) and primer pair D-KanC (951 bp) to confirm *GPI13/gpi13* deletions.
- Lane 2.** Expected PCR product when using primer pair A-KanB (555 bp) to confirm *gda1/gda1* deletions.
- Lane 3.** Expected PCR product when using primer pair D-KanC (1012 bp) to confirm *gda1/gda1* deletions.
- Lane 4.** 250 bp DNA ladder
- Lane 5.** 1 kb DNA ladder



- Lane 1:** Expected PCR product when using primer pair D-KanC (882 bp).
- Lane 2:** 1 kb DNA ladder



Lane 1. Expected PCR product when using primer pair A-KanB (689 bp)

Lane 2. Expected PCR product when using primer pair D-KanC (922 bp)

Lane 3. 1kb DNA ladder

Figure 3.7 B-E. Gene deletions were confirmed for true hyper-excretors and for hypo-excretor *nsr1/nsr1* by diagnostic PCR. Primer sequences and expected sizes for PCR products were obtained from http://www-sequence.stanford.edu/group/yeast_deletion_project/strain_heterozygous_diploid.txt.

In summary, of the 178 gene deletants screened, seven (*YGR192CΔ* (*tdh3/tdh3*), *YMR006CΔ* (*plb2Δ*), *YLL031CΔ* (*GPI13/gpi13*), *YKL165CΔ* (*MCD4/mcd4*), *YGR159CΔ* (*nsr1/nsr1*), *YGR020CΔ* (*vma7/vma7*), and *YEL042WΔ* (*gda1/gda1*) were identified as hyper-excretors of the reporter protein by single wavelength fluoresce of which four (*tdh3/tdh3*, *MCD4/mcd4*, *gda1/gda1*, and *GPI13/gpi13*) were corroborated as true hyper-excretors by multi-wavelength fluorescence spectroscopy and immunoblotting with anti-GFP antisera.

Cell-free supernatants of all seven potential hyper-excretors were also analyzed for levels of intracellular protein by immunoblot analysis using the cytosolic protein, phosphoglycerate kinase (PGK) as the marker protein and anti-PGK anti-serum (Figure 3.3C). The specificity of mouse anti-PGK antibodies for yeast PGK was corroborated by western blotting of cell extracts from wild-type cells (Figure 3.5). More PGK was observed in supernatants from wild-type cells than from any of the gene deletants tested likely because of more robust protein expression from wild-type cells than from the mutants.

The four confirmed mutants, *MCD4/mcd4*, *GPI13/gpi13*, *tdh3/tdh3* and *gdal/gdal* and unconfirmed strain *nsr1/nsr* were further examined for total protein present in the culturing medium relative to wild-type cells (Figure 3.6). An estimated 60-90 femtograms of excreted protein per cell was determined with overlapping variability among all tested strains (Figure 3.6).

Strains assayed for total protein in culture supernatants were also subjected to diagnostic PCR for confirmation of the deleted gene. The correct replacement of the gene with the KanMX marker was verified in the mutants by the appearance of PCR products of the expected size using primers that span the left and right junctions of the deletion module within the genome. Two ORF-specific confirmation primers were chosen (A and D). The "A" and "D" primers are positioned 200-400 bp from the start and stop codons of the gene, respectively. The "KanB" and "KanC" primers are internal to the KanMX4 module (Figure 3.7A). For homozygous and heterozygote deletants, the junctions of the disruption were verified by amplification

of genomic DNA using primers "A" and "KanB" and primers "KanC" and "D". PCR products of the expected sizes were obtained for all five genes (Figure 3.7 B-F)

Confirmed hyper-excretors were also analyzed for cell-surface fluorescence relative to wild-type cells. All strains were grown to early log phase, washed in distilled water and re-suspended in 10 mM Tris-HCL, pH 7.5 to equal cell concentrations prior to fluorescence analysis. To estimate relative cell-surface fluorescence intensities, the samples were exposed to continuous excitation and photographed under the fluorescent microscope with different exposure times. Each strain's series of exposure times were compared side by side by visually matching the exposure time for each strain that had identical or close to identical overall intensity to another strain. Under the assumption that the intensity is proportional to the exposure time and the samples quantum yield (ϕ),

$$I \propto \text{exposure time} \times \phi$$

the strain's relative quantum yields were determined as 1/exposure time for exposures that were matched in intensity. For instance, wild type and *GPI13/gpi13* exposures were compared (Figure 3.8A and 3.8C, respectively) and it was visually estimated that the 1/30th sec exposure for *GPI13/gpi13* cells and the 1/15th sec exposure of wild-type cells were of the same overall intensity. Therefore, the relative quantum yields were estimated as 30 and 15 for the *GPI13/gpi13* and wild type strains, respectively. In other words, the intrinsic fluorescence of *GPI13/gpi13* cells is twice that of the wild-type cells. By the same principle, the intrinsic fluorescence of *MCD4/mcd4* cells is ~ 1.5-2.0 times that of wild-type cells (compare figures 3.8A and 3.8B) and *tdh3/tdh3* and *gdal/gdal* cells are ~ 2-fold less bright than wild type (Figure 3.9 A-C). In the case of *GPI13/gpi13* cells,

inspection of cell-surface fluorescence revealed that the cells have a cell separation defect that results in multi-budded cells with increased levels of fluorescence at the separation septa (Figure 3.8D). *gdal/gdal* Cells also appear to exhibit cell separation defects that leads to the formation of large cell aggregates (Figure 3.9C).

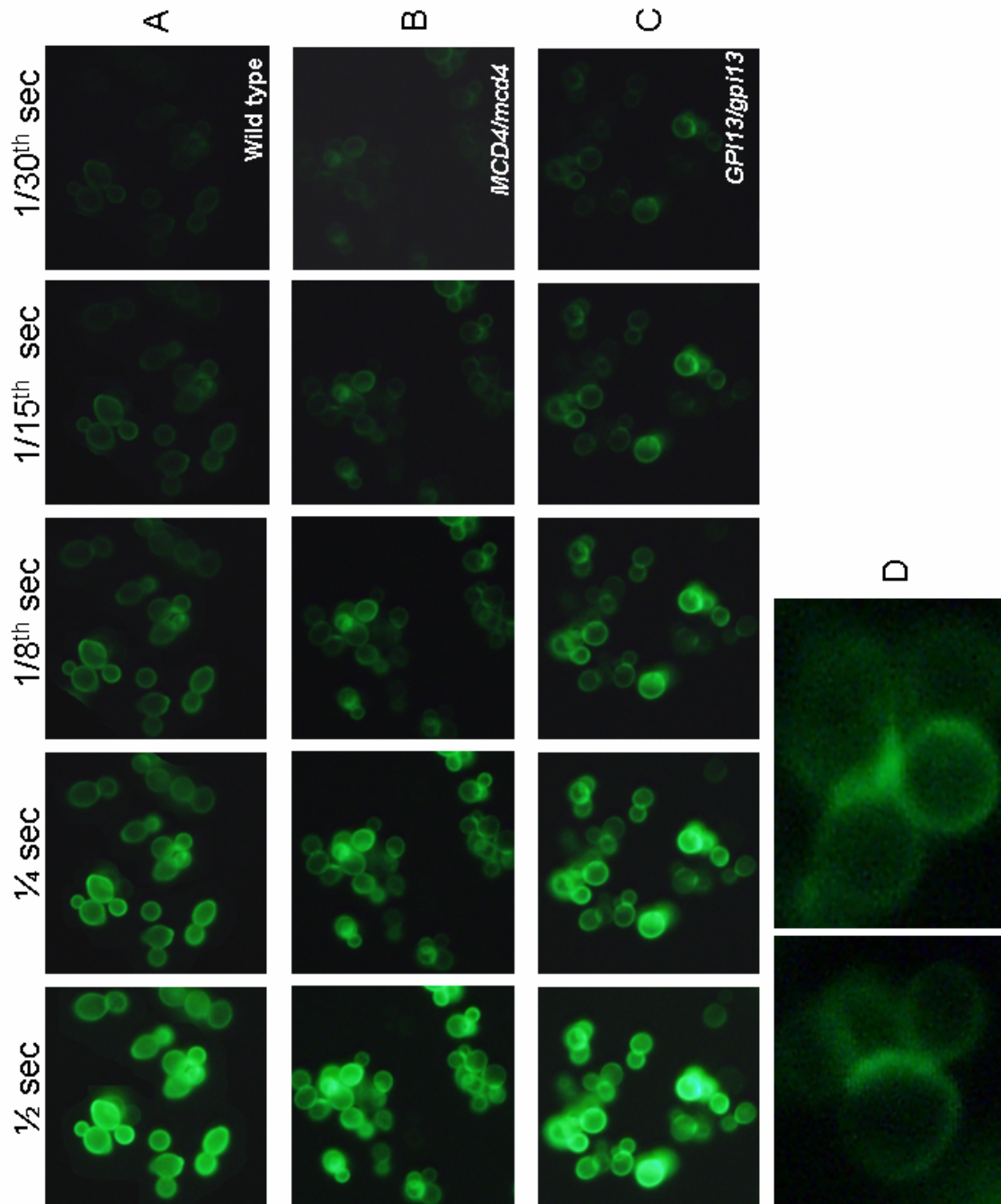


Figure 3.8. Visualization of cell surface fluorescence by fluorescence microscopy. Cells were grown to early log phase (OD_{660} 0.3-0.4) at 18 °C in CSM-URA containing 1 M sorbitol and buffered to pH 6.5 with 50mM MOPS. Cells were harvested, washed with dh20 and re-suspended in 10 mM Tris-HCL pH 7.5 prior to fluorescence analysis. Images were captured at exposure times of $\frac{1}{2}$ - $\frac{1}{30}$ of a second for estimation of cell surface fluorescence as described in Materials and Methods. Both *MCD4/mcd4* and *GPI13/gpi13* cells hyper-express GFP-Sag1p at the cell surface relative to wild type cells. Table 3.3 list ~ cell surface fluorescence for all examined strains relative to wild type.

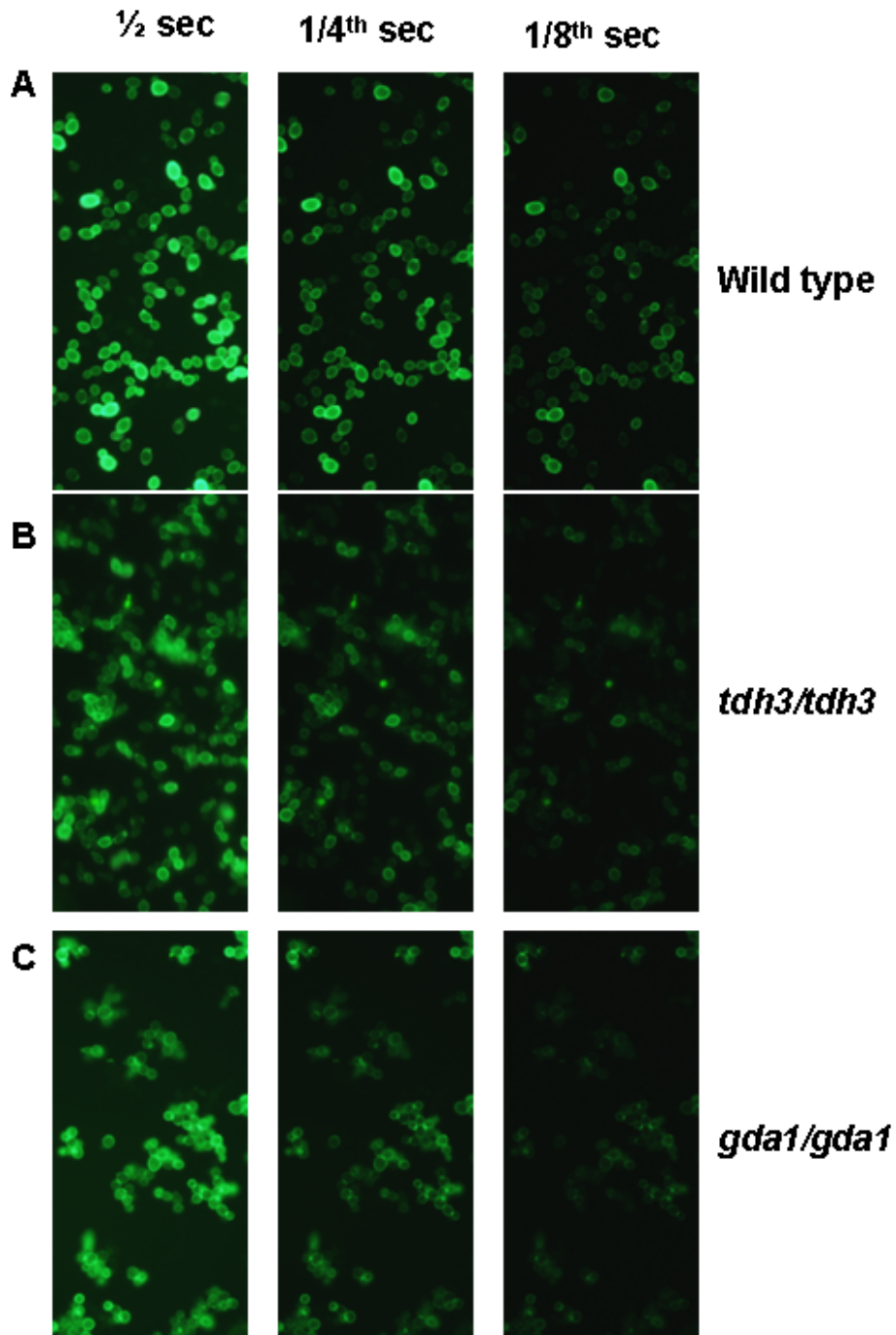


Figure 3.9. Visualization of cell surface fluorescence by fluorescence microscopy. Cells were grown to early log phase (OD_{660} 0.3-0.4) at 18 °C in CSM-URA containing 1 M sorbitol and buffered to pH 6.5 with 50mM MOPS. Cells were harvested, washed with dh20 and re-suspended in 10 mM Tris-HCL pH 7.5 prior to fluorescence analysis. Images were captured at exposure times of $\frac{1}{2}$ - $\frac{1}{8}$ th of a second for estimation of cell surface fluorescence as described in Materials and Methods. Both *tdh3/tdh3* and *gda1/gda1* cells hypo-express GFP-Sag1p at the cell surface relative to wild type cells. Table 3.3 list ~ cell surface fluorescence for all examined strains relative to wild type cells.

Table 3.3. Cell surface fluorescence for GFP-Sag1p hyper-excretors relative to wild type cells.

Mutant	Cell surface fluorescence relative to wild type (WT)
<i>MCD4/mcd4</i>	~1.5-2.0 fold > WT
<i>GPI13/gpi13</i>	~2.0-4.0 fold > WT
<i>tdh3/tdh3</i>	~ 2.0 fold < WT
<i>gda1/gda1</i>	~ 2.0 fold < WT

3.4. Discussion

3.4a. General Approach

We have developed a high-throughput approach to screen for genes required for anchoring GPI-CWPs to the fungal cell wall. In the present work, 178 mutants bearing deletions in genes suspected to play a role in cell wall biogenesis were screened for deficiencies in anchoring a GPI-CWP reporter protein to the cell wall. We used the carboxyl end of the cell wall GPI-mannoprotein α -agglutinin tagged with GFP at its N-terminus (GFP-Sag1p) as the reporter protein. The screen was performed using parameters determined to increase GFP-Sag1p yields (expression from the *GPDI* promoter and growth at lower temperature in the presence 1 M sorbitol (Chapter 2). The rationale for the screening assay is that mutants deficient in anchoring GPI-CWPs would fail to properly cross-link the reporter protein to the wall and either retain the marker protein inside the cell (hypo-excretors) or release it into the growth medium (hyper-excretors). We were able to validate this idea in the cell-wall mutants *cwp1/cwp1*, *kre1/kre1* and *KRE5/kre5* known to hyper-excrete GPI-CWPs, although *cwp1/cwp1* and

kre1/kre1 cells required growth in the presence of the aspartyl protease inhibitor Pepstatin A to show hyper-excretion of GFP-Sag1p. At the concentration used (1 μ M), pepstatin A does not seem to affect growth rate or cell viability. It is possible that pepstatin A enhances GFP yields by inhibiting extracellular aspartyl protease activity in *cwp1/cwp1* and *kre1/kre1* cells. Since hyper-excretion of GFP-Sag1p was observed in *KRE5/kre5* cells grown without pepstatin A, it may be that in this mutant, GFP-Sag1p is excreted at large enough amounts to override extracellular protease activity. Furthermore, since certain aspartyl proteases are GPI-anchored to the wall, deletion of genes involved in anchoring GPI-proteins to the wall may alter aspartyl protease activity in the medium to different degrees that would proportionally affect GFP-Sag1p yields.

As GPI-anchored aspartyl proteases likely play a role in maintaining cell wall integrity and stability [122, 123], and may regulate GPI-CWP turnover [124] we chose to perform the screen without the use of pepstatin A for concerns that it would add to cell wall damage. As was shown with *KRE5/kre5* cells, mutants that hyper-excrete GFP-Sag1p can still be identified without the use of pepstatin A. However, we propose that application of the screening assay in the presence of pepstatin A would significantly increase the sensitivity of the assay to allow for selection of mutants that hyper-excrete only but slightly more GFP-Sag1p than wild-type cells as well as of mutants that hypo-excrete the reporter protein relative to wild-type cells. In support of this idea, we observed that null mutants of the homologous GPI-mannoproteins, Dcw1p and Dfg5p, which may be involved in transporting GPI-CWPs from the plasma membrane to the cell wall, hyper-excrete GFP-Sag1p when grown in the presence of pepstatin A and appear as hypo-excretors when grown without pepstatin A. Furthermore, we found that pepstatin A

did not lead to increases in cytosolic protein in culture supernatants as would be the case if cell death and cell lysis were occurring. Additionally, pepstatin A did not seem to affect growth rate or cell viability in *dcw1/dcw1* and *dfg5/dfg5* cells. (see Chapter 1V for details).

Large-scale screening for GFP-Sag1p excretion levels was carried-out using a 96-well microplate reading fluorimeter because this method proved extremely simple, reproducible and fast. However, this approach yielded approximately 40% false positives. Despite this result, we consider the microplate screening assay useful for narrowing-down the group of mutants deserving of closer inspection by secondary screens in more comprehensive genomic screens. In this study, seven mutants were identified as excretors of significantly more than wild type levels of GFP by the microplate approach. Inspection of GFP excretion levels by dot-blot immunoanalysis, confirmed 4 of the seven hits as real hyper-excretors. The 4 hyper-excretors were further confirmed by continuous wavelength fluorescence spectroscopy, which allowed for the subtraction of background/interference fluorescence from culture supernatants that in the microplate fluorescence assay contributed to the selection of false positives.

To investigate the possibility that higher GFP excretion levels in hyper-excretors might be due to cell lysis or leakage of intracellular protein/components due to cell wall damage, their cell-free supernatants were examined for intracellular protein levels. The cytosolic protein PGK was used as a marker for intracellular protein and its levels assayed by dot blot immunoanalysis. Surprisingly, we observed more PGK in supernatants from wild-type cells than in those from any of the mutants analyzed. This might be because of generally more robust protein expression from the healthier wild-

type cells than from the cell wall-compromised mutants. Also, when total protein levels in mutant and wild type supernatants were examined, no significant difference in total protein was observed among all tested strains. It is possible that at any given time, individual cells express equivalent amounts of total protein and that differences exist rather at the level of which proteins are expressed and in what proportion. It is also possible that for true GFP-Sag1p hyper-excretors, the larger levels of GFP-Sag1p in the growth media are not substantial enough to lead to dramatic increases in total excreted protein.

3.4b. Genes identified as required for GPI-CWP anchorage to the cell wall

Four of the selected 178 cell-wall mutants exhibited clear deficits in anchoring our GPI-CWP reporter protein to the cell wall. Of the four mutants, two are missing genes essential for growth (*YKL165CΔ* (*MCD4/mcd4*) and *YLL031CΔ* (*GPI13/gpi13*)), and two are deleted for the non-essential ORFs (*YGR192CΔ* (*tdh3/tdh3*) and (*gda1/gda1*). A thorough description on the putative functions of these genes and additional findings from this study are presented below.

3.4b1. MCD4 and GPI13

MCD4 and *GPI13* are phosphoethanolamine transferases involved in GPI-anchor biosynthesis. As in other organisms, phosphoethanolamine (EtN-P) transferases form part of the GPI anchor biosynthetic complex where they function to add ethanolamine phosphate side chains to the mannose residues of the glycan part of the GPI-anchor [150-152]. To date, three EtN-P transferases have been described in *S. cerevisiae*: Mcd4p, Gpi7p/Las21p and Gpi13p which add EtN-P groups to the first, second and third

mannose residues, respectively, of the tetra and penta mannose chains of the glycan core of the GPI anchor [152] (Figure 1.2). All three enzymes have mammalian counterparts [153, 154]. In fungi, Mcd4p and Gpi13p are essential proteins that reside on the luminal side of the ER membrane, thus addition of EtN-P to the first and third mannoses occurs there. The essentiality of *GPII3* is expected because it adds EtN-P to the C6 hydroxyl group of the third mannose of the GPI anchor and it is through this EtN-P group that the GPI-anchor is linked to protein via an amide bond [60]. In *gpi13_{ts}* mutants, GPI anchors are not attached to proteins through other EtN-P groups and reduction of GPI anchoring leads to overall cell wall fragility [155]. Our studies show that cells heterozygous for a *GPII3* deletion hyper-excrete GFP-Sag1p and have increased cell-surface fluorescence relative to wild-type cells. It is likely that in these cells the synthesis of GPI-proteins is up-regulated to compensate for the high failure rate of forming the protein-GPI amide linkage. This would also help explain the relatively strong fluorescence that we observed in these cells at sites of active cell wall synthesis such as during daughter cell growth and the formation of new budding cells. We also observed that *GPII3/gpi13* cells appear to have a septation defect that leads to the formation of multi-budded cells. This is similar to what has been observed in *gpi7Δ* cells and other mutants deficient in GPI anchor biosynthesis. In this class of mutants, defects in GPI synthesis lead to deficits in anchor addition to precursor GPI-proteins and to subsequent decreases in GPI-protein targeting to the plasma membrane and the cell wall, where they are required for cell wall formation, remodeling and integrity. In the case of *gpi7Δ* cells, defects in the targeting of GPI-anchored cell wall enzymes (Cts1p, Scw11p, Dse1p, Dse3p, Eng1p and Egt2p) responsible for digesting junctions between mother and daughter cells after cytokinesis

leads to septation defects that cause the formation of aggregated multibudded cells. Faulty GPI-anchor biosynthesis in *gpi7Δ* cells has also been observed to lead to activation of the cell wall stress response [156], which in turn leads to upregulation of cell wall biosynthetic and remodeling enzymes many of which are GPI-proteins themselves [83, 156]. Consistent with this is the observation that *gpi7Δ* cells hyper-express and hyper-excrete the GPI-CWPs, Cwp1p and Ssr1p [144]. Similar responses may occur in *GPI13/gpi13* cells that would lead to the cytokinesis defects and over production and hyper-excretion of GPI-CWPs that we observed in this strain. Although these defects are predictable in *GPI13/gpi13* cells, this study provides the first experimental evidence that *GPI13* is required for normal GPI-protein anchorage to the fungal wall and that heterozygote deletions of this gene are haplo-insufficient. Notably, although *GPI13* is essential for growth in fungi, it is dispensable in mammals in which an alternative protein can compensate for *GPI13* mutations [151]. *GPI13* may thus be an excellent target for antifungal drug design.

Mcd4p is believed to catalyze the addition of EtN-P to mannose one of the GPI anchor (Figure 1.2). Experiments with temperature conditional *mcd4* mutants strongly indicate that Mcd4p is required for GPI anchoring since these mutants, like other GPI-anchor biosynthetic mutants, exhibit cell wall fragility and are defective in ER-to-Golgi transport of multiple GPI-anchored proteins [153]. This deficit in targeting GPI-proteins to their final destination is believed to cause the aberrant phenotypes observed in *mcd4^{ts}* cells such as cell separation defects and abnormal bud site emergence and cell morphology [152]. Since deficits in GPI-anchor biosynthesis inevitably compromise cell wall integrity, it seems logical to assume that *mcd4* mutations can result in activation of

the cell wall stress response and the subsequent upregulation of GPI-mannoproteins responsible for repairing and stabilizing cell wall integrity. This would help explain the increase in cell surface GFP-Sag1p and in the levels of secreted GFP-Sag1p that we observed in *MCD4/mcd4* cells relative to wild-type cells. Like Gpi13p, Mcd4p is essential for fungal growth and dispensable for mammalian cell viability [153]. The value of *MCD4* as a novel antifungal target is corroborated by findings that the terpenoid lactone compound BE49385A, which inhibits the modification of mannose one of the GPI-anchor with EtN-P, is lethal to yeast cells [157]

In a different study, treatment of MDCK mammalian cells with the amino sugar, mannosamine, lead to hyper-excretion of a plasma membrane GPI-marker protein (). A similar effect was observed in *Trypanosoma brucei* (). Mannosamine, has been shown to drastically inhibit GPI anchor biosynthesis and to block the incorporation of GPI glycans into GPI-anchored proteins without affecting the synthesis of the protein component (). It is conceivable that *GPII3* and *MCD4* deletions, by interfering with normal GPI- anchor biosynthesis can generate similar effects in fungal cells as those caused by mannosamine in mammalian and *Trypanosoma brucei* cells [158].

3.4b2. TDH3

The glyceraldehyde-3-phosphate dehydrogenase (GAPDH) is considered a classical glycolytic protein and its role in glycolysis has been well characterized. In mammals, GAPDH displays diverse activities that are unrelated to glycolysis in different subcellular locations. In bacteria and yeast, GAPDH has been found on the cell surface where it may have differing roles. For instance, in *Staphylococcus aureus* and some

streptococci, a cell-surface GAPDH is involved in the interaction with host cells and ligands [159, 160]. In the yeast, *kluveromyces marxianus*, cellular flocculation depends on the expression of a cell-surface GAPDH [161]. When a *C. albicans* cDNA library was screened for sequences that encode immunogenic proteins by using pooled sera from patients with high levels of anti-*C. albicans* antibodies, a cDNA clone coding for GAPDH was obtained [162]. GAPDH is thus considered a potentially useful antigen for the diagnosis of candidiasis and is suspected to play a role in infection. A potential role for GAPDH in virulence is further supported by observations that it tightly binds to extracellular matrix proteins such as fibronectin and laminin and may therefore participate in the adhesion of fungal cells to host tissues [65, 163].

The presence of a classic cytosolic enzyme at the cell surface was initially considered a possible artifact until experiments were done that showed the ability of GAPDH to direct intracellular proteins to the cell wall [16, 164, 165]. For instance, when a fusion of intracellular *S. cerevisiae* invertase (*scSUC2*) to *C. albicans TDH3* was expressed in a Suc⁻ *S. cerevisiae* strain, invertase activity was effectively detected at the cell surface of the Suc⁻ strain. Intracellular invertase is not brought to the cell surface, thus invertase activity detected in cell walls from Suc-cells expressing the *TDH3*-invertase fusion was assumed to result from regions in *TDH3* capable of targeting the fusion protein to the cell wall [65]. Cell wall localization of GAPDH was further established in *S. cerevisiae* by indirect immunofluorescence and flow cytometry analysis with a polyclonal antibody against *S. cerevisiae* GAPDH [162]. In *C. albicans* and *S. cerevisiae*, the GAPDH protein was detected at the outer surface of the cell wall and in the cytoplasm of wild-type cells by immunoelectron microscopy [163]. GAPDH is

now considered a bona fide cell wall protein in fungi and since its secretion appears to occur independently of the presence of a conventional N-terminal secretion signal, an alternative mechanism to the classical yeast secretory pathway has been proposed [166]. The existence of such a pathway would also be extended to other yeast cytosolic proteins that have been found to incorporate to the cell wall.

3.4b3. *GDA1*

GDA1 encodes a guanosine diphosphatase (GDPase) involved in protein and glycosphingolipid O-mannosylation at the Golgi [167]. GPI-CWP N- and O-mannosylation begins at the ER where the first mannosyl residues are added by mannosyltransferases that use dolichol phosphate mannose as the mannose donor [168, 169]. Subsequent elongation of the mannan chains proceeds at the Golgi where the mannose residues are donated by the nucleotide sugar GDP-mannose [170, 171]. GDP-mannose is synthesized in the cytosol and translocated into the Golgi lumen by a specific membrane carrier [170-172]. Following mannosylation of luminal protein and lipid acceptors, GDP is converted to GMP by Gda1p. GMP then exits the Golgi lumen in a coupled, equimolar exchange, with cytosolic GDP-mannose [171]. In the absence of Gda1p, GDP can not be converted to GMP and entry of GDP-mannose into the Golgi is impaired resulting in defects in Golgi mannosylation [46]. For instance, membranes prepared from the *C. albicans* null *gda1/gda1* strain showed a 90% decrease in the ability to hydrolyze GDP compared to wild type membrane preparations [173]. This mutant also showed severe defects in O-mannosylation and reduced cell wall phosphate content. Since GPI-CWPs contain phosphate groups in their N- and O-linked mannan chains [48], a reduction in the phosphate content of the wall is taken as an indication of reductions in

the levels of GPI-CWP at the wall [173]. Alternatively, the lower phosphate levels may result because shorter O-linked mannose chains are unable to act as substrates for phosphomannan addition. Whether GPI-CWPs with shorter O-mannan chains can still anchor to the cell wall, are degraded inside the cell or excreted into the growth medium remains to be determined. Our results show much lower than wild type levels of GFP-Sag1p at the wall in *gda1/gda1* cells, and the reporter protein is hyper-excreted into the growth medium. It is possible that poorly O-mannosylated proteins are excluded from being cross-linked to the wall and rather end-up as excreted protein. However, observations that *C. albicans gda1/gda1* cells are more susceptible to the action of β -1,3 glucanases implies a thinner outer layer of GPI-CWPs, which when properly formed acts to protect the underlying β -1,3 glucan network from glucanases [68, 174]. The increased access to cell-wall glucan in *gda1/gda1* cells may result from lower GPI-CWP levels at the wall, although the possibility that it may be a consequence of under-mannosylation of anchored GPI-CWPs can not be excluded. Shorter mannan chains would be unable to form the tight meshwork that forms through cross-links of longer mannose chains via disulfide bridges and that limit the cell wall's porosity [174, 175]. A thinner mannan-meshwork would thus lead to increased cell wall porosity. The GPI-CWP hyper-excretion phenotype, relative to wild-type cells that we observed in *gda/gda1* cells may be due to this increased porosity in the wall, which would make retention of GPI-CWP precursors less efficient. Notably, we did not see increases in the level of intracellular protein in the growth medium of these cells, which implies that increased GFP levels in the medium is not due to leakage of intracellular components .

3.4c. Advantages of the screening approach

The value of our experimental design lies in its functionality as a high-throughput approach to uncover genes required for fungal adhesin attachment to the fungal wall. Previous studies demonstrate hyper-excretion of fluorescently labeled GPI-protein in cells deficient in this process, although no approach has been taken to survey the genome in its entirety. Genome-wide surveys for genes encoding GPI-mannoproteins have been done in silico [146] although such assays are limited by the extent and quality of experimental data available. Our genome-wide screen will offer complementary experimental data to these computer-based surveys, and thus significantly contribute to uncovering genes involved in fungal cell wall development. Another experimental approach has been to use mass spectrometry to identify and quantify cell wall GPI-protein. Though this approach has been applied to normal cells, it has only been extended to a few cell-wall mutants [18, 176], as the technique is not amenable for high-throughput screening. Our genome-wide approach has been specifically designed to handle systematic growth of hundreds of strains at a time. Hyper and hypo-excretion of the marker is reproducibly assayed in a 96-well plate reading fluorimeter. Therefore the procedure is easily replicable and adaptable to a range of fungi and growth conditions. Importantly, our set up facilitates determination of growth stage by simply reading optical density directly from the test tube where the cells are growing. The tubes are inserted into a spectrophotometer for readings to calculate cell concentrations. This is a convenient feature that allows us to assay for GPI-protein attachment to the wall at any point during the cell growth cycle.

3.4d. Other applications for the screening assay

1. Direct screening for antifungal activity in libraries of compounds. Such assays would use standard strains of fungi, each expressing a species-appropriate version of the marker. Such marker proteins would be prepared by standard molecular biology techniques and expressed under promoters appropriate to the organism. We have demonstrated this application in *Saccharomyces cerevisiae*, and it could be easily adapted to any fungus in which there is a protein expression system [177-180].
2. The assay could be adapted to screen for mutations affecting cell wall anchorage of GPI cross-linked proteins in any species of fungus. The marker protein, or another one adapted to the specific species would be expressed from an engineered strain of fungus, mutagenized, grown, and the mutants screened for strains that hyper-excrete or hypo-excrete the marker protein relative to the parental strain.
3. A similar approach could be used to screen for drugs active against other organisms with GPI-anchored surface proteins. Malaria and trypanosomes are disease-causing organisms in this category. A standard strain expressing a similar fluorescent marker protein could be treated with drug candidates one at a time, and the growth supernatants assayed for hyper-excretion or hypo-excretion of the marker protein.

Chapter 4

The homologous genes *DCWI* and *DFG5* are required for anchoring of GPI-mannoproteins to the fungal cell wall

4.1. Introduction

In an effort to identify enzymes involved in transporting GPI-mannoproteins from the plasma membrane to the cell wall in fungi, Kitagi et al. searched the ORFs of the *S. cerevisiae* genome database for homologs of bacterial mannosidases known to participate in similar enzymatic reactions [64]. They identified genes for two putative proteins that share significant homology with bacterial family 75 of glycosidases/transglycosidases. Together with glycosyltransferases, glycosidases form the major catalytic machinery for the synthesis and breakage of glycosidic bonds in a cell. Dcw1p and Dfg5p are GPI-mannoproteins of the plasma membrane, although in *C. albicans* Dfg5p also localizes to the cell wall [148]. A *dcw1/dcw1* deletion rendered the cells hypersensitive to the cell-wall-digesting enzyme Zymolyase, whereas deletion of *DFG5* led to no observable phenotypes [64]. Both single deletants exhibited normal morphology and grew normally in rich and complete synthetic media [64]. *DCWI* and *DFG5* are functionally redundant since their combined deletion leads to synthetic lethality and can be rescued by over-expressing a *DFG5* allele from the *GALI* promoter. The double mutant hyper-excretes cell wall GPI-mannoproteins and becomes hyper-sensitive to cell-wall disrupting agents following repression of *DFG5* expression from the *GALI* promoter [64]. In *S. cerevisiae*, *DFG5* and *DCWI* are required for bud formation [147] while *DFG5* is required for agar invasion and growth at alkaline pH [181]. In *C. albicans*, these genes have similar

functions: at least one of them is required for growth [148], and *DGF5* is required for hyphal development [148]. Clearly, Dcw1p and Dfg5p play an important role in cell wall biogenesis. It has been hypothesized the proteins may be the ones to cleave the GPI anchor and transglycosylate the GPI-anchor remnant protein to cell wall polysaccharides. However, their role in this process remains far from clear.

Here we present new findings that support a role for Dcw1p and Dfg5p in the cross-linking of GPI-protein to the fungal wall. Null mutants of these genes fail to properly anchor a GPI-CWP reporter protein (GFP-Sag1p) to the wall. The null mutants hyper-excrete the reporter protein and localize less of the protein at the wall relative to wild-type cells. When examined for levels of cytosolic protein in the growth medium, as evidence of possible cell death and lysis, we were unable to detect any, whether the cells were grown in the presence of the aspartyl protease inhibitor pepstatin A or not. This was true for both mutant and wild-type cells. Growth in the presence of pepstatin A was required for hyper-excretion of the GPI-CWP reporter protein in *dcw1/dcw1* and *dfg5/dfg5* cells, compared to wild-type cells, and did not affect growth rate or lead to increases in cell death. In a different experiment, cultures of *dcw1/dcw1*, *dfg5/dfg5* and *GPI13/gpi13* cells showed abundant amounts of cytosolic protein in the growth media when grown in the presence of the more general protease inhibitor PMSF.

4.2. Materials and Methods

4.2a. Strains, media, plasmids, yeast transformation and growth conditions

The yeast strains utilized in this study are part of the EUROFAN collection of *S. cerevisiae* gene deletion strains and were purchased from *Invitrogen*. The strains and

their respective genotypes are listed in Table 4.1. The yeast strains were grown and transformed with plasmid pGFP-Sag1p as described in Materials and Methods (Chapter 2). For growth in the presence of pepstatin A, the reagent was added to cell solutions at early log (OD₆₆₀ 0.2-0.3) to 1 μ M concentration from 1 mM pepstatin A stock solutions prepared in methanol and kept at -20 °C. For growth in the presence of PMSF, 200 mM stock solutions were prepared in methanol and kept at -20 °C. For growth, PMSF was used at 1 mM concentrations.

4.2b. GFP quantification by dot-blot immunoanalysis and fluorescence microscopy

Strains *dcw1/dcw1*, *dfg5/dfg5*, *GPII3/gpi13* and the corresponding parental strain were assayed for levels of excreted GFP by immunoblot analysis using mouse anti-GFP as the primary antibody and HRP-labeled Goat anti-mouse as secondary antibody. Cell-surface fluorescence was visualized and relative cell-surface fluorescence intensities estimated using fluorescence microscopy. Both, immunoanalysis and quantification of cell-surface fluorescence were performed as described in Materials and Methods in Chapters 2 and 3, respectively.

4.2c. Determination of effect of pepstatin A and PMSF on growth rate and cell viability

Three mL cultures of *dcw1/dcw1*, *dfg5/dfg5*, *GPII3/gpi13* and the corresponding parental strain were grown in triplicate to early log phase (OD₆₆₀ 0.2-0.3). Pepstatin A was added to 1 μ M, and PMSF to 1mM. For controls, identical groups of cultures were similarly grown with the exception that no treatment was added. Growth was monitored for all cultures by taking regular OD measurements starting immediately after addition of the protease inhibitors. OD measurements were converted to cell concentration in

cells/mL using the conversion factor of 10^7 cells/mL per 0.3 OD units. To analyze the effect of pepstatin A on growth rate in *dcw1/dcw1*, *dfg5/dfg5* and wild-type cells, growth curves were prepared for treated and non-treated cells that compare cell concentrations over time. To examine the effect of pepstatin A in promoting cell death, treated and non-treated cells were assayed by the methylene blue dye exclusion assay as described in Materials and Methods (Chapter 2). The percentage of blue stained (dead) cells over total number of cells examined (3000 per strain) and corresponding standard errors are illustrated in bar graphs prepared using *Microcal(TM) Origin 6.0* software.

4.2d. Determination of cytosolic protein in culture supernatants

To examine the effect of pepstatin A, PMSF and combined pepstatin A and PMSF, in the levels of cytosolic protein in the growth medium of *dcw1/dcw1*, *dfg5/dfg5*, *GPII3/gpi13* and wild-type cells, cultures were grown in triplicate with and without inhibitors as described above, and their cell-free supernatants assayed for levels of the cytosolic protein phosphoglycerate kinase (PGK) by immunoblotting. Dot blot immunoanalysis was carried out as described in Materials and Methods (Chapter 2I). In summary, mid-log treated and non-treated cultures were centrifuged and 150 microliters of cell-free supernatant blotted onto nitrocellulose membranes for probing with mouse anti-PGK antiserum as the primary antibody at a concentration of 0.5 mg/mL and HRP-labeled goat anti-mouse as the secondary antibody at a concentration 1:2000 dilution.

4.3. Results and Discussion

4.3a. dcw1 and dfg5 Null mutants hyper-excrete a GPI-CWP reporter protein when grown in the presence the aspartyl protease inhibitor pepstatin A

As can be observed from figures 4.1 and 4.2, null mutants of the *DCW1* and *DFG5* genes appear as hyper-excretors of GFP-Sag1p when grown in the presence of pepstatin A. When grown without pepstatin A, *dfg5/dfg5* cells differ little from wild-type cells in the amount of excreted GFP, while *dcw1/dcw1* cells show as hypo-excretors of GFP-Sag1p relative to wild-type cells. This negative result is consistent with previous studies reporting a defective cell wall phenotype for *dcw1/dcw1* cells and no observable cell wall phenotypes for *dfg5/dfg5* cells [64]. In particular, *dcw1/dcw1* cells were found to be hyper-sensitive to the cell-wall glucanase Zymolyase, possibly because of a thinning of the GPI-CWP outer layer which acts to protect inner cell wall polysaccharides from hydrolytic enzymes [68, 175]. It can also be observed from figures 4.1 and 4.2 that pepstatin A leads to a slight decrease in the levels of GFP-Sag1p in supernatants from wild-type cells. Previous studies suggest that GPI-anchored aspartyl proteases known as yapsins may regulate GPI-CWP turnover by acting as “sheddasers” that cleave the proteins off the wall to be replaced by new ones [124]. By inhibiting this “shedding” activity, pepstatin A can lead to a decrease in the amount of GFP-Sag1p molecules that are cleaved off the wall and consequently to a lowering of the protein molecules in the medium. This provides a possible explanation as to why we see less GFP-Sag1p in supernatants from wild-type cells treated with pepstatin A than when not treated, although the effect is mild (Figures 4.1 and 4.2). In addition to inhibiting cleavage of GFP-Sag1p from the wall, pepstatin A would also prevent “shedding” of GPI-CWPs with aspartyl protease activity and thus lead to a lowering in the level of this proteolytic activity in the medium. For aspartyl proteases successfully cleaved off the wall and released into the medium, their activity would also be blocked by pepstatin A in the media. We believe

that by inhibiting “shedding” of aspartic proteases from the wall and by blocking the activity of aspartic proteases released into the medium, pepstatin A makes possible the detection of GPI-CWP hyper-excretion from *dcw1/dcw1* and *dfg5/dfg5* relative to wild-type cells. This phenotype has not been previously described for null mutants of these genes.

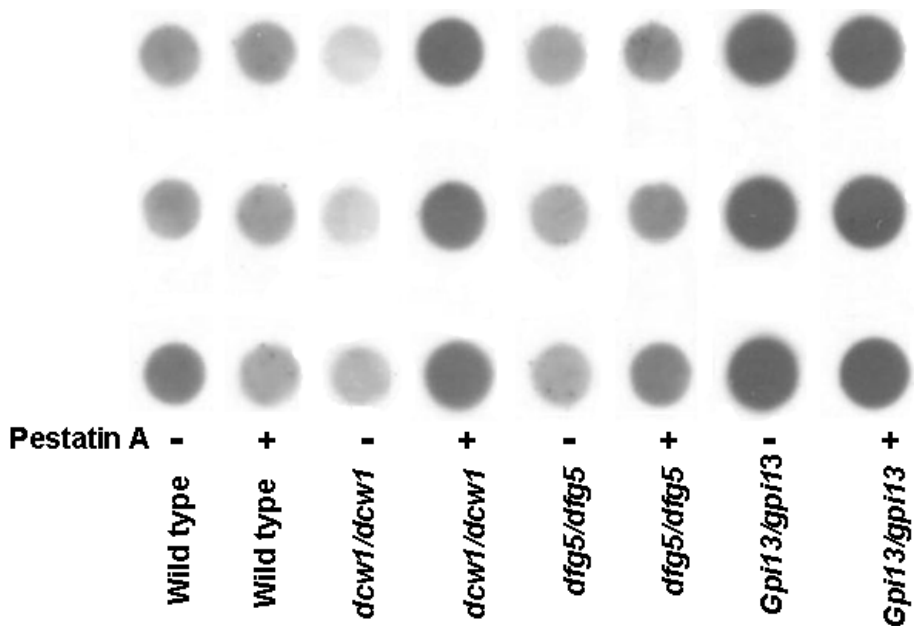


Figure 4.1. Immunoblot analysis of effect of pepstatin A on excreted GFP-Sag1p yields. Cultures were grown to early log (OD₆₆₀ 0.2) at 18 °C in CMS-URA containing 1 M sorbitol without (-) or with (+) added 1 μM pepstatin A. Cultures were harvested at mid log (OD₆₆₀ 0.6-0.8) and 100 μl of cell-free supernatant assayed for GFP levels using a BioRad dot blotter/protein concentrator. Blots were probed with monoclonal anti-GFP antiserum as the primary antibody and HRP-labeled goat anti-mouse as the secondary antibody.

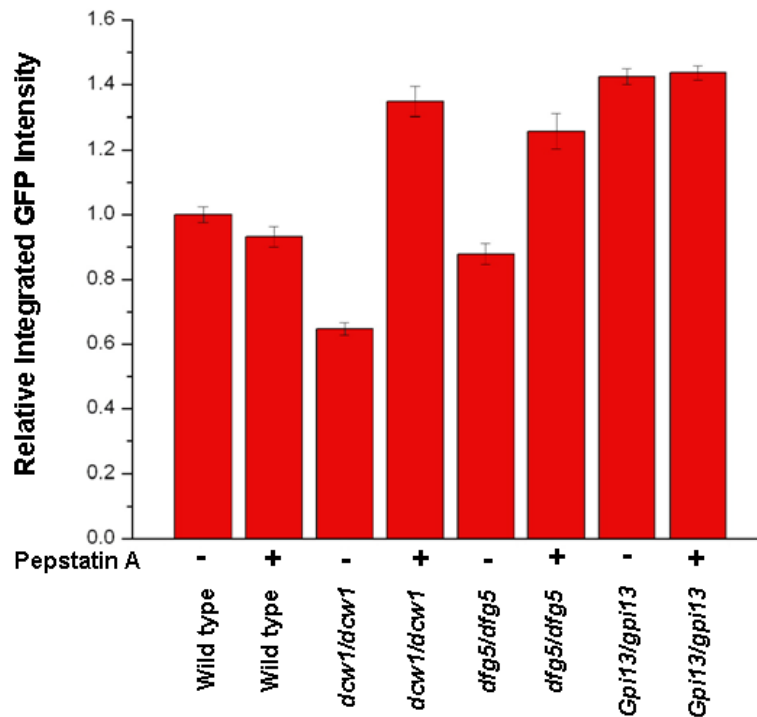


Figure 4.2. Quantification of excreted GFP-Sag1p by analysis of dot blot in figure 4.1 using ImageJ software. Integrated measures of the intensity and size (absolute intensity) were determined for each spot and their relative intensities determined using the absolute intensity of wild type cells not treated with pepstatin A as the standard or common point of comparison. That is, the absolute intensity of each spot was divided by the absolute intensity of the spot from wild type cells not treated with pepstatin A to determine relative intensities. Spots with relative intensities lower than 1 have less protein than the standard and those with relative intensities larger than 1 have more protein than the standard. The relative intensities are unitless values.

Based on their ability to hydrolyze and form new glycosidic bonds, Dcw1p and Dfg5p have been postulated as the enzymes that cleave the GPI- anchor at the plasma membrane and transfer the GPI-anchor protein remnant to non-reducing of β -1,6 glucan molecules at the wall. However, their precise role in this process remains ambiguous. Recent data shows that null mutants of these genes exhibit reduced levels of a GFP-labeled GPI-CWP reporter protein at the wall. Cells null for *dcw1*, but heterozygous for *DFG5*, fail to anchor the reporter protein to wall polysaccharides since it could not be

detected in cell wall preparations of this mutant. No attempts were made to determine the extent of excretion of the reporter protein (Mao et al. Personal communication). Mao's results are consistent with our observation that cell-surface fluorescence due to GFP-Sag1p expression is at least 1.5-2-fold lower in *dcw1/dcw1* and *dfg5/dfg5* cells than in wild-type cells (Figure 4.7). Furthermore, our observation that *dcw1/dcw1* cells excrete more GFP-Sag1p than *dfg5/dfg5* cells, relative to wild type, implies an important role for this gene in the cross-linking of GPI-proteins to cell-wall glucan following cleavage of the GPI-anchor most likely by Dfg5p. Mao's observation that *dcw1/dcw1* cells with a healthy copy of *DFG5*, completely fail to anchor the GPI-CWP reporter protein to the wall differ from our observations that anchorage can still proceed in *dcw1/dcw1* cells although to a lesser extent than in wild-type cells (Figure 4.7). This discrepancy may result from differences in reporter protein, expression yields, and/or differences in strain genetic background. Our robust expression system to enhance GFP yields may increase the number of GFP molecules at the wall to detectable levels in *dcw1/dcw1* cells. Combined with Mao's observations, our results suggest an indispensable role for Dcw1p in cross-linking GPI-CWPs to the cell wall. Notably, although we observe significant increments in the levels of excreted GFP-Sag1p in *dcw1/dcw1* and *dfg5/dfg5* cells in the presence of pepstatin A, the same does not hold true for the cytosolic protein PGK (Figure 4.3). When assayed for levels of excreted PGK, none of the cell-wall mutants examined showed increased levels of PGK in their supernatants in the presence of pepstatin A and the same was true for wild type. However, PGK was significantly hyper-excreted when the cells were grown in the presence of the protease inhibitor PMSF and when both inhibitors are used together (Figure 4.3). These findings suggest that pepstatin A's effect

in increasing GFP-Sag1p yields is not due to cell death and subsequent cell lysis and that PMSF might be causing cell lysis since large amounts of PGK were detected in supernatants from cells grown in the presence of PMSF.

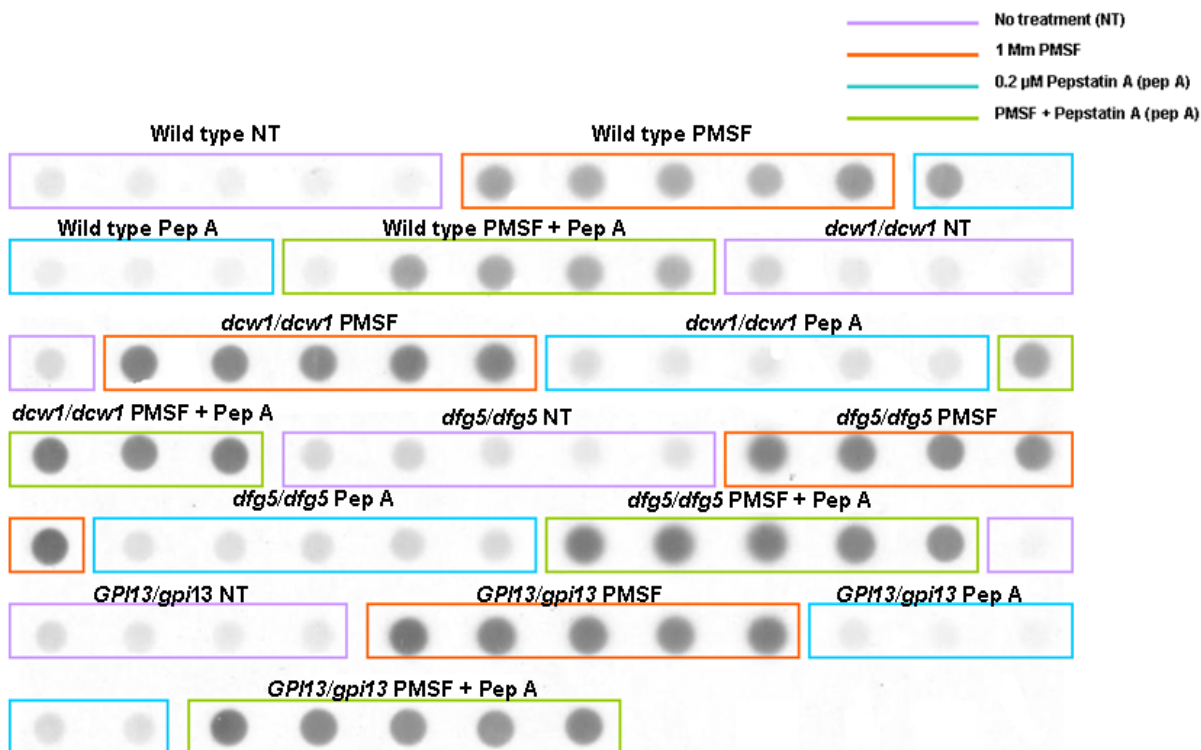


Figure 4.3. Dot blot analysis of PGK levels in cell-free supernatants of cells treated with pepstatin A, PMSF and both inhibitors together. 3 ml subclone cultures were grown in quintuple to early log phase (OD_{660} 0.2) at 18 °C in CSM-URA containing 1 M sorbitol, and treated with 1mM PMSF, pepstatin A, or both. Cultures were harvested at mid-log phase (OD_{660} 0.6-0.8) and their cell-free supernatants assayed for PGK levels using mouse monoclonal anti-PGK as the primary antibody and HRP-labeled goat anti-mouse as the secondary antibody.

It should be pointed out that *GPI13/gpi13* cells, which we found strongly hyper-excrete GFP-Sag1p in the absence of pepstatin A (Chapter 2I) are not affected by the addition of pepstatin A to the growth medium. It can be observed from figures 4.1 and 4.2 that the level of excreted GFP-Sag1p in these cells remains the same whether the cells are

grown with or without pepstatin A. This result supports our previous assumption that the level of GFP-Sag1p excretion from these cells may be abundant enough to allow for detection of the GPI-CWP hyper-excretion phenotype even on the face of GFP-Sag1p degradation by extracellular proteases. As observed for *dcw1/dcw1*, *dfg5/dfg5* and wild-type cells, pepstatin A did not lead to an increase in the level of cytosolic protein in the growth medium of *GPI13/gpi13* cells (Figure 4.3).

4.3b. Pestatin A does not affect growth rate and does not lead to increases in cell death

Our evidence that pepstatin A significantly increases yields of excreted GFP-Sag1p without compromising the cell's health is supported by observations that pepstatin A does not affect growth rate and does not lead to significant losses in cell viability. Figures 4.5 and 4.6 show growth curves for *dcw1/dcw1* and *dfg5/dfg5* cells, respectively, grown with and without pepstatin A compared to growth curves for wild-type cells treated and not treated with pepstatin A. Although *dcw1/dcw1* and *dfg5/dfg5* cells appear to grow slower than wild-type cells, it can be observed from figures 4.5 and 4.6 that their growth rates do not change by the addition of pepstatin A. In other words the cells grow at the same rate whether pepstatin A is added to the medium or not.

Cell death percentages for cells grown in the presence of pepstatin A and for non-treated cells were estimated by the methylene blue exclusion assay which permits distinguishing of dead cells from live ones based on differential permeability of the cells to the dye. Live cells have active mechanisms that can pump and keep the dye out of the cell and thus remain white/clear under the light microscope, whereas dead cells appear deep blue because of their inability to prevent entry of the dye into the cell. Figure 4.4

shows that the percentage of blue cells does not differ greatly between pepstatin A treated and non-treated cells for any of the examined strains.

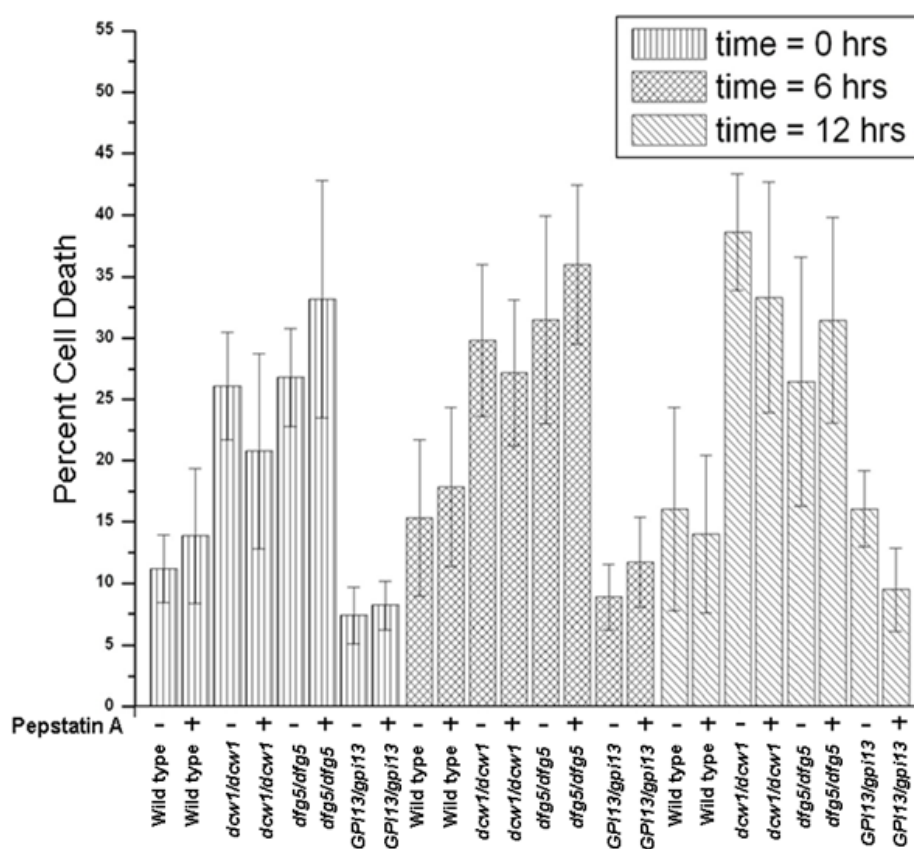


Figure 4.4. Effect of pepstatin A on cell viability. Percent cell death was determined by the methylene blue exclusion assay which stains dead cells blue. Average percentages and corresponding standard errors were based on triplicate counts of 1000 cells [total 1000 or 3000?] for each strain and taking the ratio of blue (dead) cells over total number of cells counted times 100. Cultures were grown to early log ($OD_{660\text{nm}} 0.2$) at 18°C in CSM-URA containing 1 M sorbitol, without (-) or with $1\ \mu\text{M}$ pepstatin A (+). Cell samples for staining with methylene blue were collected at 0, 6 and 12 hours after addition of pepstatin A.

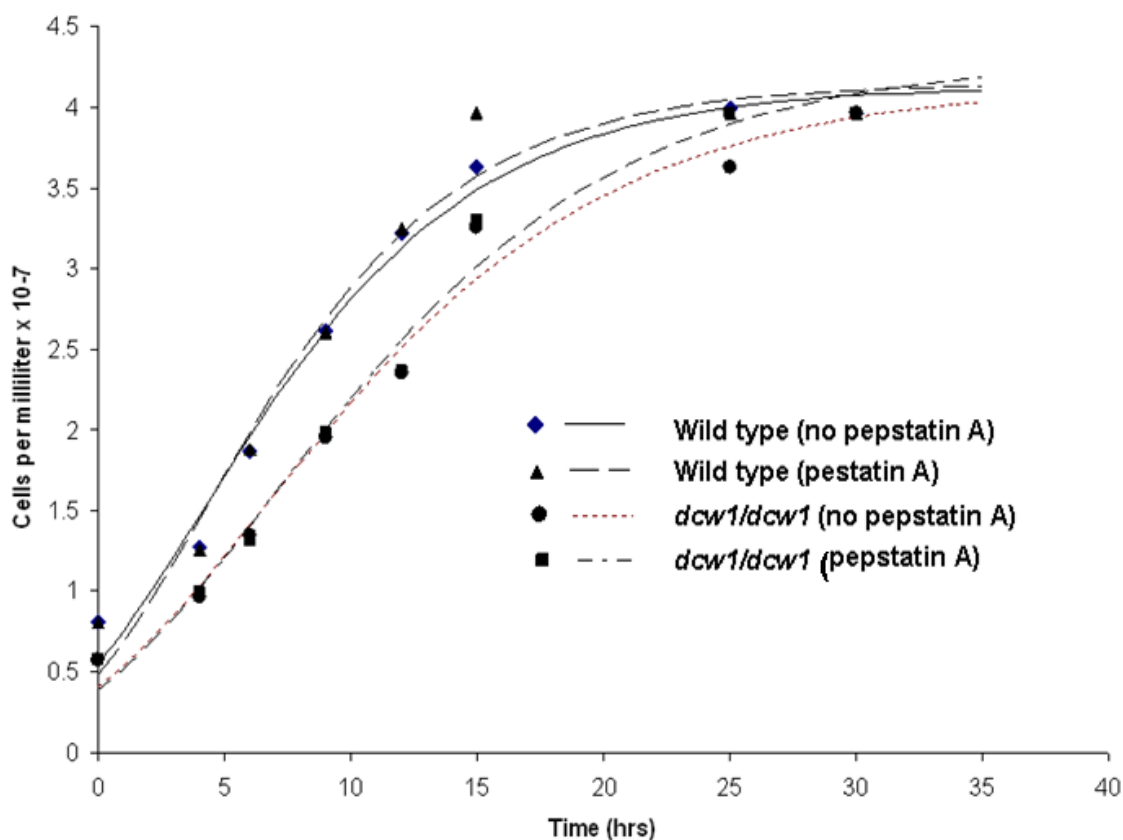


Figure 4.5. Effect of pepstatin A on growth rate of wild type and *dcw1/dcw1* cells. Cells were grown to early log phase (OD_{660} 0.2) at 18 °C in CSM-URA containing 1 M sorbitol. At T=0 hrs, cultures were split, and Pepstatin A (1 μ M) was added to half of the subcultures. OD_{660} measurements were taken at indicated intervals.

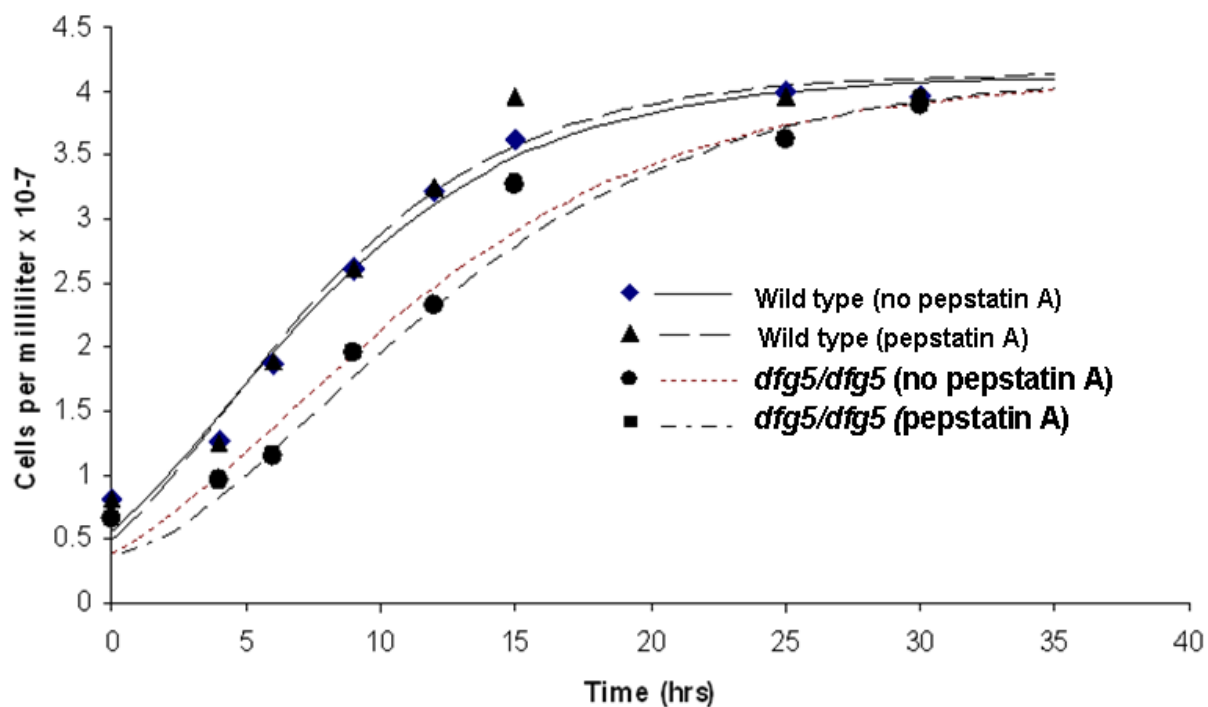


Figure 4.6. Effect of pepstatin A on growth rate of wild type and *dfg5/dfg5* cells. Cells were grown to early log phase (OD_{660} 0.2) at 18 °C in CSM-URA containing 1 M sorbitol. At T=0 hrs, cultures were split, and Pepstatin A (1 μ M) was added to half of the subcultures. OD_{660} measurements were taken at indicated intervals.

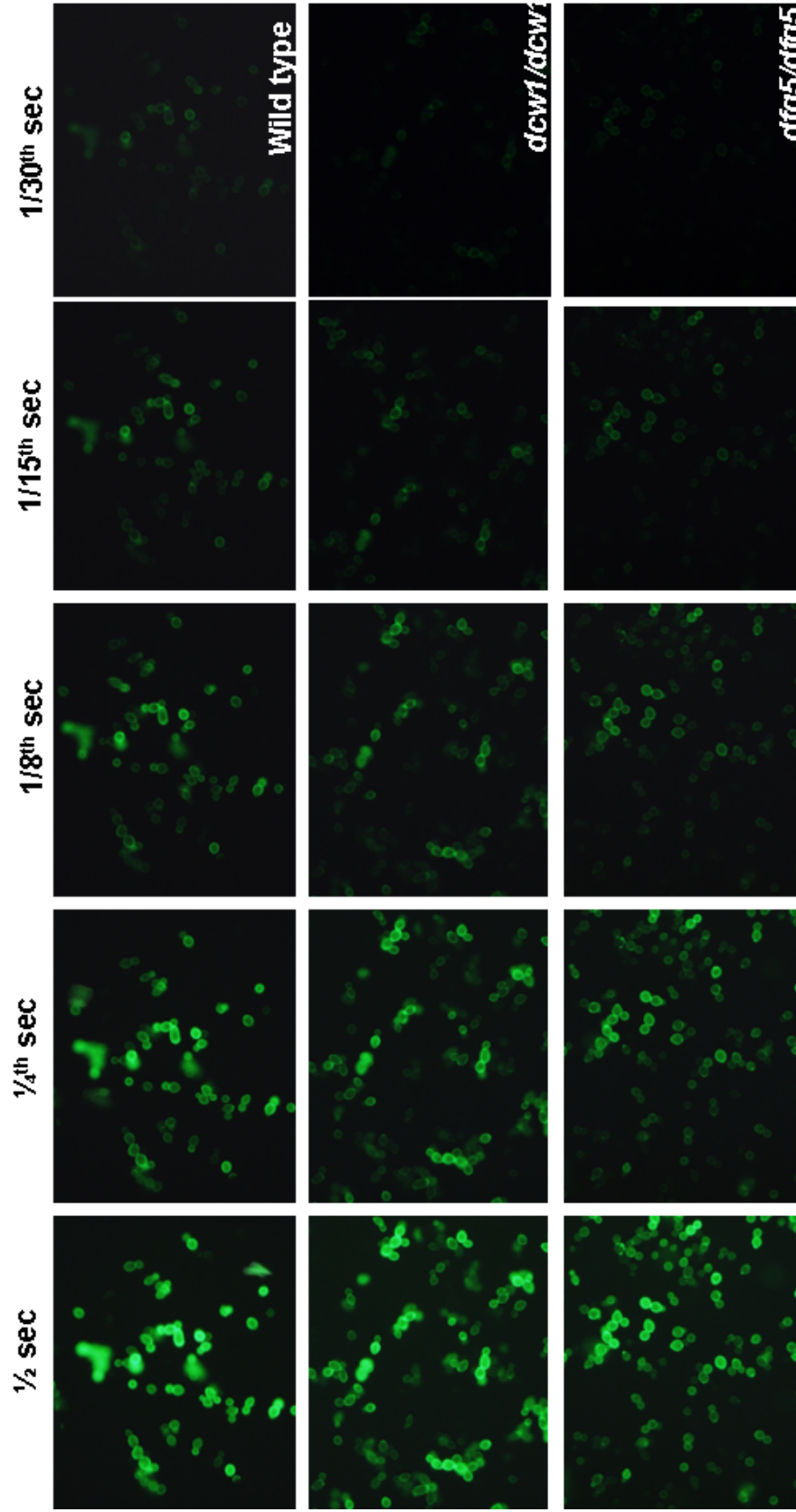


Figure 4.7. Visualization of cell surface fluorescence by fluorescence microscopy. Cells were grown to early log phase (OD_{660} 0.3-0.4) at 18°C in CSM-URA containing 1 M sorbitol and buffered to pH 6.5 with 50mM MOPS. Cells were harvested, washed with dh20 and re-suspended in 10 mM Tris-HCL pH 7.5 prior to fluorescence analysis. Images were captures at exposure times of $\frac{1}{2}$ - $\frac{1}{30}$ th of a second for estimation of cell surface fluorescence as described in Materials and Methods. Both *dcw1/dcw1* and *dfg5/dfg5* cells were estimated to exhibit ~ 1.5 -2-fold less fluorescence at the cell surface than wild type cells.

Homologs of Dcw1p and Dfg5p are widely distributed among the fungi and constitute a large family whose members are speculated to play similar roles to those of Dcw1p and Dfg5p. Although it has been previously shown that *dcw1/dcw1*, *DFG5/dfg5* cells hyper-excrete GPI-CWPs into the growth medium, we are the first to report a similar phenotype for individual null mutants of these genes. Because the hyper-excretion phenotype, relative to wild-type cells, appears graver in cells missing *DCW1* than in cells deleted for *DFG5*, our results suggest a more critical role for *DCW1* than for *DFG5* in the cross-linking of GPI-CWPs to cell-wall glucan. These results are consistent with others' observations that *dcw1/dcw1* cells exhibit more severe wall phenotypes than *dfg5/dfg5* cells. Combined with previous observations, our results suggest that *DCW1* and *DFG5* may not be redundant genes that compensate for each other's function but rather share the process of cleaving the GPI-anchor and cross-linking the anchor-protein remnant to cell-wall glucan. The mechanism may be one by which Dfg5p preferentially acts to cleave at the glycan part of the GPI-anchor while Dcw1p catalyzes cross-linking of the glycoprotein product to the cell wall. Alternatively, both Dcw1p and Dfg5p might harbor the ability to process the GPI-anchor while transglycosylation to cell-wall glucan is more optimally carried-out by Dcw1p. This would help explain why *dfg5* deletions are less detrimental to the integrity of the cell wall and our observation that *dcw1/dcw1* cells excrete significantly more GFP-Sag1p than *dfg5/dfg5* cells relative to wild-type cells. Elucidation of the enzymatic function and the role in cell wall biosynthesis of Dcw1p/Dfg5p may reveal a common and critical step in the cell wall biosynthesis of fungi. This may lead to the development of new antifungal drugs, as the cell wall biosynthesis pathway is specific to fungi and not found in higher eukaryotes such as

animals and plants. It is likely that new aspects of cell wall biosynthesis will be clarified by investigating *DCW1/DFG5*.

Chapter 5

Concluding Remarks

5.1. A need for novel antifungals

The need for novel antifungal treatments has become critical in the last decades due to the growing number of patients suffering from immunosuppression. Among the affected patients are those undergoing cancer treatments, recipients of organ transplants and medical indwelling devices as well as the critically ill, the elderly and the newborn. Adding to this need is the incremental use of currently available treatments as a preventive measure among those at most risk since this practice is rapidly leading to the emergence of resistant strains. With the exception of the echinocandins, which disrupt cell wall synthesis, currently available antifungals work to inhibit plasma membrane synthesis and can thus present serious toxicity problems to mammalian cells.

5.2 GPI-CWP anchorage to the fungal cell wall: an ideal target for antifungal drug design.

Based on the much milder toxicity effects and overall success associated with cell-wall targeted antifungals, large interest exists in developing novel drugs capable of targeting the cell wall. A condition hampering this process is the unavailability of ideal cell wall targets. To aid in the elucidation of novel cell wall targets we developed an approach to screen the fungal genome for genes required for the cross-linking of GPI-CWPs to the fungal wall. The biosynthetic pathway for the incorporation of these proteins at the wall represents an excellent target because it is essential and unique to fungi. Additionally, the fungal cell depends on an arsenal of GPI-CWPs at the wall to

build the wall, to maintain cell wall stability and proper functioning and in the case pathogenic fungi to aid in the process of infection.

To search for genes required for GPI-CWP anchoring to the cell wall we tested the idea that mutants unable to properly cross-link GPI-CWPs to the wall could be identified based on their expression patterns of a GPI-CWP marker protein. Such mutants would either retain the marker protein within the cell (hypo-excretors) or upon failing to anchor the reporter protein to the wall hyper-excrete it into the growth medium relative to wild type strains. The marker protein was made by fusing GFP to the carboxyl end of the GPI-CWP α -agglutinin and was hyper-excreted from cell-wall mutants previously shown to hyper-excrete GPI-CWPs.

5.3. Development of a robust reporting assay of deficiencies in GPI-CWP anchorage to the cell wall

To address the commonly encountered problem of low GFP yields, particularly in assays requiring excretion of GFP into the culturing medium, a robust expression system was developed that lead to significant increase in GFP yields. We observed that by expressing the GFP reporter protein from the *GPD1* promoter at lower temperature in the presence of 1 M sorbitol and at pH 6.5, GFP yields increased sufficiently to enable its detection above interference/background fluorescence, which in combination with low expression yields, has limited the use of GFP as a reporter of protein excretion. The increase in GFP yields is likely due to enhanced protein solubilization and folding which can prevent the formation of protein aggregates that can significantly lower protein yields. This assumption was based on previous studies that show that 1 M sorbitol

induces synthesis of intracellular glycerol to counterbalance higher solute concentrations outside the cell, and that glycerol promotes protein folding by promoting protein solubilization and stability. Furthermore, up-regulation of heat-shock proteins that aid in protein folding has also been reported in *S. cerevisiae* cells exposed to high osmolarity.

Other studies have shown enhanced folding of GFP and reduction in protease activity at lower temperature, which can work synergistically to further enhance protein yields. A previous study also shows that 1 M sorbitol increases transcription from the *GPD1* promoter in *S. cerevisiae* to at least 8-fold. In such study, *gpd1Δ* cells were transformed with an episomal copy of the *GPD1* gene thus transcription of the gene could be driven from the cytoplasm. These findings imply that the increased GFP yields observed in this study could also be due to enhanced transcription from the *GPD1* promoter in the presence of 1 M sorbitol.

In summary, it is likely that better GFP yields resulted from the combined effects of increased transcription under conditions that promote protein stability and better protein folding. Additionally, many studies report bottle necks at the level of post-transcriptional protein processing, thus conditions that prevent aggregation of misfolded proteins and keep the proteins stable during folding should lead to significant improvements in functional protein yields.

5.4. High-throughput application of the reporting assay to screen for genes required for GPI-CWP anchorage to the cell wall.

With a robust marker protein expression system in place it became possible to obtain measurable marker protein quantities from small culture volumes. This in turn

allowed for the scaling-up of sample analysis. For example, reproducible marker protein amounts could be detected from microliter volumes of cell-free supernatants from 3 mL cultures. Growing 3 mL cultures in 100x13 borosilicate tubes provided the advantage that cell growth could be conveniently monitored by taking OD measurements directly from the tubes. For large-scale screening of deficiencies in anchorage of the reporter protein to the cell wall, 178 gene deletants from the *S. cerevisiae* gene deletion collection were transformed in high throughput with plasmid pGFP-Sag1p encoding the reporter protein. Transformed colonies of similar size were grown in test tubes as just described to mid-log phase and 200 μ l of their cell-free supernatants assayed for GFP levels using a 96-well plate reader fluorimeter. Triplicate assays using this approach lead to the identification of seven hyper-excretors of the cell wall marker protein, relative to wild type parental strains. The seven strains were subjected to secondary screens for confirmation of the hyper-excretion phenotype. Secondary screens were based in GFP detection by immunoblotting and collection of complete fluorescence spectra that could be corrected for background/interference fluorescence. Upon secondary screens, four of the seven gene deletants were confirmed as genuine hyper-excretors. For the remaining three, GFP was barely detectable using anti-GFP antibodies. All seven mutants were also found to excrete less than wild type levels of the cytosolic marker, 3-phosphoglycerate kinase (PGK), indicating that increased GFP levels in cell-free supernatants was unlikely to be due to cell death and lysis. Confirmed hyper-excretors and a false positive were further examined for total protein excreted into the growth medium. No significant difference in total protein was observed among the examined strains.

5.5. Genes identified as required for GPI-CWP anchorage to the cell wall

Two essential genes *MCD4* and *GPI13*, previously implicated in GPI-anchor biosynthesis were found to lead to GPI-CWP hyper-excretion and to elevate GPI-CWP levels at the cell wall 2-4 fold relative to wild-type cells when one allele was deleted. The genes have been described to add ethanolamine phosphate groups to mannose residues of the GPI-anchor. *GPI13* plays a critical role as it adds the ethanolamine phosphate that links the GPI-anchor to precursor GPI-CWPs via an amide bond. *MCD4* is thought to add ethanolamine to the first mannose residue of the GPI-anchor. Both genes are essential in fungi, and not in mammals, which make them ideal targets for drug design.

The *GDA1* and *TDH3* genes are not essential for cell viability and their diploid null mutants showed substantial lowering of the GPI-CWPs marker protein at the wall and hyper-excreted the marker protein relative to wild-type cells. *GDA1* is a GDPase involved in elongation of O-linked mannan side chains of GPI-CWPs at the Golgi, and *TDH3* is a glycolytic enzyme that resides both inside the cell and at the cell wall and has been found to act as an adhesin that promotes cell-cell binding and adhesion to host substrates. In *C. albicans*, *TDH3* was also found to act as immunogen to activate a host immune response.

5.6. Pepstatin A enhances sensitivity of the screening assay

Addition of 1 μ M pepstatin A to early log cultures led to large increases in excreted GFP in mutants that would otherwise show as hypo-excretors relative to wild-type cells. Such was the case for null mutants of the transglycosidases Dcw1p and Dfg5p, which have been suggested to play a direct role in the cross-linking GPI-CWPs to the cell

wall. Pepstatin A is an aspartyl protease inhibitor, thus it may act to protect excreted GFP from proteolysis. Pepstatin A may also inhibit the “shedding” of GPI-anchored aspartyl proteases from the wall which would further lower proteolytic activity in the medium. This would be consistent with the observation that pepstatin A leads to a slight decrease of the marker protein in supernatants from wild-type cells. At the concentration used, pepstatin A was observed not to affect growth rate or to increase cell death.

Although the genomic screen was carried out without the use of pepstatin A for concerns that it would add to cell-wall damage due to previously ascribed roles to aspartyl proteases in cell-wall maintenance, the findings from this study describe and suggest conditions that may substantially increase the sensitivity of the screening assay. Importantly, because we have defined conditions that enhanced the use of GFP as a reporter of protein excretion, the assay may be applied to any fungus of interest with suitable protein expression systems.

References:

1. Singh, N., *Trends in the epidemiology of opportunistic fungal infections: predisposing factors and the impact of antimicrobial use practices*. Clin Infect Dis, 2001. **33**(10): p. 1692-6.
2. Rocco, T.R., S.E. Reinert, and H.H. Simms, *Effects of fluconazole administration in critically ill patients: analysis of bacterial and fungal resistance*. Arch Surg, 2000. **135**(2): p. 160-5.
3. Gleason, T.G., et al., *Emerging evidence of selection of fluconazole-tolerant fungi in surgical intensive care units*. Arch Surg, 1997. **132**(11): p. 1197-201; discussion 1202.
4. Wisplinghoff, H., et al., *Nosocomial bloodstream infections in US hospitals: analysis of 24,179 cases from a prospective nationwide surveillance study*. Clin Infect Dis, 2004. **39**(3): p. 309-17.
5. Rex, J.H., et al., *A randomized and blinded multicenter trial of high-dose fluconazole plus placebo versus fluconazole plus amphotericin B as therapy for candidemia and its consequences in nonneutropenic subjects*. Clin Infect Dis, 2003. **36**(10): p. 1221-8.
6. van Burik, J.H., et al., *The effect of prophylactic fluconazole on the clinical spectrum of fungal diseases in bone marrow transplant recipients with special attention to hepatic candidiasis. An autopsy study of 355 patients*. Medicine (Baltimore), 1998. **77**(4): p. 246-54.
7. Espinel-Ingroff, A. and S. Shadomy, *In vitro and in vivo evaluation of antifungal agents*. Eur J Clin Microbiol Infect Dis, 1989. **8**(4): p. 352-61.
8. Bennett, M.R., D.L. Weinbaum, and P.C. Fiehler, *Chronic necrotizing pulmonary aspergillosis treated by endobronchial amphotericin B*. South Med J, 1990. **83**(7): p. 829-32.
9. Cornely, O.A., *Aspergillus to Zygomycetes: Causes, Risk Factors, Prevention, and Treatment of Invasive Fungal Infections*. Infection, 2008. **36**(6): p. 605-606.
10. Odds, F.C., *Resistance of yeasts to azole-derivative antifungals*. J Antimicrob Chemother, 1993. **31**(4): p. 463-71.
11. Denning, D.W., *Echinocandins: a new class of antifungal*. J Antimicrob Chemother, 2002. **49**(6): p. 889-91.

12. Verstrepen, K.J. and F.M. Klis, *Flocculation, adhesion and biofilm formation in yeasts*. Mol Microbiol, 2006. **60**(1): p. 5-15.
13. Douglas, L.J., *Candida biofilms and their role in infection*. Trends Microbiol, 2003. **11**(1): p. 30-6.
14. Norice, C.T., et al., *Requirement for Candida albicans Sun41 in biofilm formation and virulence*. Eukaryot Cell, 2007. **6**(11): p. 2046-55.
15. Richard, M., et al., *Complete glycosylphosphatidylinositol anchors are required in Candida albicans for full morphogenesis, virulence and resistance to macrophages*. Mol Microbiol, 2002. **44**(3): p. 841-53.
16. Alloush, H.M., et al., *3-phosphoglycerate kinase: a glycolytic enzyme protein present in the cell wall of Candida albicans*. Microbiology, 1997. **143** (Pt 2): p. 321-30.
17. Angiolella, L., et al., *Identification of a glucan-associated enolase as a main cell wall protein of Candida albicans and an indirect target of lipopeptide antimycotics*. J Infect Dis, 1996. **173**(3): p. 684-90.
18. de Groot, P.W., et al., *Mass spectrometric identification of covalently bound cell wall proteins from the fission yeast Schizosaccharomyces pombe*. Yeast, 2007. **24**(4): p. 267-78.
19. Giusiano, G., et al., *Fluconazole and itraconazole resistance of yeasts isolated from the bloodstream and catheters of hospitalized pediatric patients*. Chemotherapy, 2006. **52**(5): p. 254-9.
20. Kollar, R., et al., *Architecture of the yeast cell wall. Beta(1-->6)-glucan interconnects mannoprotein, beta(1-->)3-glucan, and chitin*. J Biol Chem, 1997. **272**(28): p. 17762-75.
21. De Groot, P.W., A.F. Ram, and F.M. Klis, *Features and functions of covalently linked proteins in fungal cell walls*. Fungal Genet Biol, 2005. **42**(8): p. 657-75.
22. Kapteyn, J.C., et al., *Covalent association of beta-1,3-glucan with beta-1,6-glucosylated mannoproteins in cell walls of Candida albicans*. J Bacteriol, 1995. **177**(13): p. 3788-92.
23. Kapteyn, J.C., H. Van Den Ende, and F.M. Klis, *The contribution of cell wall proteins to the organization of the yeast cell wall*. Biochim Biophys Acta, 1999. **1426**(2): p. 373-83.
24. Klis, F.M., et al., *Dynamics of cell wall structure in Saccharomyces cerevisiae*. FEMS Microbiol Rev, 2002. **26**(3): p. 239-56.

25. Lu, C.F., et al., *Glycosyl phosphatidylinositol-dependent cross-linking of alpha-agglutinin and beta 1,6-glucan in the Saccharomyces cerevisiae cell wall*. J Cell Biol, 1995. **128**(3): p. 333-40.
26. Guarro, J., GeneJ, and A.M. Stchigel, *Developments in fungal taxonomy*. Clin Microbiol Rev, 1999. **12**(3): p. 454-500.
27. Kapteyn, J.C., et al., *Retention of Saccharomyces cerevisiae cell wall proteins through a phosphodiester-linked beta-1,3-/beta-1,6-glucan heteropolymer*. Glycobiology, 1996. **6**(3): p. 337-45.
28. Lipke, P.N. and R. Ovalle, *Cell wall architecture in yeast: new structure and new challenges*. J Bacteriol, 1998. **180**(15): p. 3735-40.
29. Ecker, M., et al., *Pir proteins of Saccharomyces cerevisiae are attached to beta-1,3-glucan by a new protein-carbohydrate linkage*. J Biol Chem, 2006. **281**(17): p. 11523-9.
30. Englund, P.T., *The structure and biosynthesis of glycosyl phosphatidylinositol protein anchors*. Annu Rev Biochem, 1993. **62**: p. 121-38.
31. Mayor, S., A.K. Menon, and G.A. Cross, *Transfer of glycosyl-phosphatidylinositol membrane anchors to polypeptide acceptors in a cell-free system*. J Cell Biol, 1991. **114**(1): p. 61-71.
32. Shaw, J.A., et al., *The function of chitin synthases 2 and 3 in the Saccharomyces cerevisiae cell cycle*. J Cell Biol, 1991. **114**(1): p. 111-23.
33. Cabib, E., et al., *The yeast cell wall and septum as paradigms of cell growth and morphogenesis*. J Biol Chem, 2001. **276**(23): p. 19679-82.
34. Hartland, R.P., et al., *The linkage of (1-3)-beta-glucan to chitin during cell wall assembly in Saccharomyces cerevisiae*. Yeast, 1994. **10**(12): p. 1591-9.
35. Boorsma, A., et al., *Characterization of the transcriptional response to cell wall stress in Saccharomyces cerevisiae*. Yeast, 2004. **21**(5): p. 413-27.
36. Kapteyn, J.C., et al., *The cell wall architecture of Candida albicans wild-type cells and cell wall-defective mutants*. Mol Microbiol, 2000. **35**(3): p. 601-11.
37. Ram, A.F., et al., *Loss of the plasma membrane-bound protein Gas1p in Saccharomyces cerevisiae results in the release of beta1,3-glucan into the medium and induces a compensation mechanism to ensure cell wall integrity*. J Bacteriol, 1998. **180**(6): p. 1418-24.

38. Ford, R.A., J.A. Shaw, and E. Cabib, *Yeast chitin synthases 1 and 2 consist of a non-homologous and dispensable N-terminal region and of a homologous moiety essential for function*. Mol Gen Genet, 1996. **252**(4): p. 420-8.
39. Cid, V.J., et al., *Molecular basis of cell integrity and morphogenesis in Saccharomyces cerevisiae*. Microbiol Rev, 1995. **59**(3): p. 345-86.
40. Cabib, E., et al., *Crh1p and Crh2p are required for the cross-linking of chitin to beta(1-6)glucan in the Saccharomyces cerevisiae cell wall*. Mol Microbiol, 2007. **63**(3): p. 921-35.
41. Goto, M., *Protein O-glycosylation in fungi: diverse structures and multiple functions*. Biosci Biotechnol Biochem, 2007. **71**(6): p. 1415-27.
42. Cutler, J.E., *N-glycosylation of yeast, with emphasis on Candida albicans*. Med Mycol, 2001. **39 Suppl 1**: p. 75-86.
43. Kukuruzinska, M.A. and K. Lennon, *Protein N-glycosylation: molecular genetics and functional significance*. Crit Rev Oral Biol Med, 1998. **9**(4): p. 415-48.
44. Lehle, L., S. Strahl, and W. Tanner, *Protein glycosylation, conserved from yeast to man: a model organism helps elucidate congenital human diseases*. Angew Chem Int Ed Engl, 2006. **45**(41): p. 6802-18.
45. Lamani, E., et al., *Structural studies and mechanism of Saccharomyces cerevisiae dolichyl-phosphate-mannose synthase: insights into the initial step of synthesis of dolichyl-phosphate-linked oligosaccharide chains in membranes of endoplasmic reticulum*. Glycobiology, 2006. **16**(7): p. 666-78.
46. Berninsone, P., J.J. Miret, and C.B. Hirschberg, *The Golgi guanosine diphosphatase is required for transport of GDP-mannose into the lumen of Saccharomyces cerevisiae Golgi vesicles*. J Biol Chem, 1994. **269**(1): p. 207-11.
47. Conde, R., et al., *Screening for new yeast mutants affected in mannosylphosphorylation of cell wall mannoproteins*. Yeast, 2003. **20**(14): p. 1189-211.
48. Jigami, Y. and T. Odani, *Mannosylphosphate transfer to yeast mannan*. Biochim Biophys Acta, 1999. **1426**(2): p. 335-45.
49. Humbel, B.M., et al., *In situ localization of beta-glucans in the cell wall of Schizosaccharomyces pombe*. Yeast, 2001. **18**(5): p. 433-44.
50. Breinig, F., K. Schleinkofer, and M.J. Schmitt, *Yeast Kre1p is GPI-anchored and involved in both cell wall assembly and architecture*. Microbiology, 2004. **150**(Pt 10): p. 3209-18.

51. Page, N., et al., *A Saccharomyces cerevisiae genome-wide mutant screen for altered sensitivity to KI killer toxin*. Genetics, 2003. **163**(3): p. 875-94.
52. Shahinian, S. and H. Bussey, *beta-1,6-Glucan synthesis in Saccharomyces cerevisiae*. Mol Microbiol, 2000. **35**(3): p. 477-89.
53. Levinson, J.N., et al., *Functional, comparative and cell biological analysis of Saccharomyces cerevisiae Kre5p*. Yeast, 2002. **19**(14): p. 1243-59.
54. Inoue, S.B., et al., *Characterization and gene cloning of 1,3-beta-D-glucan synthase from Saccharomyces cerevisiae*. Eur J Biochem, 1995. **231**(3): p. 845-54.
55. Ram, A.F., et al., *Identification of two cell cycle regulated genes affecting the beta 1,3-glucan content of cell walls in Saccharomyces cerevisiae*. FEBS Lett, 1995. **358**(2): p. 165-70.
56. Qadota, H., et al., *Identification of yeast Rho1p GTPase as a regulatory subunit of 1,3-beta-glucan synthase*. Science, 1996. **272**(5259): p. 279-81.
57. Mouyna, I., et al., *Identification of the catalytic residues of the first family of beta(1-3)glucanosyltransferases identified in fungi*. Biochem J, 2000. **347 Pt 3**: p. 741-7.
58. Orlean, P. and A.K. Menon, *Thematic review series: lipid posttranslational modifications. GPI anchoring of protein in yeast and mammalian cells, or: how we learned to stop worrying and love glycopospholipids*. J Lipid Res, 2007. **48**(5): p. 993-1011.
59. Li, H., et al., *Glycosylphosphatidylinositol (GPI) anchor is required in Aspergillus fumigatus for morphogenesis and virulence*. Mol Microbiol, 2007. **64**(4): p. 1014-27.
60. Tiede, A., et al., *Biosynthesis of glycosylphosphatidylinositols in mammals and unicellular microbes*. Biol Chem, 1999. **380**(5): p. 503-23.
61. Frieman, M.B. and B.P. Cormack, *Multiple sequence signals determine the distribution of glycosylphosphatidylinositol proteins between the plasma membrane and cell wall in Saccharomyces cerevisiae*. Microbiology, 2004. **150**(Pt 10): p. 3105-14.
62. Fujii, T., H. Shimoi, and Y. Iimura, *Structure of the glucan-binding sugar chain of Tip1p, a cell wall protein of Saccharomyces cerevisiae*. Biochim Biophys Acta, 1999. **1427**(2): p. 133-44.

63. Lu, C.F., J. Kurjan, and P.N. Lipke, *A pathway for cell wall anchorage of Saccharomyces cerevisiae alpha-agglutinin*. Mol Cell Biol, 1994. **14**(7): p. 4825-33.
64. Kitagaki, H., et al., *Two homologous genes, DCW1 (YKL046c) and DFG5, are essential for cell growth and encode glycosylphosphatidylinositol (GPI)-anchored membrane proteins required for cell wall biogenesis in Saccharomyces cerevisiae*. Mol Microbiol, 2002. **46**(4): p. 1011-22.
65. Delgado, M.L., M.L. Gil, and D. Gozalbo, *Candida albicans TDH3 gene promotes secretion of internal invertase when expressed in Saccharomyces cerevisiae as a glyceraldehyde-3-phosphate dehydrogenase-invertase fusion protein*. Yeast, 2003. **20**(8): p. 713-22.
66. Klis, F.M., et al., *Extraction of cell surface-associated proteins from living yeast cells*. Yeast, 2007. **24**(4): p. 253-8.
67. Smits, G.J., et al., *Cell wall dynamics in yeast*. Curr Opin Microbiol, 1999. **2**(4): p. 348-52.
68. de Nobel, J.G., et al., *The glucanase-soluble mannoproteins limit cell wall porosity in Saccharomyces cerevisiae*. Yeast, 1990. **6**(6): p. 491-9.
69. de Nobel, H., et al., *Genetics of a-agglutinin function in Saccharomyces cerevisiae*. Mol Gen Genet, 1995. **247**(4): p. 409-15.
70. Sundstrom, P., *Adhesion in Candida spp*. Cell Microbiol, 2002. **4**(8): p. 461-9.
71. Nimrichter, L., et al., *The multitude of targets for the immune system and drug therapy in the fungal cell wall*. Microbes Infect, 2005. **7**(4): p. 789-98.
72. Altamura, M., et al., *Immune responses to fungal infections and therapeutic implications*. Curr Drug Targets Immune Endocr Metabol Disord, 2001. **1**(3): p. 189-97.
73. Rast, D.M., et al., *Cell wall-associated enzymes in fungi*. Phytochemistry, 2003. **64**(2): p. 339-66.
74. Hamada, K., et al., *Screening for glycosylphosphatidylinositol (GPI)-dependent cell wall proteins in Saccharomyces cerevisiae*. Mol Gen Genet, 1998. **258**(1-2): p. 53-9.
75. Van Der Vaart, J.M., et al., *The beta-1, 6-glucan containing side-chain of cell wall proteins of Saccharomyces cerevisiae is bound to the glycan core of the GPI moiety*. FEMS Microbiol Lett, 1996. **145**(3): p. 401-7.

76. van der Vaart, J.M., et al., *The retention mechanism of cell wall proteins in Saccharomyces cerevisiae. Wall-bound Cwp2p is beta-1,6-glucosylated.* Biochim Biophys Acta, 1996. **1291**(3): p. 206-14.
77. Hamada, K., et al., *Amino acid residues in the omega-minus region participate in cellular localization of yeast glycosylphosphatidylinositol-attached proteins.* J Bacteriol, 1999. **181**(13): p. 3886-9.
78. Pittet, M. and A. Conzelmann, *Biosynthesis and function of GPI proteins in the yeast Saccharomyces cerevisiae.* Biochim Biophys Acta, 2007. **1771**(3): p. 405-20.
79. Sutterlin, C., et al., *Specific requirements for the ER to Golgi transport of GPI-anchored proteins in yeast.* J Cell Sci, 1997. **110 (Pt 21)**: p. 2703-14.
80. Weig, M., et al., *Systematic identification in silico of covalently bound cell wall proteins and analysis of protein-polysaccharide linkages of the human pathogen Candida glabrata.* Microbiology, 2004. **150**(Pt 10): p. 3129-44.
81. de Groot, P.W., et al., *Proteomic analysis of Candida albicans cell walls reveals covalently bound carbohydrate-active enzymes and adhesins.* Eukaryot Cell, 2004. **3**(4): p. 955-65.
82. Yin, Q.Y., et al., *Comprehensive proteomic analysis of Saccharomyces cerevisiae cell walls: identification of proteins covalently attached via glycosylphosphatidylinositol remnants or mild alkali-sensitive linkages.* J Biol Chem, 2005. **280**(21): p. 20894-901.
83. Jung, U.S. and D.E. Levin, *Genome-wide analysis of gene expression regulated by the yeast cell wall integrity signalling pathway.* Mol Microbiol, 1999. **34**(5): p. 1049-57.
84. Lagorce, A., et al., *Genome-wide analysis of the response to cell wall mutations in the yeast Saccharomyces cerevisiae.* J Biol Chem, 2003. **278**(22): p. 20345-57.
85. Que, Q.Q. and E.A. Winzeler, *Large-scale mutagenesis and functional genomics in yeast.* Funct Integr Genomics, 2002. **2**(4-5): p. 193-8.
86. Winzeler, E.A., et al., *Functional characterization of the S. cerevisiae genome by gene deletion and parallel analysis.* Science, 1999. **285**(5429): p. 901-6.
87. Kelly, D.E., D.C. Lamb, and S.L. Kelly, *Genome-wide generation of yeast gene deletion strains.* Comp Funct Genomics, 2001. **2**(4): p. 236-42.
88. Giaever, G., et al., *Functional profiling of the Saccharomyces cerevisiae genome.* Nature, 2002. **418**(6896): p. 387-91.

89. Muren, E., et al., *Identification of yeast deletion strains that are hypersensitive to brefeldin A or monensin, two drugs that affect intracellular transport*. *Yeast*, 2001. **18**(2): p. 163-72.
90. Zhang, N., et al., *Disruption of six novel ORFs on the left arm of chromosome XII reveals one gene essential for vegetative growth of *Saccharomyces cerevisiae**. *Yeast*, 1999. **15**(12): p. 1287-96.
91. Avaro, S., et al., *Mutants defective in secretory/vacuolar pathways in the EUROFAN collection of yeast disruptants*. *Yeast*, 2002. **19**(4): p. 351-71.
92. Chalfie, M., et al., *Green fluorescent protein as a marker for gene expression*. *Science*, 1994. **263**(5148): p. 802-5.
93. Cormack, B., *Green fluorescent protein as a reporter of transcription and protein localization in fungi*. *Curr Opin Microbiol*, 1998. **1**(4): p. 406-10.
94. Rosochacki, S.J. and M. Matejczyk, *Green fluorescent protein as a molecular marker in microbiology*. *Acta Microbiol Pol*, 2002. **51**(3): p. 205-16.
95. Margolin, W., *Green fluorescent protein as a reporter for macromolecular localization in bacterial cells*. *Methods*, 2000. **20**(1): p. 62-72.
96. Spear, R.N., D. Cullen, and J.H. Andrews, *Fluorescent labels, confocal microscopy, and quantitative image analysis in study of fungal biology*. *Methods Enzymol*, 1999. **307**: p. 607-23.
97. Zimmer, M., *Green fluorescent protein (GFP): applications, structure, and related photophysical behavior*. *Chem Rev*, 2002. **102**(3): p. 759-81.
98. Misteli, T. and D.L. Spector, *Applications of the green fluorescent protein in cell biology and biotechnology*. *Nat Biotechnol*, 1997. **15**(10): p. 961-4.
99. Cormack, B.P., et al., *Yeast-enhanced green fluorescent protein (yEGFP) a reporter of gene expression in *Candida albicans**. *Microbiology*, 1997. **143** (Pt 2): p. 303-11.
100. Chiu, W., et al., *Engineered GFP as a vital reporter in plants*. *Curr Biol*, 1996. **6**(3): p. 325-30.
101. Haas, J., E.C. Park, and B. Seed, *Codon usage limitation in the expression of HIV-1 envelope glycoprotein*. *Curr Biol*, 1996. **6**(3): p. 315-24.
102. Collins, L.A., M.N. Torrero, and S.G. Franzblau, *Green fluorescent protein reporter microplate assay for high-throughput screening of compounds against *Mycobacterium tuberculosis**. *Antimicrob Agents Chemother*, 1998. **42**(2): p. 344-7.

103. Changsen, C., S.G. Franzblau, and P. Palittapongarnpim, *Improved green fluorescent protein reporter gene-based microplate screening for antituberculosis compounds by utilizing an acetamidase promoter*. *Antimicrob Agents Chemother*, 2003. **47**(12): p. 3682-7.
104. Nakai, J., M. Ohkura, and K. Imoto, *A high signal-to-noise Ca(2+) probe composed of a single green fluorescent protein*. *Nat Biotechnol*, 2001. **19**(2): p. 137-41.
105. Rizzo, M.A., et al., *An improved cyan fluorescent protein variant useful for FRET*. *Nat Biotechnol*, 2004. **22**(4): p. 445-9.
106. Gordon, C.L., et al., *A glucoamylase::GFP gene fusion to study protein secretion by individual hyphae of Aspergillus niger*. *J Microbiol Methods*, 2000. **42**(1): p. 39-48.
107. Hraska, M., et al., *Sample topography and position within plant body influence the detection of the intensity of green fluorescent protein fluorescence in the leaves of transgenic tobacco plants*. *Plant Cell Rep*, 2008. **27**(1): p. 67-77.
108. Volfson, D., et al., *Origins of extrinsic variability in eukaryotic gene expression*. *Nature*, 2006. **439**(7078): p. 861-4.
109. Billinton, N. and A.W. Knight, *Seeing the wood through the trees: a review of techniques for distinguishing green fluorescent protein from endogenous autofluorescence*. *Anal Biochem*, 2001. **291**(2): p. 175-97.
110. Huang, D. and E.V. Shusta, *Secretion and surface display of green fluorescent protein using the yeast Saccharomyces cerevisiae*. *Biotechnol Prog*, 2005. **21**(2): p. 349-57.
111. Raser, J.M. and E.K. O'Shea, *Noise in gene expression: origins, consequences, and control*. *Science*, 2005. **309**(5743): p. 2010-3.
112. Blake, W.J., et al., *Phenotypic consequences of promoter-mediated transcriptional noise*. *Mol Cell*, 2006. **24**(6): p. 853-65.
113. Kacmar, J., et al., *Single-cell variability in growing Saccharomyces cerevisiae cell populations measured with automated flow cytometry*. *J Biotechnol*, 2004. **109**(3): p. 239-54.
114. Raser, J.M. and E.K. O'Shea, *Control of stochasticity in eukaryotic gene expression*. *Science*, 2004. **304**(5678): p. 1811-4.

115. Niebauer, R.T., A. Wedekind, and A.S. Robinson, *Decreases in yeast expression yields of the human adenosine A2a receptor are a result of translational or post-translational events*. Protein Expr Purif, 2004. **37**(1): p. 134-43.
116. Lipke, P.N., D. Wojciechowicz, and J. Kurjan, *AG alpha 1 is the structural gene for the Saccharomyces cerevisiae alpha-agglutinin, a cell surface glycoprotein involved in cell-cell interactions during mating*. Mol Cell Biol, 1989. **9**(8): p. 3155-65.
117. van der Vaart, J.M., et al., *Identification of three mannoproteins in the cell wall of Saccharomyces cerevisiae*. J Bacteriol, 1995. **177**(11): p. 3104-10.
118. Boone, C., et al., *Yeast KRE genes provide evidence for a pathway of cell wall beta-glucan assembly*. J Cell Biol, 1990. **110**(5): p. 1833-43.
119. Jentoft, N., *Why are proteins O-glycosylated?* Trends Biochem Sci, 1990. **15**(8): p. 291-4.
120. Walsh, A. and S.J. Chapman, *Sugars protect desmosome and corneosome glycoproteins from proteolysis*. Arch Dermatol Res, 1991. **283**(3): p. 174-9.
121. Meaden, P., et al., *The yeast KRE5 gene encodes a probable endoplasmic reticulum protein required for (1----6)-beta-D-glucan synthesis and normal cell growth*. Mol Cell Biol, 1990. **10**(6): p. 3013-9.
122. Krysan, D.J., et al., *Yapsins are a family of aspartyl proteases required for cell wall integrity in Saccharomyces cerevisiae*. Eukaryot Cell, 2005. **4**(8): p. 1364-74.
123. Gagnon-Arsenault, I., J. Tremblay, and Y. Bourbonnais, *Fungal yapsins and cell wall: a unique family of aspartic peptidases for a distinctive cellular function*. FEMS Yeast Res, 2006. **6**(7): p. 966-78.
124. Gagnon-Arsenault, I., et al., *Activation mechanism, functional role and shedding of glycosylphosphatidylinositol-anchored Yps1p at the Saccharomyces cerevisiae cell surface*. Mol Microbiol, 2008. **69**(4): p. 982-93.
125. Hube, B. and J. Naglik, *Candida albicans proteinases: resolving the mystery of a gene family*. Microbiology, 2001. **147**(Pt 8): p. 1997-2005.
126. Levin, D.E. and E. Bartlett-Heubusch, *Mutants in the S. cerevisiae PKC1 gene display a cell cycle-specific osmotic stability defect*. J Cell Biol, 1992. **116**(5): p. 1221-9.
127. Verna, J., et al., *A family of genes required for maintenance of cell wall integrity and for the stress response in Saccharomyces cerevisiae*. Proc Natl Acad Sci U S A, 1997. **94**(25): p. 13804-9.

128. Mager, W.H. and J.C. Varela, *Osmostress response of the yeast Saccharomyces*. Mol Microbiol, 1993. **10**(2): p. 253-8.
129. Siderius, M., et al., *The control of intracellular glycerol in Saccharomyces cerevisiae influences osmotic stress response and resistance to increased temperature*. Mol Microbiol, 2000. **36**(6): p. 1381-90.
130. Hohmann, S., M. Krantz, and B. Nordlander, *Yeast osmoregulation*. Methods Enzymol, 2007. **428**: p. 29-45.
131. Kim, S. and K. Shah, *Dissecting yeast Hog1 MAP kinase pathway using a chemical genetic approach*. FEBS Lett, 2007. **581**(6): p. 1209-16.
132. Wojda, I., et al., *Response to high osmotic conditions and elevated temperature in Saccharomyces cerevisiae is controlled by intracellular glycerol and involves coordinate activity of MAP kinase pathways*. Microbiology, 2003. **149**(Pt 5): p. 1193-204.
133. Albertyn, J., et al., *GPD1, which encodes glycerol-3-phosphate dehydrogenase, is essential for growth under osmotic stress in Saccharomyces cerevisiae, and its expression is regulated by the high-osmolarity glycerol response pathway*. Mol Cell Biol, 1994. **14**(6): p. 4135-44.
134. Meng, F., Y. Park, and H. Zhou, *Role of proline, glycerol, and heparin as protein folding aids during refolding of rabbit muscle creatine kinase*. Int J Biochem Cell Biol, 2001. **33**(7): p. 701-9.
135. Romanos, M.A., C.A. Scorer, and J.J. Clare, *Foreign gene expression in yeast: a review*. Yeast, 1992. **8**(6): p. 423-88.
136. Weber-Ban, E.U., et al., *Global unfolding of a substrate protein by the Hsp100 chaperone ClpA*. Nature, 1999. **401**(6748): p. 90-3.
137. Sacchetti, A., et al., *Green fluorescent protein variants fold differentially in prokaryotic and eukaryotic cells*. J Cell Biochem Suppl, 2001. **Suppl 36**: p. 117-28.
138. Kimata, Y., C.R. Lim, and K. Kohno, *S147P green fluorescent protein: a less thermosensitive green fluorescent protein variant*. Methods Enzymol, 1999. **302**: p. 373-8.
139. Ogawa, H., et al., *Localization, trafficking, and temperature-dependence of the Aequorea green fluorescent protein in cultured vertebrate cells*. Proc Natl Acad Sci U S A, 1995. **92**(25): p. 11899-903.

140. Shusta, E.V., et al., *Increasing the secretory capacity of Saccharomyces cerevisiae for production of single-chain antibody fragments*. Nat Biotechnol, 1998. **16**(8): p. 773-7.
141. Shusta, E.V., et al., *Directed evolution of a stable scaffold for T-cell receptor engineering*. Nat Biotechnol, 2000. **18**(7): p. 754-9.
142. Lussier, M., et al., *Large scale identification of genes involved in cell surface biosynthesis and architecture in Saccharomyces cerevisiae*. Genetics, 1997. **147**(2): p. 435-50.
143. Terashima, H., et al., *Up-regulation of genes encoding glycosylphosphatidylinositol (GPI)-attached proteins in response to cell wall damage caused by disruption of FKS1 in Saccharomyces cerevisiae*. Mol Gen Genet, 2000. **264**(1-2): p. 64-74.
144. de Groot, P.W., et al., *A genomic approach for the identification and classification of genes involved in cell wall formation and its regulation in Saccharomyces cerevisiae*. Comp Funct Genomics, 2001. **2**(3): p. 124-42.
145. Roemer, T., et al., *Large-scale essential gene identification in Candida albicans and applications to antifungal drug discovery*. Mol Microbiol, 2003. **50**(1): p. 167-81.
146. De Groot, P.W., K.J. Hellingwerf, and F.M. Klis, *Genome-wide identification of fungal GPI proteins*. Yeast, 2003. **20**(9): p. 781-96.
147. Kitagaki, H., K. Ito, and H. Shimoi, *A temperature-sensitive dcw1 mutant of Saccharomyces cerevisiae is cell cycle arrested with small buds which have aberrant cell walls*. Eukaryot Cell, 2004. **3**(5): p. 1297-306.
148. Spreghini, E., et al., *Roles of Candida albicans Dfg5p and Dcw1p cell surface proteins in growth and hypha formation*. Eukaryot Cell, 2003. **2**(4): p. 746-55.
149. Cubitt, A.B., et al., *Understanding, improving and using green fluorescent proteins*. Trends Biochem Sci, 1995. **20**(11): p. 448-55.
150. Toh-e, A. and T. Oguchi, *Genetic characterization of genes encoding enzymes catalyzing addition of phospho-ethanolamine to the glycosylphosphatidylinositol anchor in Saccharomyces cerevisiae*. Genes Genet Syst, 2002. **77**(5): p. 309-22.
151. Taron, C.H., et al., *Glycosylphosphatidylinositol biosynthesis defects in Gpi11p- and Gpi13p-deficient yeast suggest a branched pathway and implicate gpi13p in phosphoethanolamine transfer to the third mannose*. Mol Biol Cell, 2000. **11**(5): p. 1611-30.

152. Gaynor, E.C., et al., *MCD4 encodes a conserved endoplasmic reticulum membrane protein essential for glycosylphosphatidylinositol anchor synthesis in yeast*. Mol Biol Cell, 1999. **10**(3): p. 627-48.
153. Yada, T., et al., *Its8, a fission yeast homolog of Mcd4 and Pig-n, is involved in GPI anchor synthesis and shares an essential function with calcineurin in cytokinesis*. J Biol Chem, 2001. **276**(17): p. 13579-86.
154. Kinoshita, T., M. Fujita, and Y. Maeda, *Biosynthesis, remodelling and functions of mammalian GPI-anchored proteins: recent progress*. J Biochem, 2008. **144**(3): p. 287-94.
155. Flury, I., A. Benachour, and A. Conzelmann, *YLL031c belongs to a novel family of membrane proteins involved in the transfer of ethanolaminephosphate onto the core structure of glycosylphosphatidylinositol anchors in yeast*. J Biol Chem, 2000. **275**(32): p. 24458-65.
156. Fujita, M., et al., *GPI7 involved in glycosylphosphatidylinositol biosynthesis is essential for yeast cell separation*. J Biol Chem, 2004. **279**(50): p. 51869-79.
157. Hong, Y., et al., *Pig-n, a mammalian homologue of yeast Mcd4p, is involved in transferring phosphoethanolamine to the first mannose of the glycosylphosphatidylinositol*. J Biol Chem, 1999. **274**(49): p. 35099-106.
158. Lisanti, M.P., et al., *Mannosamine, a novel inhibitor of glycosylphosphatidylinositol incorporation into proteins*. EMBO J, 1991. **10**(8): p. 1969-77.
159. Modun, B. and P. Williams, *The staphylococcal transferrin-binding protein is a cell wall glyceraldehyde-3-phosphate dehydrogenase*. Infect Immun, 1999. **67**(3): p. 1086-92.
160. Taylor, J.M. and D.E. Heinrichs, *Transferrin binding in Staphylococcus aureus: involvement of a cell wall-anchored protein*. Mol Microbiol, 2002. **43**(6): p. 1603-14.
161. Moreira, R.F., et al., *Flocculation of Saccharomyces cerevisiae is induced by transformation with the GAP1 gene from Kluyveromyces marxianus*. Yeast, 2000. **16**(3): p. 231-40.
162. Gil-Navarro, I., et al., *The glycolytic enzyme glyceraldehyde-3-phosphate dehydrogenase of Candida albicans is a surface antigen*. J Bacteriol, 1997. **179**(16): p. 4992-9.

163. Delgado, M.L., et al., *The glyceraldehyde-3-phosphate dehydrogenase polypeptides encoded by the Saccharomyces cerevisiae TDH1, TDH2 and TDH3 genes are also cell wall proteins*. Microbiology, 2001. **147**(Pt 2): p. 411-7.
164. Pardo, M., et al., *Two-dimensional analysis of proteins secreted by Saccharomyces cerevisiae regenerating protoplasts: a novel approach to study the cell wall*. Yeast, 1999. **15**(6): p. 459-72.
165. Edwards, S.R., R. Braley, and W.L. Chaffin, *Enolase is present in the cell wall of Saccharomyces cerevisiae*. FEMS Microbiol Lett, 1999. **177**(2): p. 211-6.
166. Nombela, C., C. Gil, and W.L. Chaffin, *Non-conventional protein secretion in yeast*. Trends Microbiol, 2006. **14**(1): p. 15-21.
167. Lopez-Avalos, M.D., et al., *The UDPase activity of the Kluyveromyces lactis Golgi GDPase has a role in uridine nucleotide sugar transport into Golgi vesicles*. Glycobiology, 2001. **11**(5): p. 413-22.
168. Orlean, P., C. Albright, and P.W. Robbins, *Cloning and sequencing of the yeast gene for dolichol phosphate mannose synthase, an essential protein*. J Biol Chem, 1988. **263**(33): p. 17499-507.
169. Orlean, P., *Dolichol phosphate mannose synthase is required in vivo for glycosyl phosphatidylinositol membrane anchoring, O mannosylation, and N glycosylation of protein in Saccharomyces cerevisiae*. Mol Cell Biol, 1990. **10**(11): p. 5796-805.
170. Dean, N., Y.B. Zhang, and J.B. Poster, *The VRG4 gene is required for GDP-mannose transport into the lumen of the Golgi in the yeast, Saccharomyces cerevisiae*. J Biol Chem, 1997. **272**(50): p. 31908-14.
171. Berninsone, P., et al., *Regulation of yeast Golgi glycosylation. Guanosine diphosphatase functions as a homodimer in the membrane*. J Biol Chem, 1995. **270**(24): p. 14564-7.
172. Warit, S., et al., *Glycosylation deficiency phenotypes resulting from depletion of GDP-mannose pyrophosphorylase in two yeast species*. Mol Microbiol, 2000. **36**(5): p. 1156-66.
173. Herrero, A.B., et al., *The Golgi GDPase of the fungal pathogen Candida albicans affects morphogenesis, glycosylation, and cell wall properties*. Eukaryot Cell, 2002. **1**(3): p. 420-31.
174. De Nobel, J.G., et al., *Cyclic variations in the permeability of the cell wall of Saccharomyces cerevisiae*. Yeast, 1991. **7**(6): p. 589-98.

175. De Nobel, J.G., et al., *An assay of relative cell wall porosity in Saccharomyces cerevisiae, Kluyveromyces lactis and Schizosaccharomyces pombe*. *Yeast*, 1990. **6**(6): p. 483-90.
176. Yin, Q.Y., et al., *Mass spectrometry-based proteomics of fungal wall glycoproteins*. *Trends Microbiol*, 2008. **16**(1): p. 20-6.
177. Madzak, C., C. Gaillardin, and J.M. Beckerich, *Heterologous protein expression and secretion in the non-conventional yeast Yarrowia lipolytica: a review*. *J Biotechnol*, 2004. **109**(1-2): p. 63-81.
178. Buckholz, R.G. and M.A. Gleeson, *Yeast systems for the commercial production of heterologous proteins*. *Biotechnology (N Y)*, 1991. **9**(11): p. 1067-72.
179. Fowler, T. and R.M. Berka, *Gene expression systems for filamentous fungi*. *Curr Opin Biotechnol*, 1991. **2**(5): p. 691-7.
180. Cregg, J.M., T.S. Vedvick, and W.C. Raschke, *Recent advances in the expression of foreign genes in Pichia pastoris*. *Biotechnology (N Y)*, 1993. **11**(8): p. 905-10.
181. Mosch, H.U. and G.R. Fink, *Dissection of filamentous growth by transposon mutagenesis in Saccharomyces cerevisiae*. *Genetics*, 1997. **145**(3): p. 671-84.